الجمهورية الجزائرية الديمقراطية الشعبية
People's Democratic Republic of Algeria
وزارة التعـليـم العالي والـبحـث الـعلـمي
Ministry of Higher Education and Scientific Research
جامـعة الشهيد حمة لخضر الوادي
University of Echahid Hamma Lakhdar -El OUED
كلية العلوم الطبيعية الحياة
Faculty of Natural and Life Sciences
قسم البيولوجيا الخلوية والجزيئية
Department of Cellular and Molecular Biology

THESIS

SUBMITTED TO OBTAIN 3rd CYCLE LMD DOCTORATE DEGREE IN BIOLOGICAL SCIENCE
Specialty: Applied Biochemistry

THEME

Green synthesis, characterization of silver and zinc oxide nanoparticles using plant extract and evaluation of their biological activities

Presented by: Mrs. AZZI Manel

Graduated 00/00/2024

Jury Members:

Mr. CHOUIKH ATEF	**Professor**	**University of El-Oued**	**President**
Mrs. MEDILA Ifriqya	**Professor**	**University of El-Oued**	**Supervisor**
Mrs. TOUMI Ikram	**Professor**	**University of El-Oued**	**Co-supervisor**
Mrs. MAHBOUB Nasma	**MCA**	**University of El-Oued**	**Examiner**
Mr. BOUAL Zakarya	**Professor**	**University of Ouargla**	**Examiner**
Mr. MESBAH Said	**MCA**	**University of Ouargla**	**Examiner**
Mr. LAOUINI Salah Eddine	**Professor**	**University of El-Oued**	**Invited**

2023/2024

Acknowledgements

Above all, I'm grateful to God, the Almighty, for providing me with endurance and fortitude. I would first want to extend my sincere gratitude to Mrs. Medila Ifriqya and Mrs.Toumi Ikram, professors from Echahid Hamma Lakhdar University, for their guidance and supervision of this effort. Their availability, counsel, and faith in me made it possible for me to complete this work. My profound appreciation is extended to Mr. LAOUINI Salah, a professor from Echahid Hamma Lakhdar University, for his tremendous help.

My deepest gratitude goes out to Pr. CHOUIKH Atef director of the Biology, Environment, and Health Laboratory, deserves special recognition for all of his efforts in providing the needs of the laboratory and for agreeing to chair my thesis' dissertation. Additionally, I would like to express my gratitude to the committee members, Pr. BOUAL Zakarya, Dr. MAHBOUB Nasma, and Dr. MESBAH Said for consenting to review and assess my work.

I would also like to thank Dr. HAMIDATOU Mehieddine for his help in anatomy and pathology cytology.

Dr. MEHDI Selman, Dr. KHALEF Yahya, I want to thank you so much for all of your hard work, precious efforts, and scientific advice.

Thank you also to Dr. MESSAI Md Atmane, Dr. AZZI Imane, Pr. ISSAADI Fares, Dr. LAIB Ibtissam and Dr. GHARAISSA Noura, for their aiding, encouragement and their permanent support during these years of work.

And I express my thanks to Mr. TLIBA Ali, Mr. KHENOUFA Amor, and the biology laboratory managers to have benefited from his precious help, his encouragement, his advice and his good humors.

I also want to thank all of my teachers for teaching me the fundamentals of science.

My gratitude to all of my colleagues BENINE Chaima, HAMDI Mohammed, GAMIL Hacen and BIKI Abdelmalek, HAMIDI Bachir for their unwavering support and encouragement . I send them my warmest kindness and best wishes.

To my parents for their prayers, encouragement and support me in every way

To my husband and his great role and continuous encouragement to complete this work

To my two sons, Thabet and Ghaith, for their patience and bearing with me the hardship of this work

My sisters Imane and Ihsane for their constant support for me

My brothers Nacereddine and Diaeddine for encouraging me

ABSTRACT

The primary aim of this study is to biosynthesize Ag/Ag_2O NPs and ZnO NPs using *Olea europaea* var. Chemllali leaves aqueous extract. Additionally, the biological effects of these nanoparticles will be assessed both in vitro and in vivo. Qualitative, quantitative analysis and HPLC analysis was used for the identification of specific phenolic components of the extract. However, Ag/Ag_2O NPs and ZnO NPs have been green synthesized and characterized using more then one technique (UV, FTIR, XRD, and SEM-EDX). Furthermore, antioxidant, antibacterial, antimutagenic, anticoagulant activities have been used to evaluate the in vitro activities. For in vivo study using Wistar male rats, to evaluate the extent of toxicity of these nanoparticles, and to assess protective effect of this nanoparticles against metrubizin toxicity. Some biochemical and hematological indicators, also histopathological and oxidative stress parameter of liver, kidney and spleen were mesured. Phytochemical analysis revealed the presence of many seconder metabolites in aquous extract, also quantified of the total phenolic, flavonoids and condensed tanins content. Additional analyze by HPLC,we have identified eight phenolic compounds; when quercetin (1945.90 µg/g) was the most abundant element. After characterization of biogenic nanopartilces, we confirmed that Ag/Ag_2O NPs and ZnO NPs were biosynthesized. The average size distribution of Ag/Ag_2O NPs is principally 45 nm, and 18.79 nm for ZnO NPs size. For antioxidant activities of the *O.europaea* leaf extract, Ag/Ag_2O NPs and ZnO Nps is shown to be dose-dependent, as the scavenging activity, TAC and FRAP, the most notable antioxydant activities were observed with 200 µg/mL of Ag/Ag_2O Nps. The antibacterial activity in solid agar was found also to be dose-dependent of Ag/Ag_2O NPs against *S.aureus*, *E.coli*, and *P. aeruginosa*, while the ZnO nanoparticles at higher dose was less effective. However, antibacterial kinetic study in liquid medium revealed inhibitory effects of nanoparticles on bacterial growth of *E. coli* and *S. typhimurium* cells at 200ug/ml, but the growth of *B. cereus* and *MS-S. aureus* cells was suppressed in the initial hours, with almost all bacterial cells exhibiting retarded growth after this period. This tow nanoparticles biosynthetised showed strong anti-mutagenicity against *S. typhimurium* TA98, when the percent inhibition of ZnO NPs was stronger (76.24%) then Ag/Ag_2O NPS (70%) at 250 µg/plat. All nanoparticles (ZnO and Ag/Ag_2O NPs) prevented coagulation similarly to the positive control (EDTA). Toxicity study of nanoparticles revealed no mortality for ZnO NPs (50 mg/kg and 100 mg/kg b.w) and Ag/Ag_2O NPs (2.5 mg/Kg) for single dose during the 28-days. In contrast, one rat that received a higher dose of 5 mg/kg b.w of Ag/Ag_2O NPs died after 24 h, and we showed signs of toxicity in this group. Moreover, the findings in metribuzin-treated rats induced for 21 days significant changes in hematological, biochemical parameters and imbalance in oxidative stress status and deterioration of the liver, the kidney and the spleen structure compared to the control group. However, the treatment with ZnO NPs (2.5 mg/Kg , 5 mg/Kg) mitigated most of toxic effects and the restored most of previous parameters. As for Ag/Ag_2O NPs, most of the effects of low concentration (0.062mg/Kg) were generally beneficial. On the other hand, the effect of high concentration (0.125mg/Kg) was hopeless and even toxic, as demonstrated by the analyzes and histological images of the organs studied. En conclusion, this work realizes the potential for green synthesis of nanoparticles from *O. europaea* (ZnO NPs and Ag/Ag_2O NPs), as these particles have shown to be highly biological efficient and varied among them, While Ag/Ag_2O NPs was toxic to a certain degree.

Key words: biosynthesize . *O.europaea* , ZnO NPs, Ag/Ag_2O NPs, antibacterial, antimutagenic, toxicity .

الملخص

الهدف الأساسي من هذه الدراسة هو التخليق الحيوي لـ Ag/Ag_2O NPs و ZnO NPs باستخدام المستخلص المائي أوراق نبات الزيتون *O.europaea*. بالإضافة إلى ذلك، سيتم تقييم التأثيرات البيولوجية لهذه الجسيمات النانوية. تم استخدام التحليل النوعي والكمي وتحليل HPLC لتحديد المكونات الفينولية المحددة للمستخلص. وبعدها، تم التصنيع الحيوي للجزئيات النانوية للفضة/أوكسيد ثنائي الفضة Ag/Ag_2O NPs و أوكسيد الزنك ZnO NPs، قد وتم فحص خصائصها باستخدام أكثر من تقنية (UV، FTIR، XRD، وSEM-EDX). علاوة على ذلك، تم إختبار مدى نشاطيتها في المختبر المضادة الأكسدة، والمضادة الجراثيم، والمضادة الطفرات، وكذا المضادة لتخثر الدم. و قد تم أيضا إجراء دراسة على الجسم الحي باستخدام ذكور فئران ويستار، لتقييم مدى سمية هذه الجسيمات النانوية، وتقييم التأثير الوقائي لهذه الجسيمات النانوية ضد سمية المبيد ميتروبيزين. حيث تم قياس بعض المؤشرات البيوكيميائية والدموية وكذلك مؤشرات الإجهاد التأكسدي وفحص لأنسجة الكبد والكلى والطحال. كشف التحليل الكيميائي النباتي عن وجود العديد من المستقلبات الثانوية في المستخلص المائي، كما تم قياس كمية الفينول الكلي والفلافونويدات والتانينات المكثفة. وتحليل آخر بواسطة HPLC، حيث حددنا ثمانية مركبات فينولية؛ من بينها الكيرسيتين (1945.90 مكغ / غ) هو العنصر الأكثر وفرة. بعد التخليق الأخضر الجسيمات النانوية، أكدنا أن Ag/Ag_2O NPs و ZnO NPs قد تم تصنيعهما حيويًا. وبلغ متوسط حجم توزيع Ag/Ag2O NPs 45 نانومتر، و18.79 نانومتر لحجم ZnO NPs. بالنسبة للأنشطة المضادة للأكسدة لمستخلص أوراق O.europaea، Ag/Ag_2O NPs وZnO Nps تبين أن مدى النشاطية يعتمد على زيادة الجرعة، حيث لوحظ نشاط الكسح، TAC وFRAP، الأقوى في تركيز 200 ميكروغرام/مل من Ag/ Ag2O NPs.وكذلك وجد أن النشاط المضاد للبكتيريا في الأجار الصلب يعتمد أيضًا على زيادة الجرعة لـ Ag/Ag2O NPs ضد *S.aureus* و*E.coli* و*P. aeruginosa*، بينما كانت جزيئات أكسيد الزنك النانوية عند الجرعة الأعلى أقل فعالية. ورغم ذلك، كشفت الدراسة الحركية المضادة للبكتيريا في الوسط السائل عن تأثيرات مثبطة للجسيمات النانوية على النمو البكتيري لخلايا *E. coli* و *S. typhimurium* عند 200 مكغ/مل، ولكن نمو *B. cereus* و *MS-S. aureus*. تم تثبيط الخلايا البكترية في الساعات الأولى، حيث أظهرت جميع الخلايا البكتيرية تقريبًا نموًا متأخرا بعد هذه الفترة. كما أظهرت هذه الجسيمات النانوية المصنعة حيويًا مقاومة قوية للطفرات ضد *S. typhimurium* TA98، حيث كانت نسبة تثبيط ZnO NPs أقوى (76.24%) ثم (70%) Ag/Ag_2O NPS عند 250 مكغ/وعاء. جميع الجسيمات النانوية (ZnO NPs و Ag/Ag_2O NPs) منعت التخثر بشكل مشابه بالمقارنة مع الشاهد (EDTA). أما في ما يخص التجارب داخل الجسم الحي، أظهرت دراسة السمية للجسيمات النانوية عدم وجود وفيات لأكسيد الزنك 50) NPs ملغ/كلغ و100 ملغ/كلغ من وزن الجسم) و2.5) Ag/Ag_2O NPs ملغ/كلغ) للجرعة الواحدة خلال 28 يومًا. وعلى النقيض من ذلك، مات فأر واحد تلقى جرعة قدرها 5 ملغم/كغم من Ag/Ag_2O NPs بعد 24 ساعة، كما ظهرت علامات السمية واضحة جدا في هذه المجموعة. علاوة على ذلك، أدت النتائج التي تم إجراؤها على الفئران المعالجة بالميتريبوزين لمدة 21 يومًا إلى حدوث تغييرات كبيرة في مؤشرات الدم والكيمياء الحيوية وعدم التوازن في حالة الإجهاد التأكسدي وتدهور بنية الكبد والكلى والطحال مقارنة بالمجموعة الشاهدة. في حين أن المعاملة بأكسيد الزنك (2.5 ملغ/كلغ و 5 ملغ/كلغ) خففت معظم التأثيرات السامة وأعادت معظم التغيرات السابقة إلى الحالة الطبيعية. أما بالنسبة لـ Ag/Ag_2O NPs، فإن معظم تأثيرات التركيز المنخفض (0.062 ملغ/كلغ) كانت مفيدة بشكل عام. بينما تأثير التركيز العالي (0.125 ملغ/كلغ) كان ذو أثر سلبي بل وساماً، كما يتضح من التحاليل والصور النسيجية للأعضاء المدروسة. في الختام، هدف هذا العمل إلى إمكانية التوليف الأخضر للجسيمات النانوية من *O. europaea* حيث أظهرت هذه الجسيمات كفاءة بيولوجية عالية ومتنوعة فيما بينها، في حين أن Ag/Ag_2O NPs كان أكثر سمية إلى حد ما.

الكلمات المفتاحية:التصنيع الحيوي، *O. europaea*، ZnO NPs، Ag/Ag_2O NPs، مضاد للبكتيريا، مضاد للطفرات، سمية

RESUME

L'objectif principal de cette étude est de biosynthétiser les NP Ag/Ag_2O et les NP ZnO en utilisant l'extrait aqueux de feuillies de *O. europaea* Var. Chemllali . De plus, les effets biologiques de ces nanoparticules seront évalués in vitro et in vivo. Des analyses qualitatives / quantitatives et des analyses HPLC ont été utilisées pour l'identification de composants phénoliques spécifiques de l'extrait. Cependant, les NPs Ag/Ag_2O et les NPs ZnO ont été biosynthétisés et caractérisés à l'aide de plusieurs techniques (UV, FTIR, XRD et SEM-EDX). De plus, des activités antioxydantes, antibactériennes, antimutagènes et anticoagulantes ont été utilisées pour évaluer les activités in vitro. Pour une étude in vivo utilisant des rats mâles Wistar, pour évaluer l'étendue de la toxicité et pour évaluer l'effet protecteur de ces nanoparticules contre la toxicité de la métrubizine. Certains indicateurs biochimiques et hématologiques, ainsi que les paramètres de stress oxydatif et histopathologiques du foie, des reins et de la rate ont été mesurés. L'analyse phytochimique a révélé la présence de nombreux métabolites secondaires dans l'extrait aqueux, ainsi que la teneur totale en composés phénoliques, flavonoïdes et tanins condensés. Une autre analyse par HPLC, nous avons identifié huit composés phénoliques ; lorsque la quercétine (1945,90 µg/g) était l'élément le plus abondant. Après caractérisation des nanoparticules biogéniques, nous avons confirmé que les NP Ag/Ag_2O et les NP ZnO étaient biosynthétisées. La distribution de taille moyenne des NP Ag/Ag_2O est principalement de 45 nm et de 18,79 nm pour la taille des NP ZnO. Pour les activités antioxydantes de l'extrait de feuille d'*O.europaea*, Ag/Ag_2O NPs et ZnO Nps se révèlent dépendantes de la dose, car pour l'activité de piégeage, TAC et FRAP, les activités antioxydantes les plus notables ont été observées avec 200 µg/mL d' Ag/Ag_2O Nps. L'activité antibactérienne dans la gélose solide s'est également avérée dépendante de la dose des NP Ag/Ag_2O contre *S.aureus*, *E.coli* et *P. aeruginosa*, tandis que les nanoparticules de ZnO à dose plus élevée étaient moins efficaces. Cependant, une étude cinétique antibactérienne en milieu liquide a révélé des effets inhibiteurs des nanoparticules sur la croissance bactérienne des cellules *d'E. coli* et de *S. typhimurium* à 200 ug/ml, mais concernant la croissance de *B. cereus* et de *MS-S.aureus* a été supprimée dans les premières heures, presque toutes les cellules bactériennes présentant un retard de croissance après cette période. Ces deux nanoparticules biosynthétisées aussi ont montré une forte anti-mutagénicité contre *S. typhimurium* TA98, lorsque le pourcentage d'inhibition des NP de ZnO était plus fort (76,24 %) que celui de l' Ag/Ag_2O NPS (70 %) à 250 µg/plat. Toutes les nanoparticules (ZnO et Ag/Ag_2O NP) ont empêché la coagulation de la même manière que le contrôle positif (EDTA). L'étude de toxicité des nanoparticules n'a révélé aucune mortalité pour les NP de ZnO (50 mg/kg et 100 mg/kg p.c.) et les NP d' Ag/Ag_2O (2,5 mg/Kg) pour une dose unique pendant les 28 jours. En revanche, un rat ayant reçu une dose plus élevée de groupe 5 mg/kg de NP Ag/Ag_2O est mort après 24 heures et nous avons montré des signes de toxicité dans ce groupe. De plus, les résultats chez les rats traités à la métribuzine ont induit pendant 21 jours des changements significatifs des paramètres hématologiques et biochimiques et un déséquilibre du statut de stress oxydatif et une détérioration de la structure du foie, des reins et de la rate par rapport au groupe témoin. Cependant, le traitement avec des NP de ZnO (2,5 mg/Kg, 5 mg/Kg) a atténué la plupart des effets toxiques et restauré la plupart des paramètres précédents. Quant aux NP Ag/Ag_2O, la plupart des effets d'une faible concentration (0,062 mg/Kg) ont été généralement bénéfiques. En revanche, l'effet d'une concentration élevée (0,125 mg/Kg) s'est avéré désespéré et même toxique, comme le démontrent les analyses et les images histologiques des organes étudiés. En conclusion, ce travail réalise le potentiel de synthèse verte de nanoparticules d'*O. europaea* (NP ZnO et NP Ag/Ag_2O), car ces particules se sont révélées très efficaces sur le plan biologique et variées, tandis que les NP Ag/Ag_2O étaient toxiques pour un certain degré.

Mots clés : Biosynthesiser . *O. europaea* , NPs ZnO, NPs Ag/Ag_2O, antibactérien, antimutagène, toxicité**.**

LIST OF FIGURES

LIST OF TABLES

LIST OF ABBREVIATION

Ag^{+}	Silver ion
Ag/Ag_2ONPs	Silver /Silver Oxide nanoparticles
$AlCl_3$	Aluminum chloride
ALP	Alkaline phosphatase
ATCC	American Type Culture Collection
Au^{+}	Gold cation
DMSO	Dimethyl sulfoxide
DNA	Deoxyribonucleic acid
DPPH•	2,2-diphenyl-1-picrylhydrazyl
DTNB	5,5′-Dithiobis-(2-nitrobenzoic acid)
EDTA	Ethylenediaminetetraacetic acid
EDX	Energy Dispersive X-ray
$FeCl_3$	Ferric chloride
FTIR	Fourier Transform Infrared Spectrometer
GSH	Glutathione
H_2O_2	Hydrogen peroxide
LPO	Lipid peroxidation
MDA	Malondialdehyde
MHB	Mueller Hinton Broth
NPs	Nanoparticles
PLT	Platelet
RBC	Red Blood Cell
ROS	Reactive oxygen species
SEM	Scanning electron microscopes
SPR	surface plasmon resonance
T_3	Triiodothyronine
TBA	Thiobarbituric Acid
TBS	Tris buffer saline solution
TCA	Trichloroacetic Acid
UV	Ultraviolet
UV-VIS	UV-VIS: Ultraviolet-visible spectroscopy
WBC	White Blood cell

XRD	X-ray diffraction
Zn^{+2}	Zinc ion
ZnO NPs	Zinc oxide Nanoparticles

Summary

CHAPTER III Pesticides

INTRODUCTION

Introduction

The small size of nanomaterials to biological medium is what is making them appealing for use in biological applications. Furthermore, because of their extremely high surface area to volume ratio, they are active building blocks that can be functionalized with a variety of functional groups and adorned with different medications. Nanomaterials have been employed as microscopic sensors to study and identify illnesses, as agents of communication between species, or as therapeutic agents to address a range of medical issues. Nanoparticles have advanced biological applications significantly because of their wide range of uses (Horikoshi *et al.,* 2013).

Nanoparticles can be incorporated using different methodologies, including chemical, physical and biological organic compounds. Although the chemical synthesis technique requires a fairly short time frame for the development of a large quantity of nanomaterials (Osman *et al.,* 2024), For the purpose of stabilizing and adjusting the size of the nanoparticles, this technique needs the capping operators. The synthetic chemical mixtures used in the stabilization, maintenance, and amalgamation of nanoparticles are hazardous and lead to unfavorable and polluted byproducts. The desire to create environmentally friendly, non-lethal designed protocols for the amalgamation of nanoparticles has led to a fashioning interest in biological methodologies that do not include the use of any hazardous or dangerous substances as byproducts. Interest in "green nanotechnology" is growing (Singhal *et al.,* 2011).

Many biological approaches for both extracellular and intracellular nanoparticles synthesis have been described till date using micro-organisms including fungi, bacteria and plants (Mukherjee *et al.,* 2001), which is simple, fewer energy intensive, eco-friendly and minimize the usage of toxic materials, and maximize the efficiency of the process (Raveendran and Wallen, 2003).

The greatest class of naturally occurring antioxidants are thought to be plant-based polyphenols, which have remarkable potential as medications, food additives, and nutraceuticals. The fundamental idea behind green synthesis techniques is that the phytochemicals found in plant components serve as both a natural reductant and a stabilizer of nanoparticles (Tahir *et al.,* 2017).

Other research suggest that plant extracts, as opposed to microbe-based synthesis, could be used to quickly produce highly stabilized nanoparticles. Therefore, the plant extract

may be a useful method for lowering the primary material of nanoparticles and stabilizing that (Iravani, 2011) .

In this sense, the olive *(Olea europaea* L. 1753) is a tiny tree that is native to warm temperate and tropical regions of the world and belongs to the Oleaceae family. The tree, commonly known for its fruit, is a major source of olive oil and has a significant economic impact in the Mediterranean region (Boskou, 1996).
The Quran recounts the story of the olive tree and its fruit, olives, multiple times in the context of its religious significance. Al-Nur (SURA 24) celebrates olives as a wonderful fruit (Quran 24:35).

In recent years, there has been a tremendous amount of interest in the health benefits of different herbal teas. One of the most popular and traditional herbal teas used by Mediterranean people to treat various ailments is olive leaf tea. Because of this, scientists from a wide range of disciplines are becoming more interested in the possible health benefits of olive leaves. Numerous research have recently reported on the antibacterial, antioxidant, hypoglycemic, antiatherosclerotic, and antihypertensive properties of olive leaves (Sedef and Karakaya, 2009) .

This work, therefore, extends the frontier of *Olea europaea* L to the field of nanobiotechnology for health and pharmaceutical uses.

Over the past few decades, the use of pesticides in agriculture to reservation crops for animals and humans has resulted in their unwanted accumulation in the environment (Dbira *et al.,* 2014). The Pesticides and herbicides arexenobiotic, poisonous, and sometimes non biodegradable and can lead to a many serious ecological and health problems (Hamza *et al., 2015)* .

In fact, pesticides represent a main concern for human health and contribute significantly to many disease states counting neurodegeneration, cancer and other chronic health effects (Hernández *et al.,* 2013), when ,the complexity of kidney and liver problems today seems to have increased. We may come into contact with chemicals and other environmental contaminants frequently like pesticide, causal to some of this complexity. There has been a significant rise in the amount of drug or other hazardous chemicals consumed, which could harm the organs.

Nanomaterials have been used in medicine and pharmacy due to their powerful antioxidant activity in scavenging free radicals produced in the process of oxidative injury caused by exposure to this food and environmental pollutants (Wasef *et al.,* 2021).

In light of these worries, the functional effects of zinc and silver oxyde nanoparticles in the domains of xenobiotic detoxification and antioxidant effects provide a potential solution in the control of metribuzin toxicity.
Based on this information, the goal of our thesis is to green synthesize, characterize, and study the biological activities of silver and zinc oxide nanoparticles using *O. europaea* leaf aqueous extract. We also try to estimate their antibacterial and antimutagenic activities. Additionally, evaluate the protective effect of these nanoparticles against the negative effects of the pesticide metribuzin on biochemical parameters and oxidative stress in various rat tissues, as well as comparing their effects.

Three chapters make up the first part. A bibliographic review of *Olea europaea* plant is included in the first chapter. The second chapter discusses nanoparticles, while the third chapter addresses pesticides.

The experimental work is covered in the second part. Section one is based on an in vitro study and involve extracting plant extract, characterizing these compounds both quantitatively and qualitatively, synthesizing and describing silver and zinc oxide nanoparticles, and testing their biological activities using assays for antioxidant, antibacterial activity, antimutagenicity and anticoagulant activity. the second section : This section is based on an in vivo investigation that assessed the acute toxicity and protective efficacy of biosynthesised silver and zinc oxide nanoparticles against metabolic, physiological, and histological alterations brought on by experimental metribuzin used on rats.

This is followed by an analysis and discussion of the results, ending with a conclusion as a general summary of the most important results we have reached through this work.

FIRST PART

Bibliographic Synthesis

CHAPTER I

Olea europaea

1. Generality

Among the plants that are most frequently mentioned in writing is the olive. Seven times in the Quran, the olive tree and olive oil are mentioned, and the olive is lauded as a wonderful fruit. Prophetic medicine has proposed the health benefits of olive trees and olive oil. The Prophet Mohamed (PBUH) is told to have said: "Take oil of olive and massage with it - it is a blessed tree" (Sunan al-Darimi, 69:103). In the Holy book Quran fruits and fruits bearing plants have been cited. Olive is mentioned in Sura VI (Anam) V: 99 Olive has also been praised as a blessed tree and fruit in the Holy Quran (Quran, Chapter 24 Al-Noor, Verse 35) (Azhar *et al.*, 2011) (Ryan and Robards, 1998).

Given that the Bible has multiple accounts of olives in both the Old and New Testaments, the olive tree and its fruit are also significant in the context of religion.(Ryan and Robards, 1998).

2. Botanical description

The olive tree is a short, dense tree that can grow up to 10 meters tall in trees or shrubs. Its trunk is twisted and organically bowed, with a considerable diameter (Figure 1-a). It contains numerous opposing branchlets among its reedy branches. (Hashmi *et al*.,2015).

The leaves are mucronate, shortpetioled, opposite, ovate lanceolate or lanceolate, green above, and hoary at the base (Figure 1-b). The flowers are much smaller than the leaves, arranged in short, erect, axillary racemes (Figure 1-c). The calyx is short and has four teeth, while the corolla is small and white with four broad, oval segments. When ripe, the ovoid, blackish-violet fruit is usually 1-2 cm long, smaller on wild plants than on orchard cultivators, has two cells, nauseatingly bitter flesh, and a sharp, pointed stone inside. Bark has a light grey tint (Shu, 1996) (Sarwar, 2013).

The olive fruit is an oval-shaped drupe with an average width and length of 2-3 cm with a pulp-to-stone ratio of 3.0-6.5. The skin, or epicarp, pulp, or mesocarp, and stone, or endocarp, are the three main components of an olive fruit (Figure 1-d). Wax covers the epicarp, or skin, which changes color from pale green to purple, brown, or black during the growth period. The hard endocarp (stone), which contains the seed or kernel, can make up anywhere from 13 to 30% of the fruit weight, whereas the mesocarp, which has soft, pulpy flesh, makes up 84–90% of the overall fruit mass. There are 2-4 g of oil per 100 g of seed. Olive fruits can weigh anything between 2 and 12 grams, while certain types can weigh up to 20 grams (Boskou *et al*., 2006) (Niaounakis and Halvadakis, 2006).

The only highly productive edible oil extracted by physical means from *Olea europaea* fruit is virgin olive oil. It can be distinguished from the others thanks to its sensory attributes and nutritional qualities (Khan *et al.,* 2007).

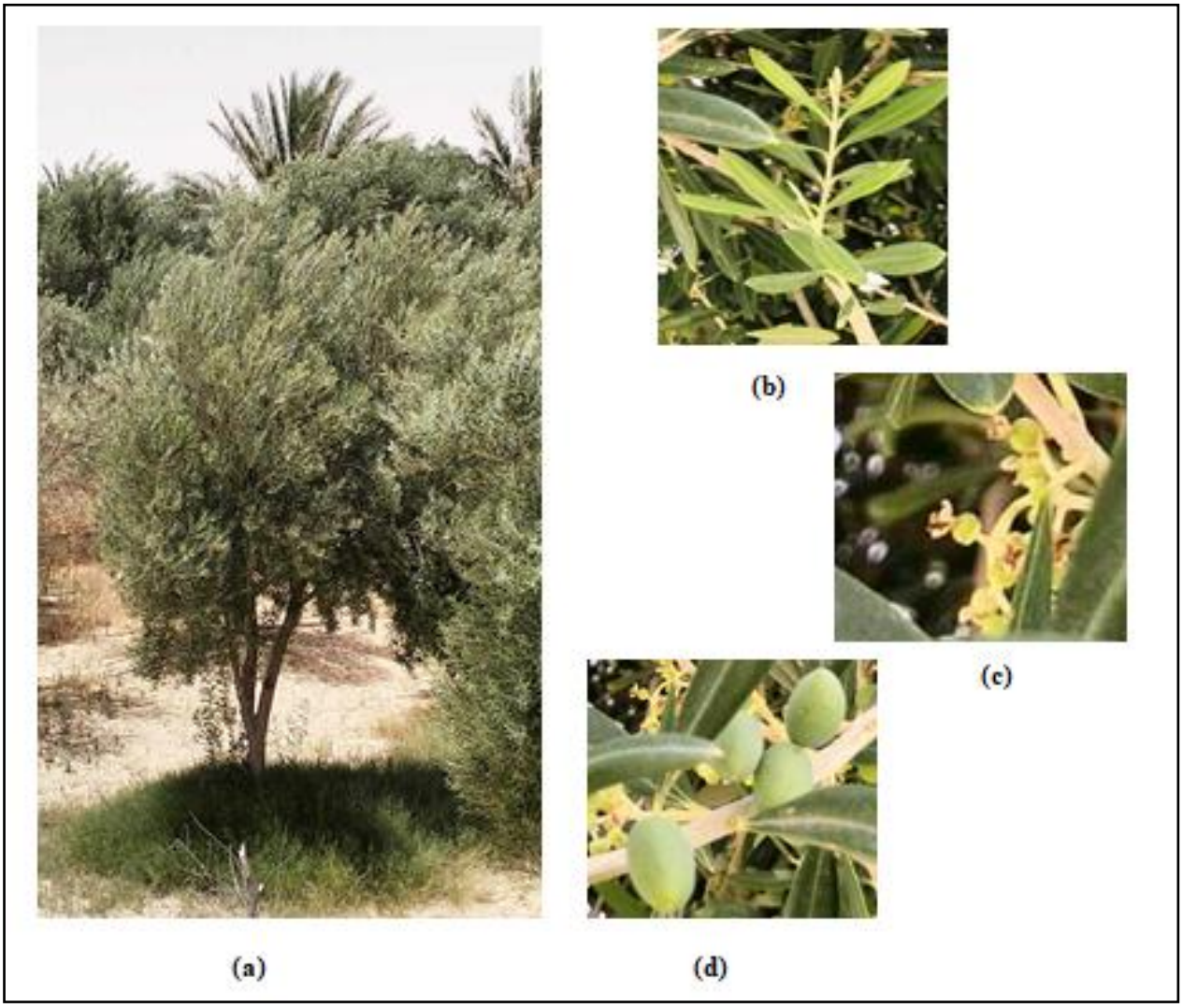

Figure (1): a- Olive tree. **b-** Olive leaves. **c-** Olive flowers . **d-** Olive fruits.(Original photo)

3. Geographic distribution

Native to the Mediterranean region and some parts of Asia, the olive tree (*Olea europaea* L.) is now widely grown throughout the world for olive oil and olives (Ghanbari *et al.,* 2012). The Oleaceae family is best grown in Asia and Malaysia, especially in tropical and temperate regions of Asia (Pérez *et al*., 2005). similar to the continuous coastal regions of northern Africa, western Asia, northern Iran near the southern tip of the Caspian Sea, and southeast Europe. In the perspective of religion, olive trees and their fruit are significant. (Robards and Ryan, 1998).

4. Classification

Kingdom: Plantae

Division: Angiosperms

Class: Eudicots

Order: Lamiales

Tribe: Oleaceae

Sub-tribe: Oleinae

Genus: Olea

Sub- genera: Paniculatae - Tetrapilus - Olea

Species: *europaea*

Sub- species: *cuspidate* - *Laprrinie* - *Maroccana* - *Cerasiformis* - *Guanchica* - *Europaea* (Green, 2002) (Ben Salem *et al.*,2014)

The Oleaceae family, sometimes known as the dicotyledon family, is made up of 30 genera of deciduous trees and shrubs, including the olive tree and its about 600 species of relatives (Grohmann, 1981). (Atta-ur-Rahman, 2023). According to Bartolini and Petruccelli (2002), the family is divided into multiple tribes: Fontanesieae, Forsythieae, Jasmineae, Myxopyreae, and Oleeae.

Although the genus Olea is well-known by almost 80 names, its namesake comes from the Greek "elaia" and the Latin word "oleum" (Médail *et al*., 2001). However, it is recognized as Olivo (Spanish), Oliva (Russian, Latin, and Italian), Olivo (English, French, and German), Zaitun (Arabic-Persian, Hindi, Urdu, and several Indian languages), and Zayit (Hebrew) in other languages (Goodner *et al.*, 2000).

There are several species in the genus Olea (Bracci *et al.*, 2011), but *Olea europaea* L. is by far the most well-known (Kaniewski *et al.*, 2012).According to Sarwar (2013), it is the only species in this genus that is utilized as food.

5. Bioactive compounds

5.1. Phenolic compound and flavenoids:

Low molecular weight polyphenols like oleuropein (up to 60–90 mg/g dry leaves weight), tyrosol, hydroxytyrosol, derivatives of elenolic acid, caffeic acid, p-coumaric acid, tocopherol, and vanillic acid, as well as flavonoids like luteolin, diosmetin, luteolin-7-glucoside, apigenin-7-glucoside, rutin, and diosmetin-7-glucoside, have been linked to the potential health benefits of olive leaves (Bianco and Uccella, 2000; Tasioula-Margari and Ologeri, 2001; Ryan *et al.,* 2003).

Moreover, compared to individual phenolics, the combined phenolic compounds exhibit noticeably stronger antibacterial activity (Lee, 2010).

According to Ghanbari *et al*. (2012), *O. europaea* is the most rich phenolic compound, accounting for up to 14% of its dry weight, and has a host of health benefits.

Several phenolic compounds, such as 7-deoxyloganic acid, loganin, secologanin, loganic acid, secologanoside, rosmarinic acid, ferulic acid, shikimic acid, taxifolin, protocatechuic acid, gallic acid, and cinnamic acid, were identified through tandem HPLC-MS analysis of olive pomace extracts (Peralbo-Molina *et al.*, 2012).

O. europaea leaves contain some flavonoids as well. From the leaves of *O. europaea*, apigenin-7-O-rutinoside, rutin, and luteolin-7-O-glucoside were extracted. Flavone glycosides, namely luteolin-7,4′-O-diglucoside, diosmetin, and apigenin-7-O-glucoside, were detected through analysis and quantification of leaves from several farmers (Meirinhos *et al.,* 2005). (Savournin and Associates, 2001).

Based on the aglycones apigenin, kaempferol, quercetin, and hesperitin, reversed-phase HPLC revealed that *O. europaea* leaves contained considerable amounts of flavonoids (Ficarra *et al.*, 1991; De Laurentis *et al.*, 1997).

According to Qidwai *et al*., (2017), the average phenolic content and flavonoid content of olive leaf extracts, measured in milligrams, are 16.9–25.6 mg and 9.5–24.1 mg, respectively. The findings showed that compared to water extract, ethanolic, methanolic, and acetone extracts had the highest phenolic and flavonoid concentration. Their findings revealed a statistically significant link between the analysis of phytoconstituents and leaf extracts (of all the solvents).

5.2. Secoiridoid glycosides

Secoiridoids such oleoside, ligstroside, I methyloleuropein, and oleuropein are the fundamental elements of olive leaves (Servili *et al.*, 2009). As the precursors of different indole alkaloids, sescoiridoids are chemical components of leaves that are glycosidically bonded and generated by terpene secondary metabolisms. The majority of secoiridoids are produced from a class of glucoside oleosides known for having both glucoside and elenolic acid residues.One of the secoiridoids, oleeuropein (Oleeuropein 1), is a fundamental phenolic molecule present in olive

leaves and is responsible for the distinctively bitter flavor of several olive cultivars (Soler-Rivas *et al.,* 2000).

The oleosidic skeleton shared by the secoiridoid glucosides of the Oleaceae family, primarily in its aglycone form, renders the sugar moiety of oleeuropein, an ester of 2-(3,4-dihydroxyphenyl) ethanol (hydroxytyrosol), insoluble in oil. (Rivas and Soler, 2000).

Oleuropein is the main component of the olive plant among the several components that have already been found. From a quantitative and historical perspective, this is the most significant element of the glucosidic portion of *O.europaea*. Actually, the oleuropein is the world's first isolated secoiridoid. Both an orhto-diphenolic and a mono-terpenic unit are found in the oleuropein molecule (Bianco and Ramunno, 2006). In the 1950s, oleuropein was isolated by Panizzi *et al.* (1960). After figuring out how it was made, they concluded that this component was among the most significant ones in charge of giving olive plant fruits and leaves its bitter flavor. It was the active ingredient in the olive extracts that gave them their well-known hypotensive effect. Recently the accurate quantitative determination of oleuropein content in olive and olive oil was proposed by Sindona *et al.,* (2005).

The methanolic extract of *O. europaea's* boron-deficient leaves, peel, pulp, seeds, and wood has been shown to contain oleeuropein (Soler-Rivas *et al.,* 2000; Pérez-Bonilla *et al.,* 2006; Ryan *et al.,* 1999).

The primary active ingredient of olive leaf extract, a naturally occurring part of the secoiridoid family. Oleuropein has been demonstrated in numerous studies to have a broad spectrum of pharmacologic and health-promoting qualities, including immunostimulant, antioxidant, anti-inflammatory, spasmolytic, cardioprotective, hypotensive, and anti-arrhythmic actions (Karakaya *et al.,* 2015). (Hassen and others, 2015).

Numerous characteristics of oleuropein have been attributed to its antioxidant capabilities. Oleuropein can hydrolyze to provide glucose, hydroxytyrosol, tyrosol, and elenolic acid. Olive leaf contains oleeuropein and hydrolysis products, both of which have significant biological properties. According to Hasen *et al*. (2015), hydroxytyrosol is thought to be primarily connected with the health advantages of olive products.

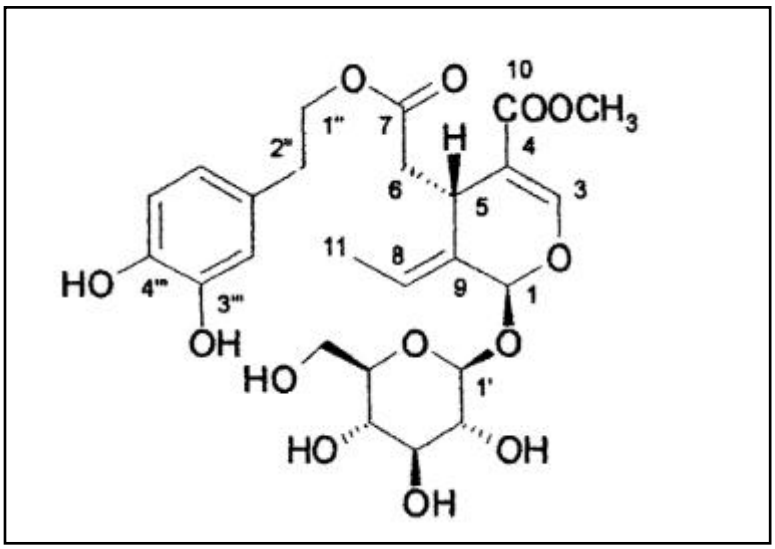

Figure(2): Chemical structure of oleuropein **(**Bianco and Ramunno, 2006).

5.3. Lipids

From the fruits of *O. europaea,* triacylglycerols, galactolipids, and fatty acids were extracted. The separation of a diacylglycerol with an oleic and an elenoic acid remaining from olive pulp (Hashmi *et al.*, 2015).

Fatty acids existing in olive oil include palmitic (C_{16}:0), palmitoleic (C_{16}:1), stearic (C_{18}:0), oleic (C_{18}:1), linoleic (C_{18}:2), and linolenic (C_{18}:3). Myristic (C_{14}:0), margaric (C_{17}:0) and gadoleic (C_{20}:1) acids are found in trace amount . Also traces of 11-*cis*-vaccenic and eicosenoic acids have been detected using C-13 Nuclear Magnetic Resonance spectroscopic method (Boskou *et al.*, 2006).

5.4. Triterpenoid

Isolation from the ethyl acetate soluble fraction of *O. europaea* leaves yielded various triterpenoids, including urs-2β,3β-dihydroxy-12-en-28-oic acid, β-amyrin, oleanolic acid, and erythrodiol. Hashmi *et al.*, (2015) extracted other triterpene acids from the leaves, including ursolic acid, betulinic acid, uvaol, and remnant of maslinic acid..

6. Biological activities

Studies on epidemiology conducted in the Mediterranean area have confirmed the positive health effects of a diet high in fruits, vegetables, legumes, and grains. The most significant of these are olives, which are abundant in vitamins, polyphenols, and flavonoids that are antioxidants and help prevent disease**.**

6.1. Skin care

The study found that olive leaf extract, specifically oleuropein, prevented skin thickness increases caused by radiation exposure. Additionally, it suppressed increases in the number of 8-hydroxy-2'-deoxyguanosine-positive cells, melanin granule area, and matrix metalloproteinase13 (MMP-13) production.

This finding revealed that *O. europaea* extract may be crucial in reducing radiation-induced skin aging, early wrinkling, pigmentation, and thickness (Azhar *et al.*, 2011).

6.2. Antimicrobial Activity

Additionally, phenolic compounds found in *Olea europaea* leaves were assessed against a wide range of microorganisms that have been linked to respiratory and intestinal tract infections in humans, including fungi, *Cryptococcus neoformans,* and *Candida albicans*, as well as Gram positive and Gram negative bacteria, including *Escherichia coli, Pseudomonas aeruginosa*, and *Bacillus cereus*. According to Pereira *et al.* (2007), the results demonstrated an uncommon combination of antibacterial and antifungal action at low dosages against the mentione.

d species, indicating that they may have use in nutraceuticals. A study was done to evaluate the antifungal activity of several aliphatic aldehydes from O. europaea fruit (hexanal, nonanal, (E)-2-hexenal, (E)-2-heptenal, (E)-2-octenal, and (E)-2-nonenal) against different strains of *Microsporum canis, Candida spp*., and Trichophyton mentagrophytes. The virulence factor elastase, which is crucial for the dermatophytes' colonization, was examined for its capacity to be inhibited by these composites. With the exception of *Candida spp*., all examined strains were inhibited by the aldehydes, which exhibited a broad spectrum effect. The elastase activity was reduced by (E)-2-nonenal and (E)-2-octenal in a dose-dependent manner (Battinelli *et al*., 2006).

Olea europaea leaf extract exhibited antibacterial efficacy against *Helicobacter pylori, Campylobacter jejuni,* and *Staphylococcus aureus* (including meticillin-resistant *S. aureus*) (Sudjana *et al.,* 2009). *O. europaea* was identified as a possible source of promising antimicrobial agents for the treatment of intestinal or respiratory tract infections in the body after it demonstrated antimicrobial activity against *Salmonella typhi*, *Haemophilus influenzae, Vibrio parahaemolyticus, Moraxella catarrhalis, and Staphylococcus aureus* (Bisignano *et al.,* 1999).

Certain bacteria, including *Klebsiella peneumoniae, Escherichia coli, and Bacillus cereus*, can also be inhibited from developing in vitro by oleeuropein, vanillic, and p-coumaric acids (Aziz et al., 1998).

and aflatoxin formation can be significantly decreased in the presence of 6 mg/mL oleuropein (Gourama and Bullerman, 1987).

Research is still ongoing to determine whether oleuropein has antibacterial properties in the human body through in vivo tests (Soler-Rivas *et al.,* 2000).

Olive leaves are resistant to insect and microbiological damage. According to research conducted in vitro, the leaves are a potent antibacterial agent that can combat a wide range of infections (Ben Salem *et al.*, 2014).

6.3. Anticancer Activity

It has been demonstrated that oleeuropein's anti-cancer action inhibits the migration and proliferation of several high-grade human cancer cell lines in a concentration-dependent way (Carrera-González and associates, 2013).

It has a protective effect against the oxidation of low-density lipoprotein, as demonstrated by the estimate of the decreased production of thiobarbituric acid-reactive substances (TBARS, which are naturally occurring in organic specimens and include lipid hydroperoxides and aldehydes that increase in dose in response to oxidative stress), malondialdehyde (a composite that results from the breakdown of lipid peroxides composed of polyunsaturated fatty acid), and 4-hydroxynonenal (4-HNE), which are by-products of lipid peroxides (Armstrong and Browne, 1994) (Visioli *et al.*, 1995).

To elucidate the underlying mechanisms of action, oleeuropein's activity on human colon adenocarcinoma (HT-29) cells has been assessed in relation to its hydrolysis product, hydroxytyrosol. The assay for sulforhodamine B (SRB) was employed to identify cell proliferation, whereas Western blot and flow cytometry were utilized to evaluate apoptosis and modifications in HIF-1α and p53 regulation, respectively. The results of cell growth inhibition showed that hydroxytyrosol was more active than oleuropein, while oleuropein demonstrated a significant rise in the presence of an apoptotic population. The findings showed that oleuropein stimulates the p53 pathway, which modifies the HIF-1α response to hypoxia and inhibits the development of HT-29 cells by inducing apoptosis (Cárdeno *et al*., 2013).

6.4. Antidiabetic and antihyperlipedemic activity

According to Azhar *et al.* (2011), the olive leaf has antihypertensive and cholesterol-lowering properties in humans.

For a period of six weeks, rabbits placed on a control, hyperlipid, or hyperlipid diet supplemented with *O. europaea* enhanced with hydroxytyrosol demonstrated the anti-atherosclerotic effect of *O. europaea.* Compared to the rabbits in the plant extract group, the rabbits in the high-lipid diet group exhibited greater levels of triglycerides, cholesterol, and LDL as well as a thick layer of lipid deposit in the aortic intima. These findings confirmed the anti-artherosclerotic properties of olive leaf, which are most likely connected to the reduction of inflammation (Poudyal *et al.*, 2010).

Good antioxidants may be used to treat antidiabetic patients, according to Al-Azzawie and Alhamdani (2006), since oxidative stress reduction lowers blood glucose levels. To reduce

oxidative stress, they administered oleuropein, a potent antioxidant found in abundance in *O. europaea* fruit and leaves, to hypoglycemia alloxan-diabetic rabbits. Oleuropein (20 mg/kg body weight) was administered to the diabetic rabbits for a maximum of 16 weeks. Following therapy, it was found that the majority of antioxidants and blood glucose levels had returned to levels that were comparable to those of the rabbits in the normal control group. The results of the investigation demonstrated oleuropein's antihyperglycemic and antioxidant properties.

The effects of the leaf extract on normal and diabetic rats were compared in a study. The mice were given injections of streptozotocin to cause diabetes. The extracts were given orally to the rats at concentrations of 100, 250, and 500 mg/Kg of body weight, whilst Glibenclamide, the reference medication, was given for two weeks at a dose of 600 µg/Kg. The extract had a stronger antidiabetic impact than Glibenclamide, the medication of reference. More intriguingly, *O. europaea* raised serum insulin levels in the diabetic group and not in the normal rat population, in addition to reducing serum glucose, total urea, creatinine, uric acid, cholesterol, and triglycerides. According to the study, olive leaf extract has potential application as an anti-diabetic medication (Eidi *et al.*, 2009).

Two potential tools have been proposed to explain the hypoglycemic action of oleuropein: enhanced peripheral glucose absorption and enhanced glucose-induced insulin release. It has been discovered that oleuropein speeds up the body's absorption of glucose, resulting in lower plasma glucose levels (Ben Salem *et al.*, 2014).

Oleuropein, the main secoiridoid glycoside found in all of *O. europaea's* components, was thought to be the only factor responsible for the plant's antidiabetic properties. The G-protein coupled receptor TGR5, which is the first cell surface receptor activated by bile acids, was found to be an agonist by Sato et al. When given to mice fed a high-fat diet, oleanolic acid significantly reduced insulin and serum glucose levels and improved glucose tolerance. Based on their findings, they proposed that the antidiabetic properties of olive leaves were caused by both oleanolic acid and oleeuropein (Sato *et al.*,2007) .

6.5. Antihypertensive Activity

In rats made hypertensive by daily oral administration of dosages of L-NAME (NG-nitro-L-arginine methyl ester) at 50 mg/kg for at least one month, the olive leaf extract demonstrated blood pressure reducing action (Khayyal *et al.*, 2002).

It has been discovered that the unripe olive fruit extract possesses Ca^{+2} channel blocking action, which is thought to be the reason for its efficacy in treating cardiovascular conditions like hypertension (Gilani *et al.*, 2005).

Preparations of *O.europaea* have been widely used in folk medicine as a diuretic, hypotensive, emollient, and treatment for bladder and urinary infections throughout the European

Mediterranean region, the Arabian Peninsula, India, and other tropical and subtropical areas. (Samova *et al.,* 2003) .

Heart disease is caused by hypertension, which also, if left untreated, can lead to peripheral arterial disease, chronic renal disease, and artery stroke. It has been shown that a number of natural products work well to lower hypertension. Three triterpenoids—ursolic acid, uvaol, and oleanolic acid—isolated from *Olea europaea* leaves were investigated for their cardiotonic effects. Because of the notable concentration-response vasodepressor effects of oleanolic acid and uvaol, olive oil was suggested as a cheap and natural way to treat hypertension (Samova *et al.,* 2004).

6.6. Antioxydant activity

It is commonly acknowledged that the olive tree, through its fruits, leaves, and oil, has the highest antioxidant activity among all natural antioxidants (Servili *et al.,* 1999). It is commonly recognized that the presence of several significant antioxidant and phenolic components to prevent oxidative damage accounts for the olive tree's product extract activity in the medical and food industries (Lins *et al.,*2018).

It has long been known that the olive tree contains chemicals linked to the prevention of certain diseases, including caffeic acid, ligstroside, and antioxidants including tyrosol, hydroxytyrosol, and oleuropein (Castellano *et al.,* 2015) (Servili *et al.,* 2009) .

In the past, oleuropein was shown to have cardioprotective, lipid-regulating, and antidiabetic properties, especially in animal and cell culture models (Khan *et al.,* 2007) (Bali *et al.,* 2014) (Al-Azzawie and Alhamdani, 2006).

In living things, lipid peroxidation is linked to aging, membrane damage, heart disease, stroke, and cancer. The use of synthetic antioxidants could halt this oxidative process, but it is now known that natural antioxidants are safer than synthetic ones (Mancini Filho *et al.,* 1998).

6.6. Thyroid activities

After giving rats an aqueous extract of olive leaves for two weeks, the rats' T_3 levels rose and their circulating levels of thyroid stimulating hormone decreased. This may have happened through a feedback mechanism, but generally speaking, the extract stimulates the thyroid without affecting the pituitary (Al-Qarawi, *et al.,* 2002) .

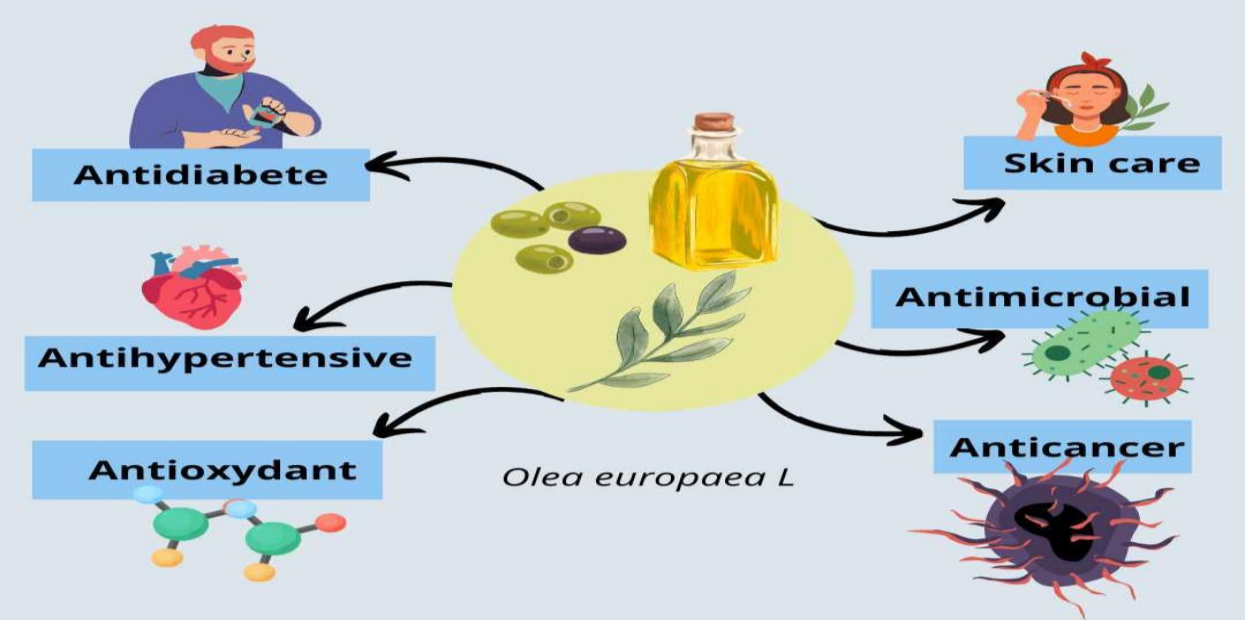

Figure(3): domain applications of *O. europaea*.

CHAPTER II

Nanoparticles

1. Nanotechnology

Nanoparticles are minuscule particles of metals and metal alloys that typically have a size range of 5 to 100 nanometers (nm) (Hussain *et al.*, 2016) .

NPs come in a variety of sizes, forms, and configurations. They may have unusual shapes or be spherical, cylindrical, conical, tubular, hollow core, spiral, etc (Ealia and Saravanakumar, 2017).

The surface area of these metals at the nanoscale is significantly higher than that of their standard sized equivalents. Moreover, they have distinct chemical and physical characteristics because of their tiny size, surface and contact effects, and quantum effects. Numerous kinds of nanoscale metals have a wide range of uses in biology, medicine, and engineering (Zhao *et al.*, 2016).

NPs have greater structures than their counterparts despite their modest size. Their unique characteristic makes them potentially useful in a variety of sectors, including biosensors, nanomedicine, and bionanotechnology (Ashe, 2011).

The size, content, crystallinity, and shape of metal nanoparticles, such as zinc oxide, TiO_2, and silver, are the primary characteristics that define their intrinsic qualities. Their mechanical, electrical, chemical, structural, optical, and morphological qualities can all be altered by shrinking them to the nanoscale. Because of these altered characteristics, the nanoparticles can interact with cell biomolecules in a novel way, which makes it easier for them to physically get within cellular structures (Rasmussen *et al.*, 2010) .

High surface reactivity is a result of nanostructured materials having a higher fraction of atoms at their surface. Consequently, nanomaterials have recently gained a great deal of significance in both bionanotechnology and the fundamental and applied sciences.

2. Synthesis of nanoparticles

The creation of nanoparticles can be approached through three primary methods: chemical, biological, and physical approaches. The chemical and biological approaches together are referred to as the bottom-up strategy, while the physical approach is also known as the top-down approach. Another name for the biological approach is "green systems of NPs".

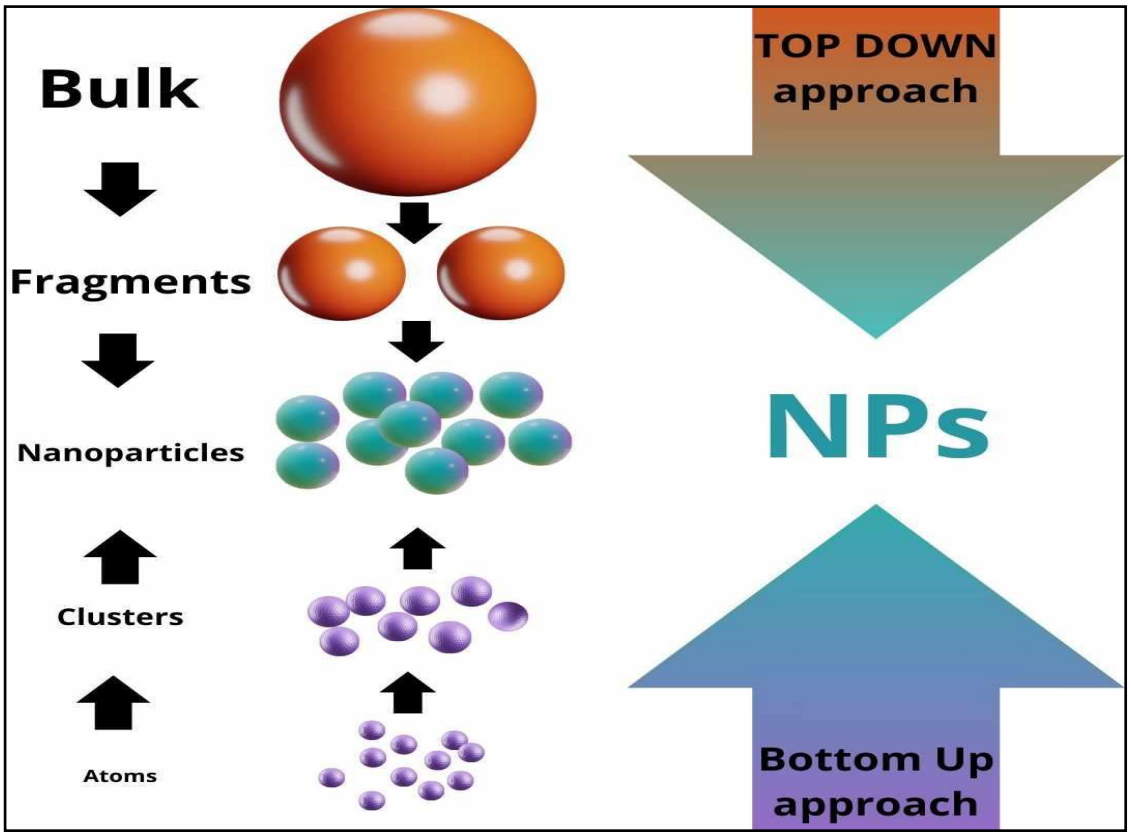

Figure (4): Top-down and bottom-up approaches to realizing nanoparticles.

2.1. Bottom-up method

Bottom-up or constructive method is the build-up of material from atom to clusters to nanoparticles.

2.1.1. Sol-gel

The sol : a colloidal solution of solids suspended in a liquid phase.

The gel : a solid macromolecule submerged in a solvent.

Because it is the easiest way to use and can synthesize the majority of nanoparticles, the most popular bottom-up strategy is this one. In this wet chemical process, a chemical solution serves as a precursor for an integrated system of discrete particles. Metal oxides and chlorides are frequently used as precursors in the sol-gel process (Anu Mary Ealia and Saravanakumar, 2017).

Following the distribution of the precursor in a host liquid through shaking, swirling, or sonication, a liquid and a solid phase make up the resulting system. Using a variety of techniques, including filtration, sedimentation, and centrifugation, a phase separation is

performed to recover the nanoparticles, and dehydration is used to eliminate any remaining moisture (Mann *et al.*, 1997) .

2.1.2. Coprecipitation

It is a wet chemical method that uses a solvent displacement technique. Solvents include acetone, ethanol, hexane, and non-solvent polymers. Phases of polymers might be natural or manufactured. The polymer-solvent quickly diffuses into the non-solvent phase of the polymer domino effect by mixing the polymer solution. The ramifications of interfacial stress at two stages in the creation of nanoparticles (Das and Srivasatava, 2016).

One of the key advantages of this technology is its inherent capacity to generate large amounts of water-soluble nanoparticles via a simple procedure. Several commercial iron oxide nanoparticle-based magnetic resonance imaging contrast agents, such as Combidex, Feridex, and Reservist, are made using this process (Baig *et al.*, 2021) .

2.1.3. Chemical vapour deposition

During CVD, vapor-phase precursors are used in a chemical process to produce a thin coating on the substrate surface (Dikusar *et al.*, 2009).

If precursors have a long shelf life, good chemical purity, strong evaporation stability, low cost, and no harmful properties, they are considered suitable for CVD. Furthermore, no pollutants should be left behind after it breaks down. Chemical vapour deposition (variations) include vapor phase epitaxy, atomic layer epitaxy, metal-organic CVD, and plasma-enhanced CVD. Benefits of this approach include the production of extremely pure, uniform, robust, and stiff nanoparticles (Ago, 2015) .

Nanoparticles produced by CVD are extremely pure, consistent, robust, and hard. The need for specialized equipment and the relatively safe gaseous byproducts are the drawbacks of CVD (Anu Mary Ealia and Saravanakumar,2017).

2.1.4. Pyrolysis

The most often utilized method in industries for producing nanoparticles on a big scale is pyrolysis. It entails setting a predecessor on fire. The precursor is injected into the furnace at high pressure through a tiny hole where it burns and can be either liquid or vapor (Kammler *et al.,* 2001).

The nanoparticles are then recovered by air classifying the combustion or byproduct gases. Certain furnaces generate high temperatures that facilitate easy evaporation by using lasers and plasma in place of flames. This technique has the advantages of being straightforward, economical, effective, continuous, and yield-maximizing (Amato *et al.,* 2013).

Hydrothermal synthesis often occurs at temperatures ranging from room temperature to extremely high temperatures. When comparing this method to biological and physical methods, there are several advantages (Patil *et al.,* 2021) .

2.1.5. Biosynthesis

The development of clean, nontoxic, and environmentally acceptable "green chemistry" processes—which can involve microorganisms like fungi, bacteria, and even plants—would be beneficial for the synthesis of nanoparticles. Consequently, it is recognized that both unicellular and multicellular organisms can create inorganic minerals extracellularly or intracellularly (Prashant Mohanpuria *et al.,* 2008) .

In theory, both microbes and plants use the same process to synthesize nanoparticles. Using a reducing agent, metal salts made up of metal ions are first reduced to atoms. After that, the acquired atoms nucleate in tiny clusters that eventually form particles. According to Shanker *et al.,* (2003), secondary metabolites were found in the water-soluble fractions of geranium leaves, and it was postulated that terpenoids helped reduce silver ions and oxidized them to carbonyl groups. Characterization examination of the study suggested a protein implicated in the surface capping of gold nanoparticles generated using geranium leaf extract and the ester C=O group of chlorophyll functioning as a reducing mediator (Shankar *et al.,*2003).

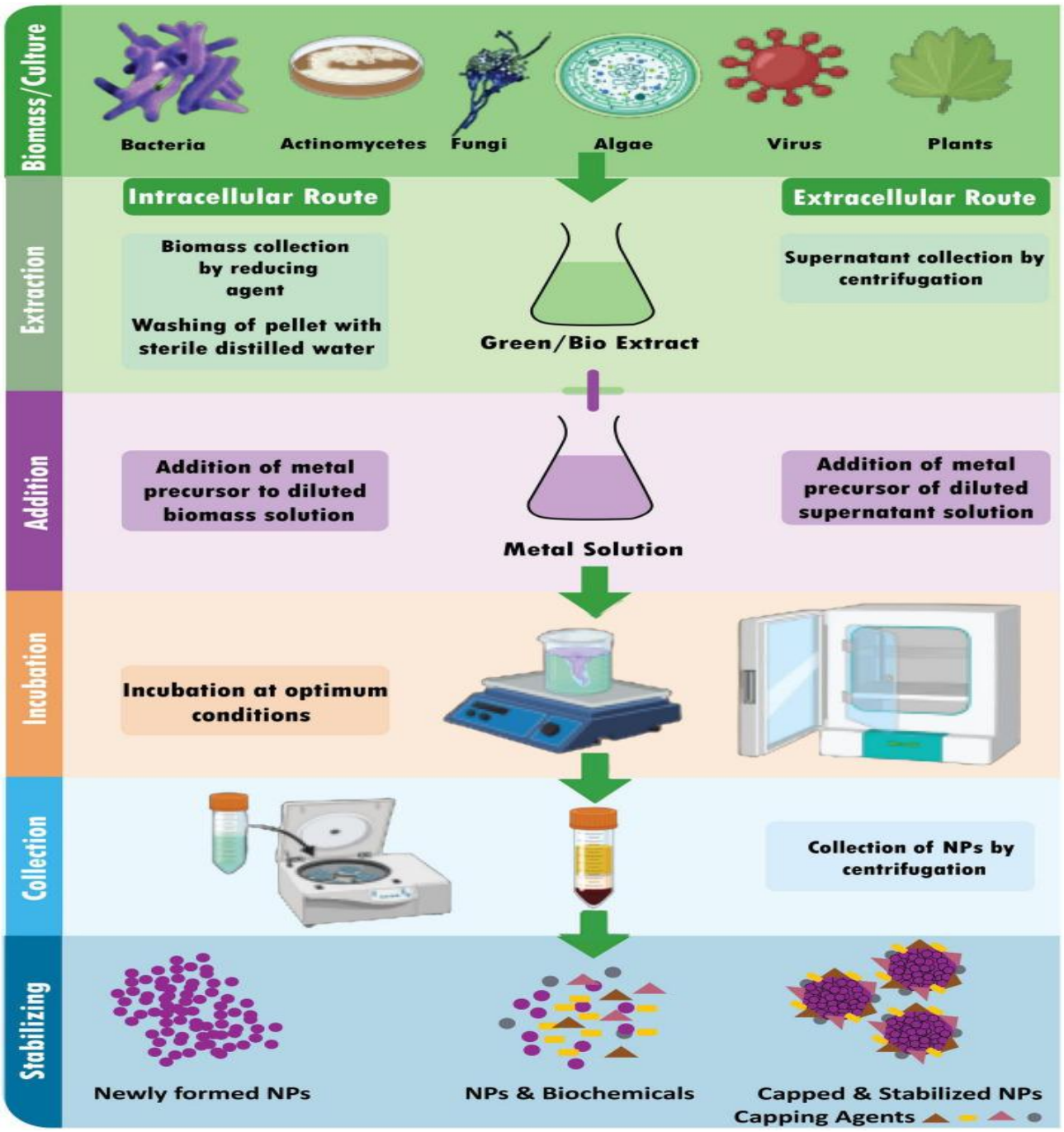

Figure(5): Schematic diagram for biosynthesis of NPs (Altammar, 2023).

2.2. Top-down method

Top-down or destructive process is the reduction of a bulk material to nanometric scale particles. It is physical approach.

2.2.1. Mechanical milling

A straightforward technique for creating nanostructures from bulk materials is mechanical milling. It is a useful procedure that yields blends of several phases and facilitates the creation

of nanocomposites. Aluminum alloys enhanced by oxide and carbide, wear-resistant spray coatings, aluminum, nickel, magnesium, and copper-based nanoalloys, and several other nanocomposite materials are all produced by mechanical milling (Prasad Yadav *et al.,* 2012) .

Ball-milled carbon nanomaterials are thought to be a novel class of nanomaterial that offers the potential to meet the needs of energy conversion, energy storage, and environmental remediation (Lyu *et al.,* 2017) .

2.2.2. Nanolithography

The construction of nanometric scale structures with at least one dimension in the nano-size range is the subject of the research of nanolithography. Numerous techniques exist for nanolithography, such as optical, multiphoton, electron-beam, and scanning probe lithography (Pimpin and Srituravanich, 2012) .

The method of printing a necessary shape or structure on a light-sensitive substance by selectively removing material to get the desired shape and structure is known as lithography. The ability to create clusters with the appropriate size and shape from a single nanoparticle is one of nanolithography's primary benefits. The drawbacks include the need for sophisticated equipment and the corresponding expense (Hulteen *et al.,* 1999) .

2.2.3. Sputtering

Sputtering is typically done in an evacuated chamber that has been supplied with sputtering gas. Gas ions are created when free electrons clash with the gas at a high voltage applied to the cathode target. Positively charged ions rapidly speed in the electric field in the direction of the cathode target, which they repeatedly strike, ejecting atoms from the target's surface (Muñoz-García *et al.,* 2009) .

On SiO2 and carbon paper substrates, WSe2-layered nanofilms are created via magnetron sputtering (Nam *et al.,* 2020) .

Sputtering is a remarkable technology because it produces nanomaterials with a composition that is identical to the target material but with fewer imperfections, and it is less expensive than electron beam lithography (Nie *et al.,* 2009) .

2.2.4. Sonication

Sonication is the most important stage in the production of nanofluids. Following magnetic stirring of the mixture in a magnetic stirrer, sonication takes place in a mechanical homogenizer, ultrasonic vibrator, and ultrasonication path. When compared to ultrasonic cleaning baths for nanoparticle applications, sonicators are notably more powerful and effective, and they have become the industry standard for sonicating probes. When processing nanomaterials (graphene, inks, carbon nanotubes, metal oxides, etc.), probe sonication is a very useful technique (Zheng *et al.,* 2010).

3. Silver nanoparticles

Silver nanoparticles are composed of silver and have a nanoscale range. Because of their small size, high surface area-to-volume ratio, and capacity to absorb and scatter visible and near-infrared light, they have special chemical and physical properties. Silver nanoparticles may exhibit additional anti-microbial properties not exhibited by ionic silver due to their very tiny size and high surface-to-volume ratios, which result in physical and chemical changes in their characterization compared to their bulk counterparts (Shenashen *et al.,* 2014).

One of the most well-liked materials at the moment is silver nanoparticles, which have been studied by nanostructures generated by nanotechnology in recent decades. Particles with high specific surface area, surface energy, surface activity, and catalytic efficacy are known as silver nanoparticles (NPs). Ag's fundamental adaptability allows for a variety of synthesis techniques, including chemical, biological, and physical synthesis techniques, to be used to create AgNPs (Penghu *et al.,*2023).

For their properties, particularly antibacterial properties (Patil *et al.,* 2021) , AgNPs are widely used in a range of applications, like as food packaging, medical products, medical devices and other fields, . With the increasing usage of silver nanoparticles products, also AgNPs can cause a variety of ecological and human health problems (Lee and Jun, 2019) (Kumar *et al.,* 2018)

As a result, we need to learn more about the toxicity of AgNPs and their adverse effects. In the heart, liver, spleen, brain, lungs, kidneys, and other organs, silver nanoparticles (NPs) can pass through biological membranes, enter cells directly, and aggregate, potentially affecting the physiology (Park *et al.,* 2010). Gaining knowledge about how these many elements impact

AgNP toxicity is crucial. Nevertheless, self-factors are sometimes the most disregarded. Furthermore, it's still unclear just how hazardous silver nanoparticles are (Penghui *et al.*, 2023) .

Table (1): Exemples of biosynthesis of silver nanoparticles using plant extract.

Plant extract	**Protocol**	**Study**
Prunus persica extract	10 mL (0.01 M) aqueous solution of silver nitrate + into the extract	(Kumar *et al.*, 2017)
Turmeric extract	2 mL of the powder + 8 mL of 1 mM $AgNO_3$ aqueous solution	(Alsammarraie *et al.*, 2018)
Boerhaavia diffusa	10 mL of the extract + 90 mL (0.1 M) $AgNO_3$ solution	(Kumar *et al.*, 2014)
Punica granatum leaf extract	leaf extract + aqueous solution of $AgNO_3$ (1 mM) (1:10 ratio)	(Saratale *et al*, 2018)
Anthocyanin extracts	$AgNO_3$ (1 mM) + extracts	(Abbasi *et al*, 2019)

4. Zinc oxid nanoparticles

Zinc oxide nanoparticles are zinc particles that range in size from 1 to 100 nm. The wide band gap semiconductor zinc oxide (ZnO) NPs have an energy gap of 3.37 eV at ambient temperature. It has shown to be highly valuable due to its electrical, optoelectronic, catalytic, and photochemical characteristics (Kumar *et al.*, 2013) .

Current research is looking into the use of zinc oxide nanoparticles in both micro and nanoscale formulations as an antibacterial agent. When ZnO particles are reduced to the nanoscale range, they begin to show notable antibacterial activity. The nanosized ZnO can then interact with the bacterial surface and/or the bacterial core where it enters the cell, displaying unique bactericidal mechanisms. These special compounds often have harmful

relationships with bacteria, which have been used for antimicrobial purposes including food production (Seil and Webster, 2012) .

It is noteworthy that a number of studies have revealed ZnO nanoparticles to be non-toxic to human cells. This has made them useful as antibacterial agents, detrimental to microorganisms, and having good biocompatibility with human cells (Colon *et al.*, 2006) (Padmavathy and Vijayaraghavan , 2008).

According to Seil and Webster (2012), nanoparticles' high specific surface area-to-volume percentages and distinctive physicochemical characteristics are usually credited with their diverse antibacterial mechanisms. Though a number of proposed procedures have been proposed and accepted, the exact mechanisms are still up for discussion. The field of nanomaterials and the phenomenon underlying nanostructured materials would benefit from studies on antibacterial nanomaterials, particularly ZnO nanoparticles (Sirelkhatim *et al.*, 2015).

Phytocompounds that are secreted by plants include vitamins, amino acids, alkaloids, terpenoids, polyphenols, and polysaccharides. These compounds can act as stabilizing or capping agents in addition to reducing agents. Additionally, these ingredients turn metal oxides or ions into zero valence metal nanoparticles. Therefore, this green approach of nanoparticle manufacturing does not require the use of capping or stabilizing chemicals.

Table (2): Exemples of biosynthesis of zinc oxide nanoparticles using plant extract.

Plant extract	**Protocol**	**Study**
Trifolium pratense (flower)	30 ml extract + 30 ml 0.5 M ZnO.	(Dobrucka *et al.*, 2016)
Catharanthus roseus (leaf)	The aqueous extract + 0.025 M Zinc acetate + pH 12	(Bhumi and Savithramma, 2014)
Murraya koenigii (seed)	20 mL of extract + 80 mL of zinc nitrate ($ZnNO_2$) + 2.0 M NaOH solution	(Sundaraselvan and Quine ,2017)
Passiflora caerulea	1 mM Zinc acetate	(Santhoshkumar *et al.*, 2017)

(Leaf)	$[Zn(O_2\ CCH_3\ )_2\ (H_2\ O)_2\ ]$ + Then 20 mL of NaOH solution + the Zinc acetate solution +25 mL of extract	
Polygala tenuifolia (root)	dried roots (10 g) + 100 mL H_2O and then filtered + Zinc nitrate (3 g) was then dissolved in the plant extract	(Nagajyothi *et al* ., 2015)

5. Applications of Nanoparticles

Because of their aforementioned special or improved physicochemical characteristics, nanomaterials are used in many different sectors for a variety of purposes. Research and development also has a number of possible uses. Here are a few instances of these applications.

5.1. Biomedical applications

Nanoparticles are made to disrupt the polymer sub-group of the cell membrane in organisms that cause sickness. The antithetical function of nanoparticles efficiently impedes the production of proteins and damages bacterial cell membranes. When compared to low doses, higher doses of silver nanoparticles caused membrane rupture and successfully broke the bacterial cell wall. Ag nanoparticles mediated by *R. apiculate* extract exhibited a slower growth rate than bacterial cells exposed to silver nitrate. This could be due to the interaction between the nanoparticles and enhanced external stimuli, which resulted in induced cell membrane rupture and cell interruption (Antony *et al.*, 2011). Another significant potential use for nanoparticles is targeted medicine delivery. ZnO and Fe_3O_4 nanoparticles were effectively employed for targeted medication delivery and tumor cell destruction.

At the same time, nanoparticles like TiO_2, ZnO, CuO, and $BiVO_4$ are being utilized more frequently in medical devices like catheters due to their antimicrobial and antibacterial properties (Joudeh and Linke, 2022). Gold nanoparticles, for example, effectively absorb light and transform it into localized heat, which can be used for cancer photothermal therapy selectively; heat produced in tumor tissue for the death of cancer cells (Huang *et al.*, 2007).

Furthermore, gold nanoparticles' distinct optical characteristics make them an excellent choice for photodynamic treatment, which uses light to induce a medication to destroy tumor cells. (Elahi *et al*., 2018) .

Effective antiviral compounds found in nanoparticles prevent the virus from spreading before it reaches the host cell. The metallic nanoparticles that are biosynthesized exhibit many coupling behaviors that allow them to interact with viral cell populations and manipulate their structural makeup. The bio-associated NPs have a potent anti-viral and anti-cell-mediated broad-spectrum agent role. Moreover, gold and silver nanoparticles significantly reduce HIV-1 lifespan prior to arrival. Additionally, nanoparticles can combat retroviruses with their antiviral capabilities (Ambrose *et al.*, 2022) .

Gold nanoparticles come in a variety of sizes and shapes, and they have unique properties that make them useful in biomedical applications. These include targeted drug delivery, photothermal therapy, antiviral therapy, anticancer therapy, medical imaging, biomarkers, biosensors, biocatalysis, and intracellular analysis (Chahardoli *et al.*, 2018) .

One of the most serious illnesses in the world is cancer. A great deal of effort has been put into finding new natural treatments that can slow the progression of cancer and even cure it, due to the many side effects of traditional cancer therapy and their unfavorable tolerance performance. The analysis of cancer can benefit greatly from the use of silver nanoparticles. The p53 tumor suppressor was urged to become active by the silver nanoparticles. Furthermore, Ag nanoparticles are used to treat fibroblasts that are not cancerous but have a stronger harmful response to cancer cells (Abdel-Fattah and Ali, 2018).

Furthermore, iron nanoparticles hold greater significance in the field of biomedicine. Iron nanoparticles made from the flat-crown (*Albizia adianthifolia*) leaf extract are used to treat the cancer cell lines MCF-7 and AMJ-13 and induce apoptosis (Sulaiman *et al.*,2018). Additionally, iron nanoparticles made from sugar apple (*Annona squamosa*) leaf extract demonstrated a potent cytotoxic response against the HepG2 cancer cell line. Similarly, iron nanoparticles produced from Babchi (*Psoralea corylifolia*) leaf extract shown anti-cancer efficacy against the Kaki-2 cell line used to study renal carcinoma. The process of creating nanoparticles via biosynthesis proved crucial for treating infections in humans (Vijayaram *et al.*, 2024) .

Moreover, the biosynthesised nanoparticles may serve as an alternative medication for the treatment of hyperglycemia. Daisy and Saipriya (2012) concur that gold nanoparticles have

superior therapeutic action in the management of diabetes. In diabetic mice exposed to AuNPs, the ratio of hepatic enzymes, including alanine movement, serum creatinine, uric acid, and alkaline phosphatase, is substantially reduced. According to Daisy and Saipriya (2012), gold nanoparticles treated to a diabetic mouse showed a decrease in the HbA (glycosylated hemoglobin) scale, which was controlling the standard scale.

According to a study by Swarnalatha *et al.* (2012), in an animal investigation, biomedically produced AgNPs from Sphaeranthus amaranthoides reduced a-amylase and a carbohydrate sugar in diabetes.

On the other hand, utilizing a rat model for an ablation and heat wound, the wound-healing capabilities of silver nanoparticles produced from Aspergillus niger extracellularly were investigated. According to a different study, silver nanoparticles (NPs) possess potent antibacterial qualities and can regulate the amount of cytokines that are produced during wound healing.(Karunakaran *et al.*, 2024).

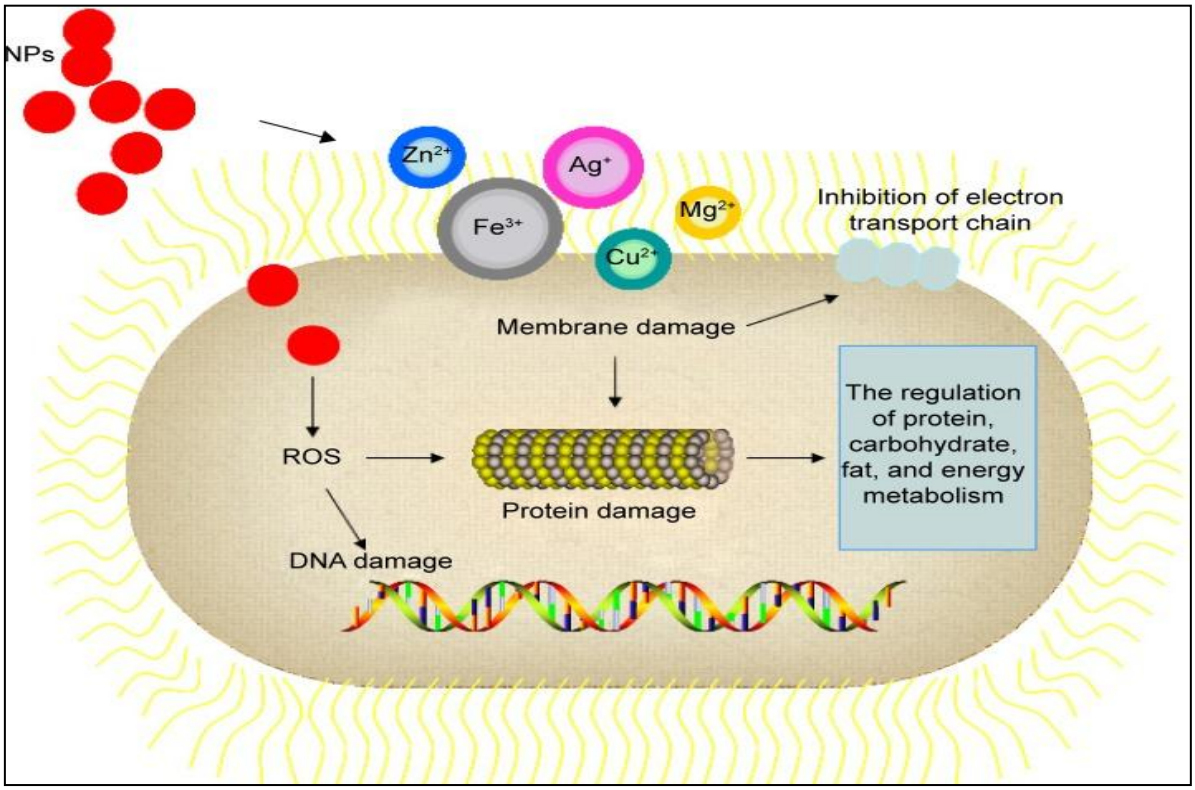

Figure (6): Methods of nanoparticles killing bacteria.

5.2. Applications in agriculture

In agriculture, nanoparticles are mostly employed as nanopesticides and nanofertilizers. Chemical fertilizers perform poorly because of volatilization and leaching. When this happens, planters typically respond by applying excessive amounts of fertilizer, which boosts crop yield but has an adverse effect on the environment (Usman *et al.,* 2020) . Because of this, the scientific community is paying close attention to the development of alternative strategies to guarantee the sustainable use of nutrients. Here, nanotechnology is applied to improve the accessibility of poorly-available nutrients, decrease the loss of mobile nutrients, and provide slow-release fertilizers. Nanomaterials that are nutrients in and of themselves or that serve as carriers or additions for the nutrients (for example, by combining with minerals) are known as nanofertilizers (Kah *et al.,* 2018). Nutrients can also be encapsulated into nanoparticles to create nanofertilizers (DeRosa, 2010) .

Since NPs have a larger surface area, a smaller particle size, and a well-established reactivity, there has been an increase in interest in using them to remediate contaminated soils, mostly through chemical oxidation, sorption, or reduction (Guerra *et al.,* 2018) .

Titanium oxides are another metal-based substance that is regularly researched for environmental cleanup. They have been thoroughly investigated for their demonstrated cheap cost, nontoxicity, semiconducting, electronic, gas sensing, and energy-converting qualities as well as for use as photocatalysts in water remediation applications, waste treatment, and air purification (Li *et al.,* 2008) .

Electronic noses (EN), which are thought of as artificial intelligence systems and the next generation of sensors, have also been developed using nanotechnology. They have been widely used in agriculture to assess plant diseases, insect infestations, soil and water pollution, and industrial processes (Hu *et al.,* 2019). The widespread use of food products and farming practices based on nanoparticles, as well as the less common usage of immobilized nano-sensors, have prompted worries about the health of humans and the environment, even while nanotechnology has revolutionized smart agriculture and decreased associated risks. Nanobio-ecointeractions are complex, making it difficult to measure their activity in soils. Therefore, it is advised to use a holistic approach to comprehend these relationships in the soil, plant, and air cycles, as well as the food chain (Hu *et al* ., 2019) .

Using adsorption, filtration, and oxidation processes, nanomaterials have been effectively used to purify air and water more efficiently than with traditional methods. AgNPs have

broad-spectrum antibacterial activity against a variety of Gram-negative and Gram-positive bacteria, as well as strains of antibiotic-resistant bacteria (Durán *et al.,* 2005) .

In a different investigation, soils were exposed to varying concentrations of ZnO and TiO2 nanoparticulates in microcosms for more than two months. The results demonstrated that the particles had an inhibitory effect on microbial activity by negatively affecting substrate-induced respirations. Meanwhile, because of these nanomaterials that altered enzyme activity, the diversity and composition of the soil bacterial community decrease (Ge *et al.,* 2011) .

5.3. Food industry

Around the world, food safety is becoming a more important concern for public health. Ensuring that food, in its prepared and eaten forms, will not cause harm to the person consuming it is the fundamental goal of food security. Food must be protected against any possibility of physical, chemical, or biological pollutants during manufacture, storage, and distribution. Recent developments in nanotechnology have revolutionized the food sector. This is because nanotechnology has several uses in the treatment, security, and safety of food. It has also made progress in extending its useful life, enhancing its nutritional content, and removing undesired substances from packaging (Singh *et al.,* 2023).

Despite toxicological concerns, nanomaterials have significant uses in a number of food industry-related processes, including food processing, preservation, and packaging. One important and potentially fruitful player in this market is TiO2 NPs. Their ability to combat microbes through photocatalysis makes them a fascinating material for food packaging (Othman *et al.,* 2014) .

In order to pack minced meet at refrigerator temperature (4 °C), for example, polyvinyl chloride doped with Ag NPs was tested; the results demonstrated that silverNPs greatly assisted to slow down bacterial growth, improving the shelf-life of minced meet from week to week (Mahdi *et al.,* 2012) .

In addition to improving product shelf life, texture, and aroma, additional nanoparticles and nanoscale food additives are utilized to influence nutritional content. They can also be used to identify food pathogens, which provide hints about the requirements of food quality (Bott *et al.,* 2014) .

6. Toxicity of nanoparticles

Because of their tiny size, nanoparticles are able to easily enter the human body, pass through a number of biological barriers, and possibly even reach the most sought-after organs. (Pourmand and Abdollahi , 2012) . According to scientific theories, particles smaller than 10 nm behave like gases, can easily permeate human tissues, and may even disrupt normal cell function (Vishwakarma *et al.*, 2010) .

Studies on the bodies of humans and animals have revealed that, in addition to the lungs and gastrointestinal system, nanoparticles are also transported to the liver, kidney, heart, spleen, and brain following inhalation and oral contact. Immune system components are engaged to help the body eliminate these NPs. Since NPs have an estimated half-life of 700 days in human lungs, they constantly endanger the respiratory system. A portion of the NPs accumulate in the liver tissues during metabolism. When compared to larger particles of the same chemical substance, nanomaterials are more harmful to human health, and it is commonly proposed that the toxicity of NPs is inversely related to their size (Bahadar *et al.*, 2016) .

It has been discovered that coming into touch with nanoparticles activates proinflammatory cytokines and chemokines, which in turn attract inflammatory cells and affect immune system homeostasis. This can result in allergy, autoimmune, or neoplastic disorders (Roy *et al.*, 2014).

In experiments, after mice were exposed to silver nanoparticles by subcutaneous injection or inhalation, Ag NPs were found in the lungs, spleen, kidney, liver, and brain (Tang *et al.*, 2009).

Furthermore, these NPs have demonstrated greater toxicity than others in terms of cell survival, reactive oxygen species generation, and lactate dehydrogenase (LDH) leakage (Hussain et al., 2005) . Foldbjerg *et al.*, (2011) have reported a dose-dependent cytotoxicity, and cellular DNA adduct formation.

CHAPTER III

Pesticides

1. Definition

Chemical compounds or biological agents are used as pesticides to draw in, entice, eliminate, or dilute any dangerous creature. They are mostly used in agriculture to shield plants from weeds, insects, and bacterial or fungal infections while they are growing, as well as to keep food safe from rodents, mice, insects, and other biological pollutants while it is being stored (Bolognesi and Merlo, 2011). Certain pesticides, including herbicides, are used to trim trees, bushes, and weeds along roadsides. They are also typically used to remove undesired aquatic vegetation in ponds and lakes. Others are employed to eradicate or halt the development of insects or fungus that damage crops (Gupta, 2011).

According to Calvert *et al*. (2008), agriculture in the United States uses the most pesticides. In Europe, overall pesticide use did not significantly decrease in the WHO European Region between 1990 and 1990, despite global efforts to encourage the sustainable use of pesticides in agriculture and a real decrease in use in individual countries (Robertson *et al.*, 2004) .

Many outdated, non-patented, more hazardous, ecologically persistent, and low-cost chemical types are utilized extensively in underdeveloped countries, leading to serious acute health issues as well as local environmental damage (Ecobichon, 2001). Consequently, the risk of pesticide exposure is higher for agriculturalists and farm workers than for normal non-agricultural workers, who make up the majority of individuals who are exposed to pesticides on a regular basis.

2. Classification

Any component or combination of compounds intended to eliminate, repel, or otherwise control a "pest," such as insects, snails, rodents, fungi, bacteria, or weeds, is referred to as a "pesticide" (Bolognesi and Merlo, 2011).

The "green revolution" led to a sharp rise in the use of pesticides, which greatly boosted output and broadened the variety of pesticide products available. To identify the optimal pesticide for the intended application, it is imperative to create a classification system that would offer critical guidance amidst the multitude of currently available chemicals. When compiling the classification of pesticides it is very hard to meet one distinct principle, so in most cases, combined approaches are preferred.

There are three common faces allowing to which pesticides may be categorized:

- **Assignment** (kind of pest, object) : (Abdollahi *et al.*, 2004)

- Insecticides (e.g, organophosphates, organochlorines, carbamates).

- Fungicides (e.g, dithiocarbamates, captan)

- Herbicides (e.g, paraquat, diquat, 2,4-dichlorophenoxyacetic acid [2,4-d]).

- Rodenticides (e.g, anticoagulants)

- Fumigants (e.g, ethylene dibromide, methyl bromide)

- **Method of pesticide influence** : (Lushchak *et al*., 2018)

- Contact: occasionally working externally to dry the pest's body or release a gas-a thin layer that obstructs regular gas exchange, or in other situations, seeping into the integument and attacking the neurological system, etc.,
- Systemic: pesticides just pass through biological barriers to impact every organ.
-Fumigants: chemical mixtures that impact the bloodstream, living things' neurological systems and enzymes, and sophisticated preparations when inhaled.
- **Chemical composition of the pesticide**

It is the most precise way to distinguish between the various classes and subclasses of compounds with a wide range of structurally varied chemical properties. From this, the most modern pesticides can be divided into the following classes based on their chemical structure: (Franco *et al.,* 2010)

- Organochlorines (e.g., endosulfan, hexachlorobenzene)

- Organophosphates (e.g., diazinon, omethoate, glyphosate)

- Carbamic and thiocarbamide products (e.g., aldicarb, carbofuran, oxamyl, carbaryl)

- Carboxylic acids and their products (e.g., pentanal, butanamide)

- Urea products (e.g., fenuron, metoxuron,..)

- Heterocyclic elements (e.g., benzimidazole, triazole derivatives)

- Hydrocarbons, ketones, aldehydes and their products (e.g., benzene, toluene, cerenox)

- Fluorine-containing elements (e.g., cryolite, acetoprole, dichlofluanid)

- Copper-containing elements (e.g.,, caocobre, macc 80)

- Metal-organic elements (e.g., mancozeb, maneb, zineb, nabam)

- Synthetic pyrethroids and others (e.g., allethrin, \n, fluvalinate)

- Phenol and nitrophenol products (e.g., dinocap, dinoseb)

3. Metribuzin

4-Amino-6-tert-butyl-3-methylthio-1,2,4-triazixin-5(4H)-one, = 4-Amino-6-(t-butyl)-4-methylthio-1,2,4-triazine-5-one

Trade name Metribuzin : Lexone, Sencor, Sencora, Sencoral, Sencorex

Chemical formula : $C_8H_{14}N_4OS$

LD_{50}: (oral): rat (male) 2200 mg/kg, (female) 2345 mg/kg.(Aiach *et al.*, 1992) .

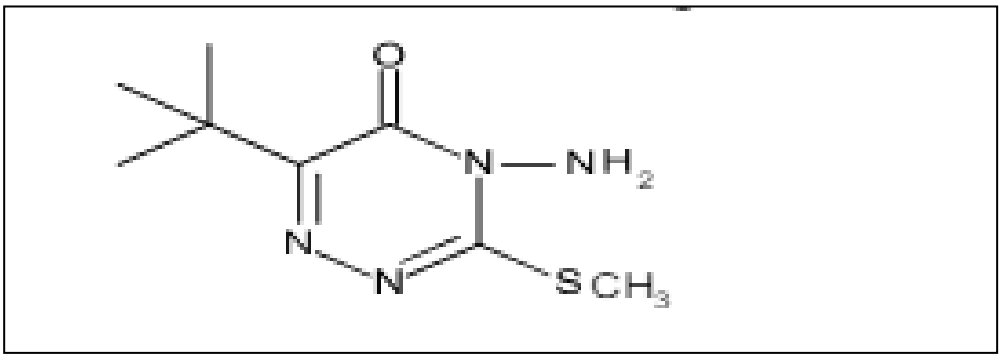

Figure: Chemical structure of metribuzin (Armenda´riz *et al.*, 2014).

Metribuzin is commonly used to selectively control specific broadleaf weeds and grassy weed species on a variety of locations, including vegetable and field crops, turf grasses (recreational areas), and noncrop areas. It was classified as a herbicide in the United States in 1973 (Armenda´riz *et al.*, 2014) .

Metribuzin belongs to the class of herbicides known as substituted as-triazinone. Interference with photosystem II electron transport in plant chloroplasts is the cause of activity (Dodge, 1983). Numerous short- and long-term investigations have examined the metabolism of metribuzin in plants since the early 1970s.(Simoneaux, 2008) .

Metribuzin is a highly effective organic herbicide that is utilized globally and in some nations. This kind of herbicide has been shown to be extremely persistent in soil and dangerous to lipid tissue (Kitous *et al.*, 2016) (Behloul *et al.*, 2017).

Chlorinated hydrocarbons and other common organic herbicides have been mostly replaced by metribuzin. Metribuzin has largely replaced a number of public herbicides, including chlorinated hydrocarbons. Furthermore, metribuzin is a useful organic pesticide that keeps harmful grasses and broadleaf weeds from growing in between different crops. The blockage of electron transfer during photosynthesis determines the manner of action (Saleh *et al.*, 2020).

Metribuzin is a herbicide of the triazinone family that dissolves readily in water (1.05 g/L) but adsorbes only weakly on sandy soils with little organic matter. The range of adsorption coefficients is 0.56 in very sandy loams and 31.7 in soils that contain 60% organic matter (Henriksen *et al.*, 2002) Metribuzin is thought to have a half-life of five to fifty days in soil, making it a short to moderate persistent compound (Huertas-Pérez *et al.*, 2006).

3.1. Exposure

Metribuzin is a pre-emergent and post-emergent herbicide used in farming to control broadleaf and grassy weeds.

Metribuzin is a chemical used in agriculture that may contaminate surface or groundwater if it is released into the environment by spray drift, tile drain effluent, and surface runoff. It is rarely found in sources or drinking water, despite its possible health impacts, and in animal testing, it mostly targets the liver. (Federal Provincial-Territorial Committee on Drinking Water, 2020) .

The people most likely to be exposed to metribuzin are those who work in agriculture. Exposure may also occur to anyone who handle, load, mix, or handle the material before to its application in the field. Additionally, eating vegetables exposes the general public, as may coming into contact with landscaping and attractive plants (Armenda´riz *et al.*, 2014) .

3.2.Kinetics of metribuzin

There are research available that look at the pharmacokinetics of metribuzin in humans, although most of them involve rats; there have also been studies with mice, dogs, and farm animals (Armenda´riz *et al.,* 2014)

3.2.1. Absorption

Metribuzin is absorbed quickly after administration, reaching peak blood and tissue levels in 4 hours, and is nearly entirely absorbed (95% to 100% based on excretion data) within 36 hours. Metribuzin's cutaneous absorption is unlikely to happen, according to a rat research (Bleeke *et al.,* 1985).

3.2.2. Distribution

Following absorption, metribuzin and its metabolites are broadly dispersed, with the thyroid and liver exhibiting the highest amounts, followed by the kidneys and then other tissues (heart, fat, ovaries, brain, muscle, plasma, and testes). Metribuzin was present in thyroid tissue ten times higher than in liver tissue (OEHHA, 2001).

3.2.3. Metabolism

Metribuzin metabolism is broad and happens quickly via a number of pathways (deamination, hydroxylation at the t-butyl side chain, hydrolytic or aminolytic cleavage of the thioalkyl moiety, and conjugation), some of which can act in combination to produce a large number of metabolites in urine, feces, and tissues, according to studies conducted in Wistar rats. Cytochrome P450 might be implicated in the first metabolism, producing reactive intermediates that react with glutathione such as desaminometribuzin, desaminodiketometribuzin (DADK), and diketometribuzin (DK), as well as metribuzin sulfoxide or deamonometribuzin sulfoxide (Bleeke et al., 1985; OEHHA, 2001). Sulfation and glutaronidation are not very important for excretion or metabolism. On the other hand, conjugation with glutathione and subsequent conversion to derivatives of mercapturic acid seem to be important processes in excretion and detoxification. The liver and kidney have the largest quantities of metribuzin and/or its metabolites, respectively. There is proof that metribuzin metabolites can bind to proteins at very high concentrations or in the absence of nonprotein sulfhydrils (Armenda´riz *et al.,* 2014).

The metabolites demethylmetribuzin (DM), tert-butylhydroxy-metribuzin, N-acetylcysteine-metribuzin (N-AC-metribuzin), desaminometribuzin, diketometribuzin, and numerous other unidentified compounds were similar in the urine and feces (OEHHA, 2001)

The liver is the organ in animals that is most frequently involved in the biotransformation of foreign substances because of its role, placement in relation to other organs, and large blood supply. Typically, biotransformation modifies a substance's toxicity so that it is either less or more dangerous to the organism than the original compound (Vander Oost *et al.,* 2003). Numerous xenobiotic metabolizing enzymes are also present in the skin, and some of them are induced, particularly by polycyclic hydrocarbon (Baron *et al.*, 2008).

The kidney is also a target for xenobiotic toxicity due to its function in the body, which is associated with high blood flow and the existence of renal xenobiotic metabolizing systems (Speerschneider and Dekant, 1995). Interestingly, stress tolerance in animals is often linked to their ability to biotransform and remove xenobiotics, with stress-tolerant species showing reduced xenobiotic sensitivity (Banaszkiewicz, 2010) .

3.2.4. Elimination

Additionally, metribuzin or its metabolites are eliminated rather quickly; one to several days after treatment, the majority of the drug can be found in the urine or feces. Wistar rats expelled 0.1% of expired air, 27.3% to 43.4% of urine, and 55.8% to 71.5% of feces (Bleeke *et al.,* 1985) (EFSA, 2010)

4.Toxcicity

Based on the length of exposure to the pesticide and the speed at which toxic symptoms manifest, there are three basic categories of pesticide toxicity in human exposure scenarios. Therefore, there are three types of exposure to the job or environment: acute, sub-chronic, and chronic (Klaassen *et al.*, 2013) .

Pesticides, which act as outward irritants, can cause pesticide poisoning, which damages internal organs or systems. Exposure to pesticides can cause mild to severe symptoms, ranging from skin irritation to headaches, nausea, and disorientation.

Exposure to pesticides can lead to serious side effects like convulsions, comas, and death. The effects vary based on the type of exposure, route, and body system. Some pesticides are reversible, while others may have irreversible consequences. While some poisons are not lethal, their harmful effects can be transient (Damalas and Koutroubas, 2016) .

Table (03): Toxicity categories of contact to a pesticide (Nesheim *et al.*,2014)

Category	Description
Acute toxicity	resulting from an unique exposure occasion (single momentary exposure).
Sub-chronic toxicity	resulting from exposure situations that happen repeatedly over a period of weeks or months .
Chronic toxicity	resulting from exposure to exposure repeatedly over several months or years

5. Pesticides-Induced Oxidative Stress

Pesticides are hazardous substances that are often employed in agriculture and other contexts worldwide, exposing people and animals to ongoing exposure. Numerous pesticides, particularly organophosphorus insecticides (OPI), are known to be neurotoxic, to severely impair mental health, and to induce "cholinergic syndrome." If not, OPI exhibits toxicity, which has been shown to have negative impacts on the body's hematological and metabolic systems (Abderrahim *et al.,* 2020) .

Because the metal ions released during their biotransformation can increase steady-state levels of reactive oxygen species (ROS), stimulate ROS-induced oxidation of lipids and proteins, or inactivate specific enzymes that have neurotoxic effects, many dithiocarbamates (DTC) also cause intraneuronal oxidative stress that results in neuronal damage (Fitsanakis *et al.,* 2002) . Many pesticides interfere with hormone synthesis, release, transport, metabolism, action, or elimination, which results in endocrine disruption (Khan and Law, 2005).

Oxidative stress is associated with an imbalance between the antioxidant defense system and the generation of oxygen free radicals. It has been identified as one of the routes via which exposure to OPI has detrimental effects on health (Mansour and Mossa ,2009). OPI toxicity can cause oxidative stress, which can change the antioxidant system and produce free radicals. Despite the fact that several studies have demonstrated that they can cause a rise in oxidative damage in cells from different organs. (Abdollahi *et al.,* 2004)

Pesticides' high liposolubility and low molecular weight enhance absorption and toxicity. Pesticides containing organophosphate (OP) and carbamate cause acetylcholine buildup by inhibiting carboxyl ester hydrolases, specifically acetylcholinesterase (Cortés-Iza and Rodríguez,2018) . Furthermore, some research suggests that the rise in reactive oxygen

species (ROS) in agricultural workers exposed to OP insecticides and bipyridyl herbicides is related to the suppression of the acetylcholinesterase enzyme. Both a rise in lipid peroxidation and a fall in antioxidant capacity can cause oxidative stress. (Ranjbar *et al.,* 2002) .

Many pesticides have different modes of action of toxicity in brain, many of which are not well-categorized. Because they permanently block acetylcholinesterase, an enzyme that hydrolyzes the neurotransmitter acetylcholine at neuromuscular junctions and brain cholinergic synapses, organophosphorus pesticides are widely recognized to be very neurotoxic (Galloway and Handy, 2003) (Van der Oost *et al.,* 2003)

Certain insecticides are known to induce oxidative stress by promoting the production of ROS. As a result, they may affect the enzymatic systems that scavenge ROS and act as antioxidants. Several contaminants can become dangerous due to pesticides by stimulating lipid peroxidation (Akhgari *et al.,* 2003)

For instance, it has been demonstrated that prolonged exposure to propiconazole causes ROS-promoted stress in a number of rainbow trout tissues, as seen by noticeably increased levels of protein carbonyl groups and lipid peroxides (Li *et al.,* 2010) .

Toxicological research has focused on pesticide-induced oxidative stress as a potential mechanism of harm for the past ten years. The liver is the first organ to undergo biotransformation after being exposed to ingested poisons such as metals, insecticides, etc. As a result, it has been noted that the liver experiences more toxic reactions than other organs, when reactive oxygen species (ROS)-induced oxidative stress has been linked to different stages of the tumor growth process, DNA damage, membrane lipid peroxidation, and mutagenesis in bodies animals (Chenikhar *et al.,* 2018) .

However, the processes causing oxidative stress in response to some pesticides remain poorly understood. The culmination of a series of events leading to an imbalance between pro-oxidant and antioxidant defense mechanisms is pesticide-induced oxidative stress. Pesticide poisoning also causes changes in antioxidant enzymes and the glutathione redox system, among other derangements of specific antioxidant processes in various tissues (Abdollahi *et al.,* 2004) .

Increases in ROS steady-state levels can increase the likelihood that they will interact with DNA and produce genotoxicity, which can result in a variety of mutations, because ROS and DNA interact differentl (Franco *et al.,* 2010).

Numerous environmental pollutants and/or their metabolites have been demonstrated to have harmful consequences, including the induction of oxidative stress. Oxidative stress can arise due to the well-known byproduct of specific metabolic pathways or the autoxidation of specific molecules, reactive oxygen species, whose concentrations can be raised either temporarily or permanently under different circumstances (Lushchak, 2011).

Since ROS may react with important biological macromolecules, their cytotoxic effects are especially intriguing. These reactions typically result in lipid peroxidation, DNA damage, and enzyme inactivation, which can ultimately cause necrosis or apoptosis, which are forms of cell death. Although primarily nonspecific, a number of hematological measures, including hematocrit or hemoglobin, protein or glucose content, may also be sufficiently sensitive indicators of specific types of pollutants to be taken into consideration as possible biomarkers for pesticide toxicity (Nieves-Puigdoller *et al.,* 2007)

Additionally, it can result in immunological abnormalities, neurobehavioral changes, developmental and reproductive toxicity, neurotoxicity, oxidative stress, and histopathologic alterations in both people and animals. (Breslin *et al.,* 1996) Also,if a pesticide has genotoxic effects, it can set off a chain reaction that results in diseases (like cancer) that are caused by DNA damage, structural changes in DNA, and the subsequent expression of mutant gene products. These events can be tracked to determine the toxicity mechanisms involved. Identifying and measuring different events in this sequence can also be used to identify biomarkers in organisms exposed to genotoxic chemicals in the environment

(Van der Oost *et al.,* 2003).

SECOND PART

Experimental Study

CHAPTER I

Material & Methods

1. Materials

1.1. Plant

Fresh olive leaves (Olea europaea L. Var. Chemlali) were harvested straight from the olive tree plantation farms in Nakhla, Algeria's El-Oued region, located at 33°16′38°N 6°57′05°E, in mid-April 2022. The leaves were then sent straight to the laboratory (LBEH). Dr. Chouikh Atef, a professor in the biological sciences department of the faculty of sciences of natural and life from Echahid Hamma Lakhedar University in El-Oued, Algeria, defined the leaves scientifically. The leaves were given a thorough cleaning and then let to air dry. The premium dried leaves were kept until they were required for the extraction processes in a dry plastic container.

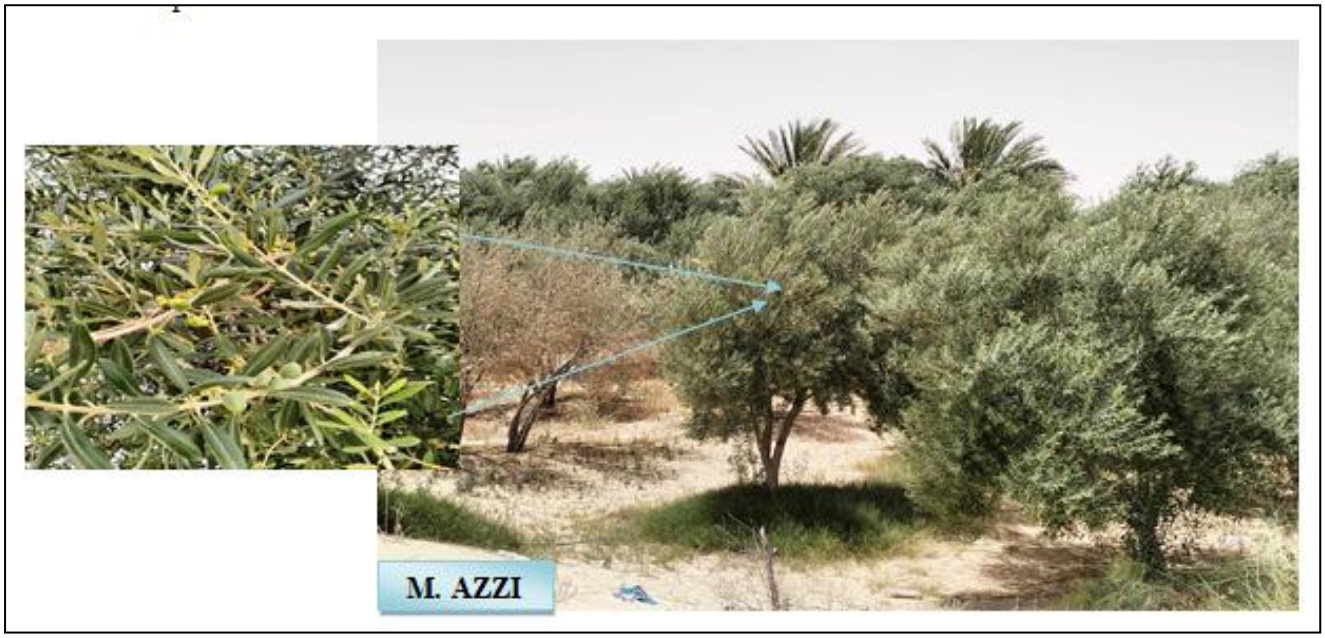

Figure (8) : *Olea* ***europaea*** L. Var. Chemlali (Original photo, 2024**).**

1.2. Animals

For this investigation, 55 adult albino Wistar rats were purchased from the Pasteur Institute in Algiers, Algeria. The Molecular and Cellular Biology Department, Faculty of Natural and Life Sciences, University of El-Oued, Algeria, animal house housed all of the rats. Under identical laboratory circumstances of photoperiod (12 hours of light and 12 hours of darkness), relative humidity of 62±3%, and room temperature of 21±3°C, the rats weighed 222.35± 2.91g. For the course of the trials, tap water and standard rat food were freely available. The local ethical committee's suggested methods were adhered to in the handling and care of the rats during all experimental procedures.

1.3. Bacterial strains

For antibacterial test using the difusion method , nanoparticles were tested for their antibacterial efficacy against 3 bacterial strains obtained from the Pasteur Institute's laboratory in Algeria, including three bacteria (Escherichia coli (ATCC 25922), Staphylococcus aureus (ATCC 25932), and Pseudomonas aeruginosa (ATCC 27853).

Also four bacterial strains were utilized as biological substrates from laboratory of treatement and valorization of hydrolic rejects,center of reaserch and water technology,in Tunisia, for evaluate kinitic antibactrial effect of nanoparticles.

Escherichia coli ATCC25922 (E. coli) and Salmonella typhimurium LSP 14/92 clone DT104 (S. typhimurium), Bacillus cereus (B. cereus) and Methicillin-resistant Staphylococcus aureus (MRSA) ST97-t267-agrI-SCCmecV (S. aureus), used it in this investigation .

1.4. Chemicals and reagents

Silver nitrate ($AgNO_3$,>99.9%), 2,2-diphenyl-1-picrylhydrazyl, free radical (DPPH, 95%), potassium ferricyanide ($K_3Fe(CN)_6$, 98%,), ammonium molybdate tetrahydrate ($(NH_4)_6Mo_7O_{24}.4H_2O$, 98%), sodium phosphate monobasic dehydrate ($NaH_2PO_4.2H_2O$, 98%), ferric chloride (FeCl3, 98%), trichloroacetic acid ($C_2HCl_3O_2$, 99%), ascorbic acid (C6H8O6 99%), sulfuric acid (H_2SO_4, 98%), methanol (CH_3OH, 99%), dimethylsulfoxide (DMSO, C_2H_6SO, 99%), were purchased from Biochem Chemophara, United Kingdom.metribuzine. However, commercial kits procured from Spinreact (Barcelona, Spain) were employed to test biochemical markers.Sigma-Aldrich provided the remaining chemicals, reagents, and organic solvents (USA).

2. Methods

2.1. Phytochemical analysis of *Olea europaea*

2.1.1. Extraction of *Olea europaea* Aqueous extract

The olive leaves (20g) were drieded and powdered and added to 200ml of distilled water. After 24 h at room temperature, the mixture was filtered with filter paper. Finally, the filtrates were evaporated in an oven at 45°C to produce dried residues (active principles), the extract was stored at 4°C in a refrigerator for subsequent experiments.

2.1.2. Phytochemical Screening

Identification of phytochemical compounds including in *O. europaea* aqueous crude extract (polyphenols, flavonoids, alkaloids, terpenoids, saponins, tannins, coumarin, glycosides, ..) carried up using the standard methods (Harborne,1973) (Trease and Evans,1989) (Sofowara,1993) (Matos,1997). (Bekro et al., 2008),

2.1.2.1. Polyphenols

2 mL of the extract received a few drops of a 2 % (w/v) $FeCl_3$ solution. $FeCl_3$ takes on a greenish or blackish-blue coloring when polyphenol derivatives are present.

2.1.2.2. Flavonoids

1 mL of H2SO4, 5 mL of diluted ammonia, and 5 mL of the extract to be analyzed. There are flavonoids present because of the appearance of yellow color.

2.1.2.3. Tannins

In a test tube, we mix 5 mL of the extract with 1 mL of a 2% aqueous ferric chloride solution (FeCl3). Tannin content indicated by greenish or bluish-blackish hue.

2.1.2.4. Alkaloids

To analyze, add 1 mL of extract to each of the two test tubes. After adding a few drops of HCl to acidify the medium, fill the first tube with drops of Mayer's reagent and the second tube with drops of Wagner's reagent. Alkaloids are present when a white or brown precipitate forms, accordingly.

2.1.2.5. Terpenoids

We added 3 mL of strong sulfuric acid, 2 mL of chloroform, and 5 mL of plant extract to a test tube. Terpenoids are responsible for the reddish-brown color.

2.1.2.6 Saponins

The aqueous extract is included in 10 mL of a test tube. The tube was shaken for fifteen seconds, and then it was permitted to stand for an additional fifteen minutes. The presence of saponins was indicated by a continuous foam height of more than 1 cm.

2.1.2.7. Cardiac glycosides

1 mL of the extract was combined with 2 mL of chloroform. Next, cautiously add H2SO4 to the test tube's inner side. An indication of the presence of a glycone portion in a cardiac glycoside is its reddish-brown hue.

2.1.2.8. coumarins

by the addition of a few ml of NaOH .

2.1.2.9.Quinones

One milliliter of crude extract was mixed with diluted NaOH. Quinines are indicated by a blue-green or red coloring.

2.1.2.10. Steroids

Five drops of pure H2SO4 were added to 1 milliliter of the extract. The color reddish brown indicates the presence of steroids.

2.1.3. Quantification of phytochemicals compounds

2.1.3.1. Estimation of total phenolics

Folin-Ciocalteu method (Slinkard and Singleton, 1977) used,to determination of the total amount of phenolics. 1 mL of 10% Folin-Ciocalteu reagent, 0.2mL of the aqueous extract of *O. europaea* was added. After 4 minutes,was added 0.8 mL of sodium carbonate (75 g/L).

At room temperature, after 2 h of incubation, the absorbance was measured at 765 nm. A gallic acid used as the standard for the calibration equation linear, the total phenolic content was expressed in ug equivalent of gallic acid per mg of extract.

2.1.3.2. Estimation of total flavonoids

To ascertain the total flavonoid content of the *O. europaea* extract, the aluminum chloride ($AlCl_3$) colorimetric method was employed (Ahn *et al.*, 2007); 1 mL of the $AlCl_3$ solution is mixed with 1 mL of the sample, the same volume for the standard, and the results are determined using a linear calibration equation with quercetin as the standard. After 30 minutes, the absorbance at 430 nm was measured against the prepared reagent blank. The findings were shown as ug of quercetin for every milligram of extract.

2.1.3.3. Estimation of condensed tannin

The amount of tannin in the *O. europaea* leaf extract was measured using the techniques described by Broadhurst and Jones (1978).

0.5 ml of the sample was well mixed with 3.0 mL of vanillin reagent (4% w/v vanillin in methanol) before 1.5 mL of 8% hydrochloric acid was added. After fifteen minutes, the absorbance of the reaction was measured at 500 nm in respect to water. The reference value of catechin was used to blot the sample amounts and the standard absorbance curve. The results were given as mg of extract divided by ug of catechin.

2.1.4. Qualitative analyze by HPLC

We used Shimadzu Prominence LC-20AL High-Performance Liquid Chromatography (HPLC) to measure the phenolic components in O.europaea leaves. Non-polar aliphatic residues were used in the reverse-phase chromatography investigations, and the mobile phase consisted of gradient elution of acetonitrile and acetic acid (0.1%). outfitted with a Shim-pack VP-ODSC18 analytical column (4,6mm x 250mm, particle size of 5mm) and a Hamilton 25l universal injector. The injection volume of the sample and reference were both 20µL, and the flow rate was 1 mL/min.

The amount of phenolics in O. europaea leaves was measured by utilizing their regression equation to compare the retention periods of the leaves with those of the respective standards, detecting absorbance at 268 nm, and obtaining UV spectra using an SPD-20A UV-vis detector (Shimadzu).

2.2. Green synthesis of nanoparticles

2.2.1. Green synthesis of Silver Nanoparticles

The Ag/Ag_2O NPs were synthesized using a green synthesis Laouini *et al.,* (2021) method with some modifications.

In a 250 mL Erlenmeyer flask, 1 mL of *Olea europaea* leaf extract was combined with 45 mL of 1 mM $AgNO_3$ aqueous solution, and the mixture was shaken for two hours at 150 rpm and 75°C. The first sign that Ag/Ag_2O NPs were being biosynthesised was the reaction mixture's color changing from bright yellow to dark brown.For twenty-four hours, the mixture was let to stand at room temperature. $AgNO_3$ solution and an aqueous extract of *Olea europaea* leaves were used to maintain controls throughout the trial. The mixture was then centrifuged for 10 minutes at 3000 rpm to get rid of any unbound phytocomponents. The Ag/Ag_2O NPs were thoroughly cleaned three times using distilled water to guarantee the elimination of any loose materials.

After 24 hours oven dry at 50 °C, the synthesized Ag/Ag_2O NPs were packed into containers for further characterizations.

2.2.2. . Green synthesis of Zinc oxyd nanoparticles

With minor modifications, zinc oxide nanoparticles (ZnO NPs) were created via a technique that was previously described by Shabnam Fakhari et al (2019). In the environmentally friendly synthesis method, 1 mL of Olea europea aqueous extract was mixed with 45 mL of a 0.5 M Zn(CH3CO2)2 solution. Using a magnet stirrer, this mixture was stirred for two hours at room temperature. The pH of 12 was then gradually reached by adding 0.02 M NaOH. The resultant mixture was continuously stirred at 150 rpm for an hour during the incubation period. The bio-reduced salt became visible as a white precipitate that collected at the flask's bottom. Several redispersions in deionized water were required for purification, and centrifugation was performed three times at 3000 rpm for 30 minutes.

The end product, a white powder, was dried in an oven set at 60°C for the entire night before being stored for later use.

2.2.3 Characterization of nanoparticles

The methods UV-Vis, FT-IR, XRD, SEM, and EDX were used to characterize AgNPs and ZnO NPs

2.2.3.1. UV-visible spectrophotometer and bandgap energy

The optical features and bandgap energy of these nanoparticles were evaluated by recording absorbance spectra using a UV-visible spectrophotometer (Shimadzu UV-2450, USA) in the wavelength range of 200–800 nm for Ag/Ag_2ONPs and ZnO NPs. The energy band gap (Eg) of the nanoparticles was determined using Tauc's equations **(equation 01)**:

$$(\boldsymbol{\alpha h v}) = \boldsymbol{A}\left(\boldsymbol{h v} - \boldsymbol{E_g^{opt}}\right)^{\boldsymbol{n}} \qquad (\mathbf{1})$$

2.2.3.2. Fourier transforms infrared spectroscopy (FTIR)

Fourier Transform Infrared Spectroscopy (FTIR) in diffuse reflection mode, performed with a Thermo scientifc-Nicolet iS5 Attenuated Total Refection, was employed to detect the functional groups present in the nanoparticless .The recorded spectra spanned from 4000 to 400 cm-1, exploiting a KBr pellet approach.

2.2.1.3. X-ray diffraction (XRD)

To assess the crystallinity and grain size of the greensynthesized nanoparticles, powder X-ray diffraction (XRD) analysis was conducted using a copper K-radiation with an X-ray difractometer (Mini Flex 600 Rigaku; λ=1.5406 Å, covering the 2θ range of 25-90By choosing the leading peak with the highest intensity, the Scherrer equation **(equation 02)** was used to calculate the crystallite size.

$$\boldsymbol{D = \frac{K.\lambda}{\beta.\theta}} \qquad (02)$$

Where D represents the size of the crystallite, k denotes the so-called form factor (0.9), $\boldsymbol{\lambda}$ is the wavelength (0.154281nm, CuKα), h stands for the Full Width at Half Maximum (FWHM), and diffraction angle is $\boldsymbol{\theta}$.

2.2.3.4. Scanning electron microscopy (SEM) and Energy dispersive spectroscopy (EDX)

This technique enables the visualization of highly magnified morphological features formed between the atomic envelopes of the substance to be analyzed's constituent elements and the electron beam. Energy dispersive spectroscopy (EDX) with a nominal resolution of 6 nm or less and scanning electron microscopy (SEM) analysis demonstrated with a TESCAN VEGA3 model (USA) at an accelerating voltage of 10 KV were used to analyze the morphology and elemental composition of the synthesized nanoparticles. A temperature-controlled sample holder (20°C to 50°C) is part of the microscope's setup.

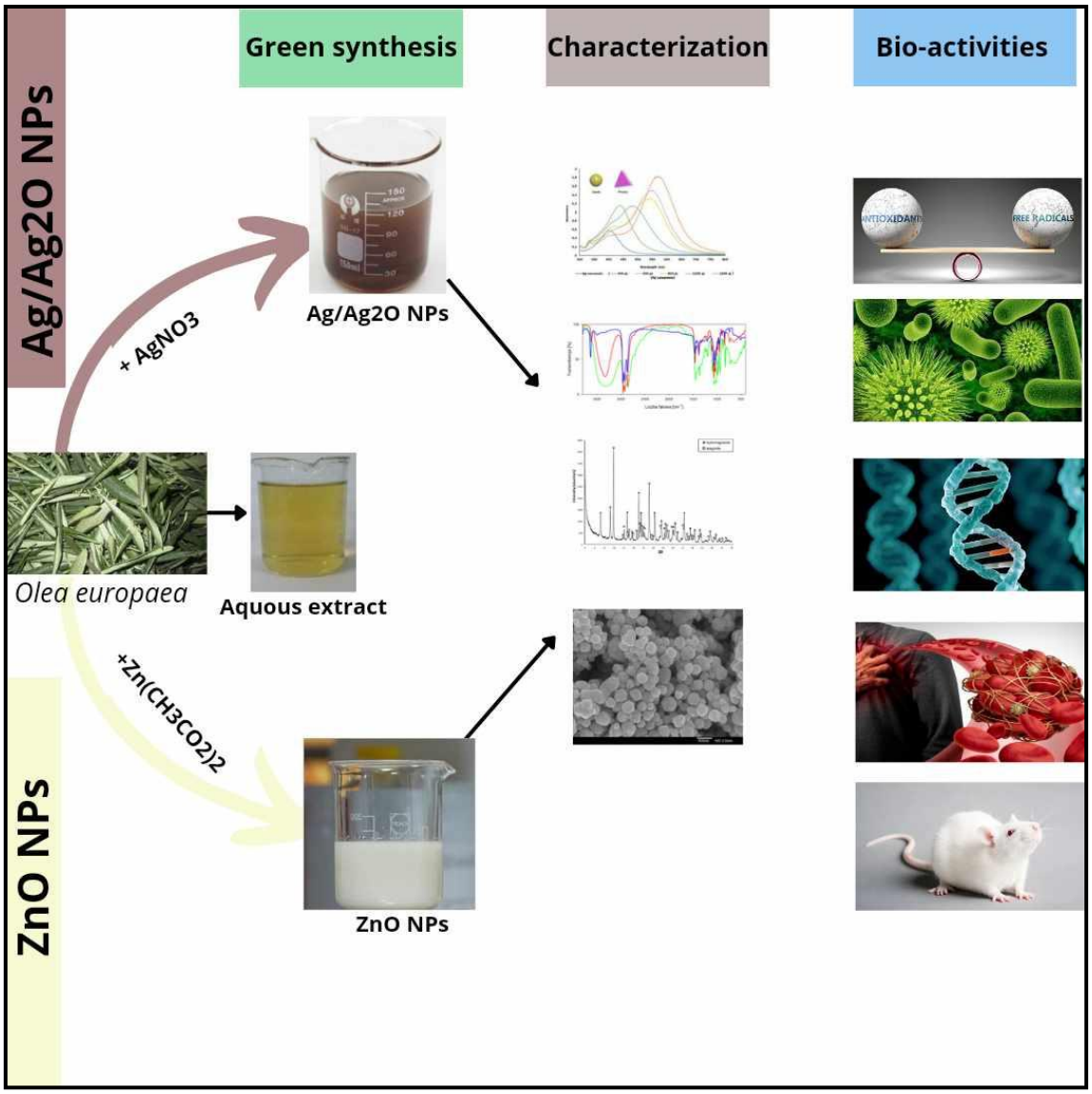

Figure (9) : Green synthesis method of Ag/Ag_2O NPs and ZnO NPs using *O.europaea* aqueous extract

2.3. In Vitro Activity of the aqueous extract of nanoparticles

2.3.1. Antioxidant activity

2.3.1.1. DPPH free-radical scavenging activity

To evaluate the scavenging activity of 2,2-diphenyl-1-picrylhydrazyl (DPPH), we used the procedure of Kumar *et al*., (2014) that the stable free radical DPPH is frequently used to assess the antioxidant component's capacity to scavenge free radicals, it was modified slightly. A volume of *Olea europaea* leaves extract at different concentrations (from 7 to 125 µg/mL) was mixed with 1 mL of methanolic solution of DPPH (0.1 mM; 3.94 mg DPPH was

dissolved in 100 mL methanol) . In a dark room-temperature environment, the mixture was agitated forcefully and left to settle for a 30 min. At 517 nm, the mixture's absorbance was measured using a spectrophotometer. The similar method was used for nanoparticles. Gallic acid was prepared as the positive control. The reaction mixture's lower absorbance showed a higher percentage of scavenging activity. The following **equation (03)** yields the free radical scavenging activity:

equation (03)$DPPH\ scavenging\ effect\ (\%) = ((A_0 - A_1)/A_0) \times 100$

Where: A_o Absorbance of the control

A_1 sample extract's absorbance after 30 minutes.

2.3.1.2. Total antioxidant capacity assay

The phosphomolybdenum method was used to assess the total antioxidant activity of the extract and nanoparticles. Gallic acid was used as a standard, 2 mL of reagent solution containing 0.6 M of sulfuric acid, 4 mM ammonium molybdate, and 28 mM sodium phosphate, mixed with 0.2 mL of samples at a concentration of 20-200 ug/mL. The tubes were incubated for 90 minutes in a hot water bath at 95 °C. The same conditions was applied for the standard. The samples were then air-conditioned at ambient temperature. At 695 nm, the absorbance of the prepared mixture was measured in comparison to a blank solution (0.2 mL of distilled water in place of the extract).

Total antioxidant activity (TAC) was measured in milligrams of GAE per milligrams of samples. (Laouini *et al.*,2021)

2.3.1.3. Ferric reducing antioxidant power assay (FRAP)

The ferric reducing power of the extract of *Olea europaea* leaves and the nanoparticles was mesured using Oraiza, 1986 methods with some modifications , 20–200 µg/mL concentrations of the samples were mixed with 1 mL of both potassium ferricyanide (1%) and phosphate buffer (0.2 M, pH = 6.6). After adding 0.5 mL of trichloroacetic acid (10% w/v). After 20 min at 50 °C incubation , the samples were centrifuged for 10 minutes. An identical amount of supernatant and deionized water, 0.125 mL of ferric chloride (0.1%), were combined. The same process for Ascorbic acid as a positive control was used.

The absorbance was measured using a UV-vis spectrophotometer at 700 nm.

Total antioxidant activity (FRAP) was measured in milligrams of AAE per milligrams of samples. (Laouini *et al.*,2021)

2.3.2. Antibacterial activity assays

2.3.2.1. Antibacterial test using the agar diffusion method

The difusion method was performed using the standard disc difusion test with modification (Bauer *et al.,* 1966) .

The strains were initially cultivated in nutrient agar, which was made with 15 g of agar, 5 g of peptone, 5 g of sodium chloride, 1.5 g of beef extract, and 1.5 g of yeast extract in 1000 ml of distilled water with a pH of 7.0. Streptomycin, a common antibiotic, DMSO as a negative control, and a sterile cork borer (6 mm) for the well were used to culture *Escherichia coli, Staphylococcus aureus, and Pseudomonas aeruginosa*. Zones of inhibition were measured after 24 hours incubation at 37 °C on agar plates. Ag/Ag_2O and ZnO nanoparticle samples were all dissolved in DMSO at concentrations of 50, 100, and 200 ug/ml.

2.3.2.2. Antibacterial kinetic study of nanoparticles

We used four different pathogens to conduct antibacterial activity tests in order to evaluate the antibacterial efficiency of nanoparticles (Ag/Ag_2O and ZnO). The methodology utilized in this study was modified based on the strategy presented by Tsuji et al. (2008) Four bacterial strains from the Center of Research and Water Technology in Tunisia, the Laboratory of Treatment and Valorization of Hydrolic Rejects, were used as biological substrates.

Bacillus cereus and methicillin-resistant *Staphylococcus aureus* are two gram-positive pathogens; *Salmonella typhimurium* and *Escherichia coli* are two gram-negative strains.

These strains were initially resurrected in liquid tryptic soy broth (TSB) medium and cultured at 37°C for 24 hours after being preserved in glycerol at -20°C. To verify bacterial purity, bacterial isolation on tryptic soy agar (TSA) medium was then carried out.

A well-isolated colony was subcultured in the same broth and incubated for 24 hours at 37°C with 150 rpm shaking in order to create a fresh culture. Every 30 minutes, samples were collected to measure the biomass concentration. The growth media exhibited a heterogeneous appearance as a result of all bacterial strains being doped with 200 µg/mL of nanoparticles.

To do an analysis of bacterial growth, the colony forming units per milliliter, or CFU/mL, were measured. CFU is a measure used in microbiology to calculate the amount of live bacteria present in a sample. The young culture was subjected to cascade dilutions, and 100 µL of the suitable dilution was distributed in triplicate on TSA agar medium.
After that, the spread petri dishes were incubated at 37°C, and colonies were counted at various intervals of time (0, 2, 6, 18, 24, 48 hours). The test was conducted three times. The bacterial growth curve was created over time using the CFU/mL values. There was a growth control in the study that had zero nanoparticles (0 ppm). Based on its proven effectiveness against every studied bacterial strain, 200 ppm was chosen.

2.3.3. Antimutagenic activity

Several histidine-dependent *Salmonella* strains were used in the Ames *Salmonella* mutagenicity assay to carry out the anti-mutagenicity test. The mutant strain of *S. typhimurium* TA98 was used in this investigation. To identify different frame shift mutagens, TA98 is employed.The Ames test, often known as the mutagenicity assay, has been amply validated as an appropriate primary test for the identification of putative mutagens and carcinogens (Maron and Ames, 1983)**.**

Following the Ames test,with some modifications. When 1-Nitropurane as mutagen, and Ag/Ag_2O NPs and ZnO Nps dispersed in DMSO.

Plate incorporation method was done for testing antimutagenicity effects of the *O. europeaea* mediatedly synthesized nanoparticles. 0,50,100,150,200,250 ug/ml concentration of Ag/Ag_2O NPs and ZnO NPs were used with the direct acting mutagens, 4-nitropurane for TA98. (Sarac N *et al.*, 2014)

Working cultures of *S. typhimurium* TA98 were prepared by inoculating nutrient broth withthe frozen cultures,followed for 24 hours incubation at 37 ◦C with moderate agitation.

In the *S. typhimurium* antimutagenicity test, 2 ml of the top agar containing 0.5 mM histidine/biotin was mixed with 100 ul for 24 hours bacterial culture, 100 ul mutagen, 100 ul test NPs at various concentrations, and 500 uL phosphate buffer. The blend was transferred onto thin glucose plates. After being incubated at 37 °C for 48 or 72 hours, viable cells and histidine-independent revertant colonies were scored on plates.

The colonies on the plates were counted at the finish of the period. For every dosage in the experiment, three different tubes were used.
- As a direct acting mutagen in the experiments, 4-nitro-purane was employed with the *Salmonella typhimurium* TA 98 strain in the presence of the main antimutagenicity assay, while positive control assays were conducted concurrently.
The antimutegenicity results were computed and expressed as a percentage of inhibition, which measures how well Ag/Ag_2O and ZnO nanoparticles were able to stop the mutagen's action in these tests.

The following formula was used to estimate the anti-mutagenic activity:

Percent Inhibition (P I(%)) = (A − B/A) × 100 **(equation 5)**

where A is the revertants/plate in the positive control, and B is the revertants/plate in the presence of mutagen and NPs.

Antimutagenicity was assessed as follows:

- P I (%) ≥ 40% (strong)

- P I (%) = 25–40% (moderate)

- P I (%) ≤ 25% (low)

2.3.4. Anticoagulante activity:

Using the Raja *et al.* (2015) approach, the anticoagulant activity of the nanoparticles was examined. In the analysis laboratory of El-Madjed in Eloued,Algeria, a surem was drawn into four vials, A, B, and C, without the use of any anticoagulant agents. Vial A was designated as the control negative. Vials B and C immediately received NPs added at a 0.5% (v/v) concentration (ZnO at 50 ppm and Ag/Ag_2O Nps at 150 ppm concentration), while vial D (which had EDTA added) was designated as the control positive. The nanoparticles' anticoagulant action was investigated.

2.4. *In vivo* activity of aqueous extract of nanoparticles

2.4.1. Acute toxicity study

Rat groups were injected with varying quantities of nanoparticles to assess their acute toxicity (Della Rosa and Stannard, 1964).

There were five groups of five Wistar rats (n=5). Ag/Ag2O NPs at doses of 5 mg/kg and 2.5 mg/kg were administered intraperitoneally into two groups. ZnO NPs were injected at doses of 100 and 50 mg/kg in the same manner, and the final group was given simply physiological saline (0.9%) as a solvent. The acute toxicity test of injecting nanoparticles was rigorously assessed using visual observations of mortality. Many bodily changes were noted once a day for 28 days, particularly following the dose and up to 12 hours after delivery, along with any injury or disease (e.g., weariness, ataxia, or lethargy).

2.4.2. Protective effect of NPs

2.4.2.1. Experiment design

For 3 weeks ,six groups, each containing five rats (n=5), the adult Wistar albino rats were randomly divided as follow:

Group I: Control rats received drinkable water, standard diet, water ad libitum.

Group II: Metribuzin was given orally at a dose of 133 mg/kg b.w. (1/20 LD50) in drinking water.

Group III: Metribuzin *133* mg/kg b.w. in drinking water + ZnO Nps by IP dose 2.5 mg/Kg b.w

Group IV: Metribuzin 133 mg/kg b.w. in drinking water + ZnO Nps by IP dose 5 mg/Kg b.w

Group V: Metribuzin 133 mg/kg b.w. in drinking water + Ag/Ag_2O Nps by IP dose 0.0625 mg/Kg b.w

Group VI: Metribuzin 133 mg/kg b.w. in drinking water + Ag/Ag_2O Nps by IP dose 0.125 mg/Kg b.w

Throughout the whole trial, intraperitoneal (i.p.) injections of physiological saline (0.9% NaCl, 1 ml/kg b.w) were administered daily.

2.4.2.2. Samples preparation

2.4.2.3. Sacrifice and Blood collection

After three weeks of treatments, 16 hours of fasting, the rats were sacrificed by decapitation under xylasine anesthesia. Serum samples were collected from the blood of each rat by centrifuging at 2500 rpm for 10 minutes for biochemical analysis.

2.4.2.4. Preparation of tissues samples

Normal saline was used to cleanse the kidneys, liver, and spleen. Half of them were preserved in 10% formaldehyde for histological analysis.For the purpose of determining the oxidative stress parameters (protein, MDA, and GSH), the remaining samples were kept at -20°C.

2.4.2.5. Hematological parameters analysis

Hematological parameters are computed using Coulter's method and a Medonic automatic hematological analyzer (Coulter Beckman -USA-).

2.4.2.6. Biochemical parameters analysis

Using the commercial kit from Spinreact, Spain, the following parameters were measured for each individual: serum glucose, urea, uric acid, creatinine, and serum lipid (cholesterol and triglyceride) Additionally, glutamate-pyruvate-transaminase (GPT) and glutamate-oxaloacetate-transaminase (GOT).(Appendix 04).

2.4.2.7. Determination of oxidative stress parameters

2.4.2.7.1. Homogenates preparation

In order to identify any oxidative stress markers in the liver, kidney, or spleen, we homogenized the produced supernatants of each organ, weighing 1g. The samples were then placed in 9 mL of Tris buffer saline (Tris 50 mM, NaCl 150 mM, pH 7.4)). Centrifuged at 3900 rpm for 20 minutes after homogenates were prepared.

2.4.2.7.2. Determination of tissue proteins

- **Principle**

  A spectrophotometer used a colorimetric approach to identify the tissue proteins by reacting the proteins' amine group (NH_2) with Coomassie blue, a reagent, to create a blue complex. The emergence of the blue hue reveals how ionized the acid medium is, and its intensity is connected with the amount of proteins present. The absorbance is measured at 595 nm. (Bradford, 1976)**.**

- **Preparation of Bradford's reagent**

After dissolving 100 mg of Coomassie blue in 50 mL of 95% ethanol, the mixture must be agitated for two hours in the dark before adding 100 mL of 85% orthophosphoric acid (H_3PO_4). In addition, one liter of distilled water was added, and the resulting solution was

purified using filter paper.
Note: This reagent is stable for 15 days at 4°C.

Five minutes after adding 1 mL of the homogenate to 5 mL of Coomassie blue, we measured the optical densities at 595 nm in relation to a blank.
A reference range of bovine serum albumin (0.1-0.2-0.4-0.6-0.8-1 mg/mL) that has been measured under similar circumstances is used to compare the protein concentration.

2.4.2.7.3. Determination of malondialdehyde (MDA) level

Place the glass test tubes in the glass vise, add 800 µL of TBA reagent and 200 µL of sample, and then screw on the caps firmly. The mixture will be cooked in a water bath at 100°C for 15 minutes. Allow the reaction's gasses to escape by leaving the tubes open for half an hour after they've been frozen in a cold water bath. After 5 minutes of centrifuging at 3000 rpm, measure the absorbance of the supernatant at 532 nm using a spectrophotometer.

(Yaki, 1976).

The concentration of thiobarbituric acid reactive compounds (TBARS) was determined using the molecular extinction coefficient of MDA (å= 1.53.105 M-1.cm-1). Equation 08 reported the results in nmol/mg of protein.

$$\mathbf{MDA\ (nmol\ /mg\ of\ prot)} = \frac{OD\ Sample}{1{,}53.10^{5}.mg\ of\ prot} \quad (8)$$

2.4.2.7.4. Determination of reduced glutathione level (GSH)

Weckbecker and Cory (1988) state that the amount of reduced glutathione is determined by measuring the optical density of 2-nitro-5-mercocapturic acid (TNB), a short-lived Ellman reagent with SH groups present in GSH that is produced by the reduction of dithio-bis-2-nitrobenzoic acid (DTNB).

800 µL of homogenate samples are combined with 200 µL of salicylic acid (0.25%). After that, the mixture was centrifuged at 1000 rpm for five minutes. Furthermore, 1000 µL of tris buffer (tris 0.4mol, 0.02mol NaCl, pH = 8.9) was mixed with 500 µL of supernatant and 25 µL of DTNB (0.01 mol/L). The absorbance of the reaction medium is measured at 412 nm after 5 minutes of incubation.

The concentration of GSH is expressed in nanomoles per milligram of protein (nmol/mg of protein) using the following equation (equation 09).

$$GSH(nM/Mg\ de\ prot) = \frac{DO \times 1 \times 1.525}{13133 \times 0.8 \times 0.5 \times mg\ de\ prot} \times d \quad (9)$$

- OD: Optical Density.
- 1.525: total volume of blend an mL.
- 13133: Absorption constant of SH groups at 412 nm.
- 0.5: Volume of the supernatant
- 1: volume of protein mixture.
- 0.8: volume of homogeneous solution without protein exists in 1 mL.

2.4.2.8. Histopathological study of liver, Kidney and spleen

After the rats were killed, the sections of their liver, kidney, and spleen were taken, and they were preserved in 10% formaldehyde until the time came to cut the slices for examination. After being washed with xylene and submerged in paraffin, the samples were dehydrated in an increasing graded series of ethanol (60, 70%, 80%, and 100%). Using a Thermo Scientific (Micron HM 325) Histoline Rotary Microtome, paraffin blocks were sectioned into 4-6 µm layers. The photograph was colored with hematoxylin and eosin. Histopathological inspection was done with a light microscope.

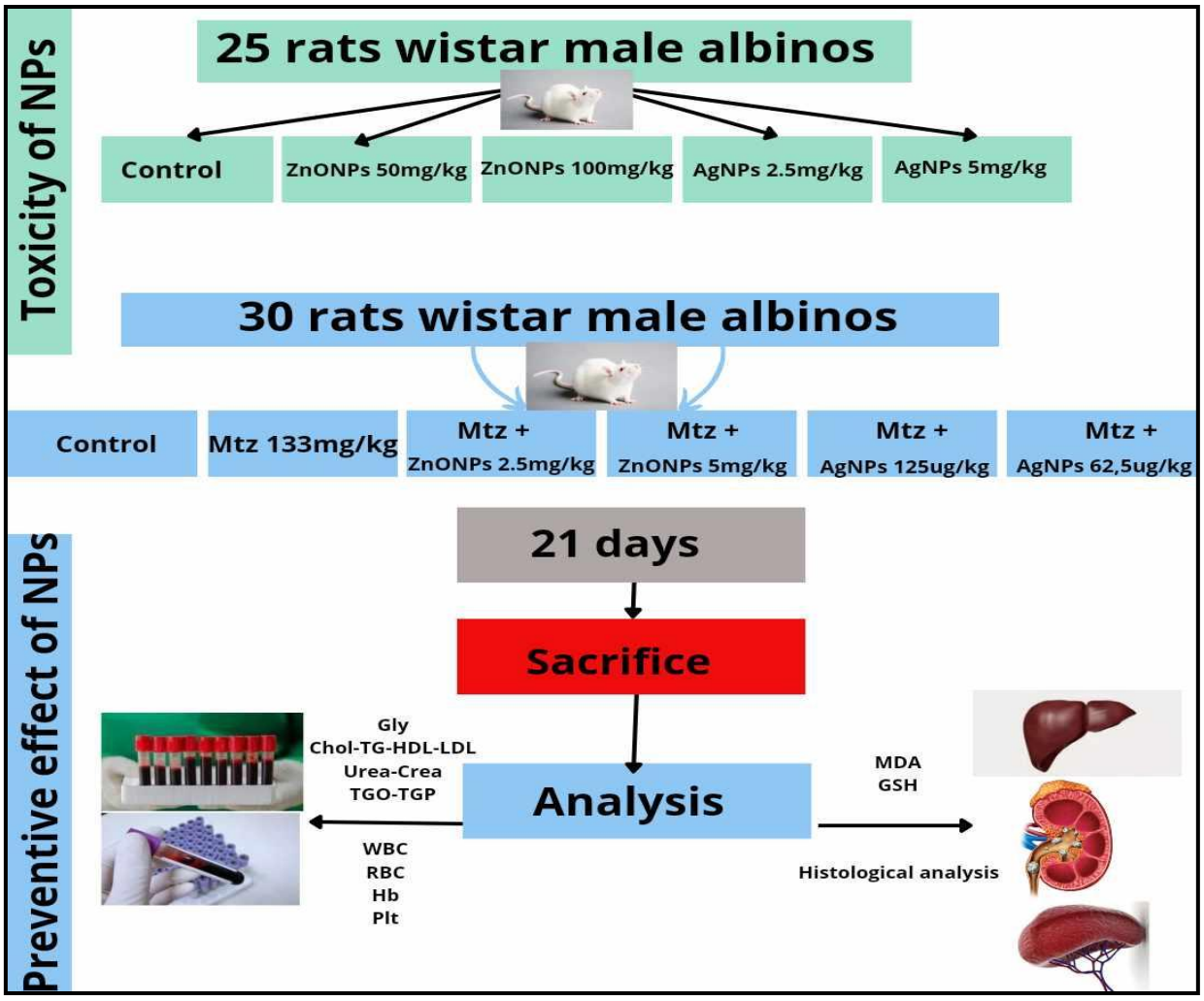

Figure (10) : A brief overview of the in vivo study's experimental protocol.

2.5. Statistical analysis

The obtained results are presented as mean ± standard error of the mean (Mean ± SE). The statistical package for social sciences(SPSS), version 22, was used to compare the means of the various groups. One-Way ANOVA and Duncan's multiple range test (DMRT) at p=0.05 were used to calculate significant differences between means. At $p \leq 0.05$, differences were deemed significant.

- ✓ Significant (* or a $P \leq 0.05$).
- ✓ Highly significant compared with the control (** or b $P \leq 0.01$).
- ✓ Very highly significant compared with the control (*** or c $P \leq 0.001$).

CHAPTER II

Results

1. Results:

1.1. Phytochemical Screening

The presence of phenolic compounds, flavonoids, glycosides, terpenoids, tannins,quinon, steroids and saponin in the *Olea europaea* extract (table 4) revealed by phytochemical analysis

Table (4): Phytochemical composition of aqueous extracts of *Olea europaea* leaves

Phytochemical composition	**Presence/ absence**
Phenol	+++ bleu
Flavonoid	+++
Tanin	+++ green
Saponine	+++
Alkaloide	-
Terpenoid	+++ red brown
Quinon	+++ red
Coumarin	-
Glycoside	+++
Cardiaglycoside	+++ brown
Steriods	+++ brown

1.1.2. Quantification of phytochemicals compounds

In this study, the total phenolic content, total flavonoids and condensed tanins of the aquous extract of the leaves of *O.europaea* var. Chemllali was found to be 143.279 ± 1.7 ug GAE/mg extract, 6.764 ± 0.025 ug QCE/mg extract,and 16.333 ± 0.12 ug CTE/mg extract respectively.

Table (5): Quantification of some phytochemicals compounds of the aquous extract of the leaves of *O.europaea* var. Chemllali.

Estimation	total phenolics ug of GAE/mg Ex	total flavonoids ug of QCE/mg Ex	condensed tannins ug of CTE/mg Ex
Means ± SE	143.279±2.7	6.764±0.025	16.333±0.12

1.1.3. Analyze qualitative by HPLC

The results of HPLC analysis showed that the *O. europaea* chromatograms **(Figure **)**. Where we have identified 08 phenolic compounds out of 72 peaks. The analysis revealed that quercetin (1945.90 µg/g) was the most abundant element with a high amount of Naringin and Vanilic acid (790.94µg/g , 702.63 µg/g respectively), a moderate quantity of Rutin, Chlorogenic acid and p- coumaric acid (595.50 µg/g , 453.80 µg/g, and 391.65 µg/g), a little amount of Vanilin and Caffeic acid (197.73µg/g, 119.58 µg/g), **(Table**)** were detected in *O. europaea* extract leaves.

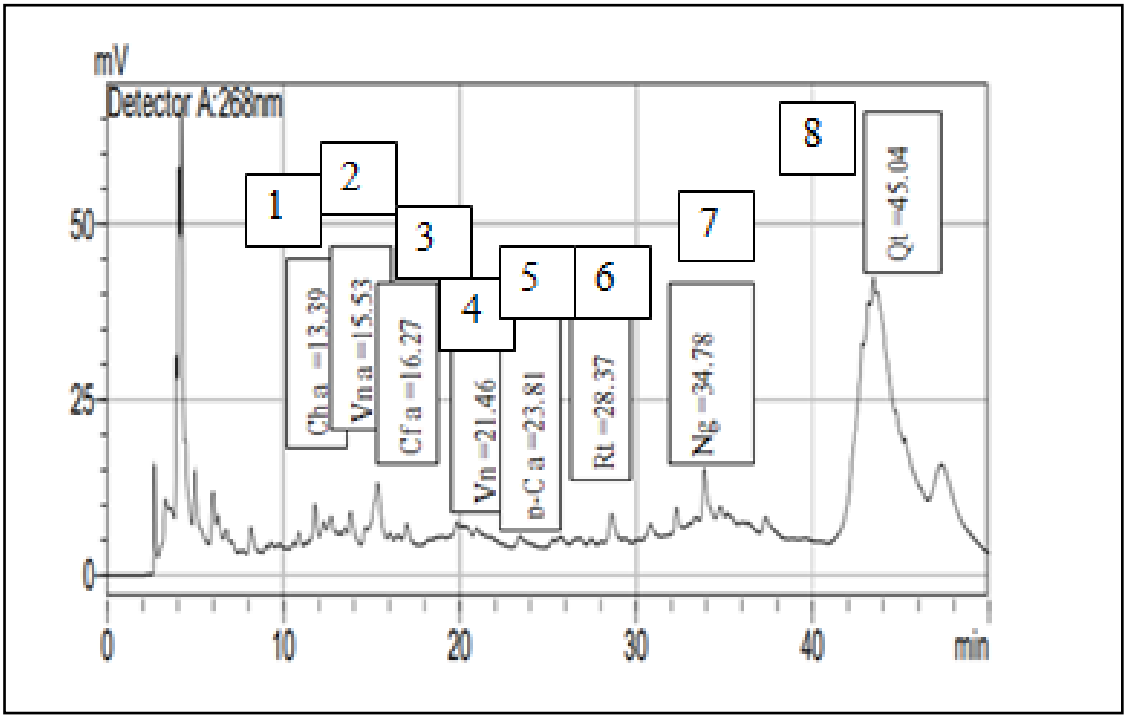

Figure(11): HPLC chromatogram's of the extract of *O. europaea* with retention time of 1:

Chlorogenic Acid, 2: Vanilic acid , 3: Caffiec Acid, 4: Vanilin , 5:p-Coumaric Acid, 6: Rutin , 7: Naringin, 8: Quercetin, respectively.

Table (6): Concentration of phenolic compounds identified in *O. europaea* aqueous extract.

Phenolic compounds	**Concentration µg/gEx**
Chlorogenic acid	453.80
Vanilic acid	702.63
Caffeic acid	119.58
Vanilin	197.73
p- coumaric acid	391.65
Rutin	595.50
Naringin	790.94
Quercetin	1945.90

1.2. Green synthesis of nanoparticles

1.2.1. Green synthesis of Ag/Ag_2O NPs

1.2.1.1. Characterization of Ag/Ag_2O NPs

1.2.1.1.1. UV-visible spectrophotometer and bandgap energy

Our data indicates the UV-Vis absorption graph in the visible light region, illustrating the formation of Ag/Ag_2O NPs, which exhibit an absorption band. A scanning wavelength analysis (200 to 800 nm), revealing presence of peaks at 440 nm and 255 nm, indicative of Ag/Ag_2O formation. Additionally, the plant extract graph was analyzed and displayed peaks at 280 nm and 325 nm. The optical absorption spectra of Ag/Ag_2O NPs are influenced by surface plasmon resonance, which shifts towards 440 nm. This shift depends on factors such as grain size, shape, aggregation state, and the surrounding dielectric medium. The energy bandgap (Eg) of Ag/Ag_2O NPs were plotted using Tauc's Eqs (Pfost *et al*.,1985) :

$$(\alpha hv) = A\left(hv - E_g^{opt}\right)^n \qquad (1)$$

through extrapolating a straight line on the energy axis, the direct and indirect Energy gap of Ag/Ag_2O NPs were valued to be nearby 2.23 and 1.34, respectively.

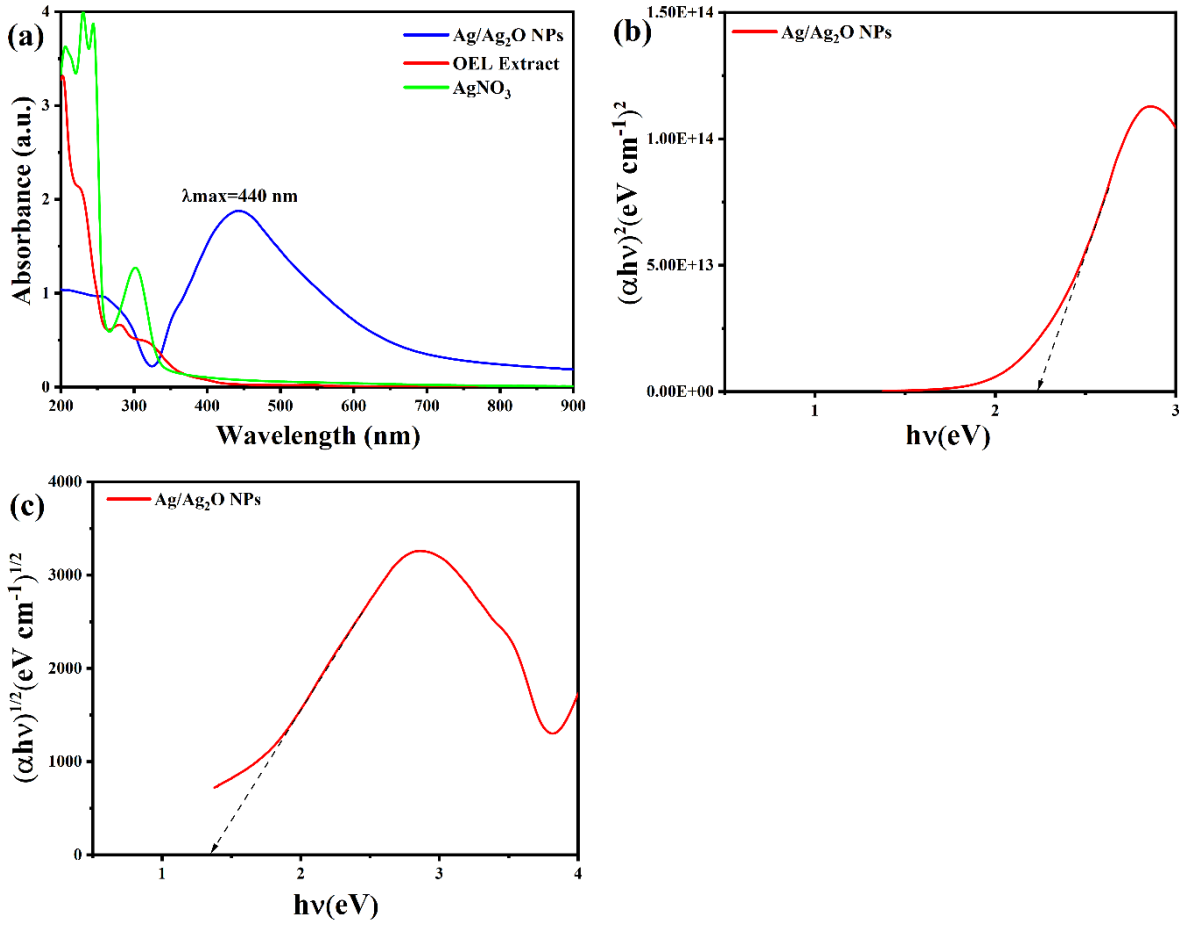

Figure(12): (a) UV-vis graph (b) direct bandgap energy (c) indirect bandgap energy of the Ag/Ag_2O NPs:

1.2.1.1.2. Fourier transforms infrared spectroscopy (FTIR)

FTIR measurement was used to identify the different functional groups in both Olea europaea leaf extract and the synthesized Ag/Ag_2O nanoparticles (NPs). Figure 13 depicts the FT-IR spectrum of the green synthesis of Ag/Ag_2O NPs using extract of *O. europaea* leaf compared with the extract. The broad band at 3400 cm^{-1} is attributed to O–H stretching frequency. Another band at 2358 cm^{-1} is assigned to symmetric carboxyl stretching (C=O). The peak at 1634 cm^{-1} corresponds to C=C stretching vibration. The absorption band located at 1430 cm^{-1} corresponds to the stretching frequency of C–C bonding in aromatic cycles. The band at 1270 cm^{-1} is associated with C–O stretching vibrations of carboxylic acids. Moreover, the

vibration band at 564 cm^{-1} corresponds to Ag–O.

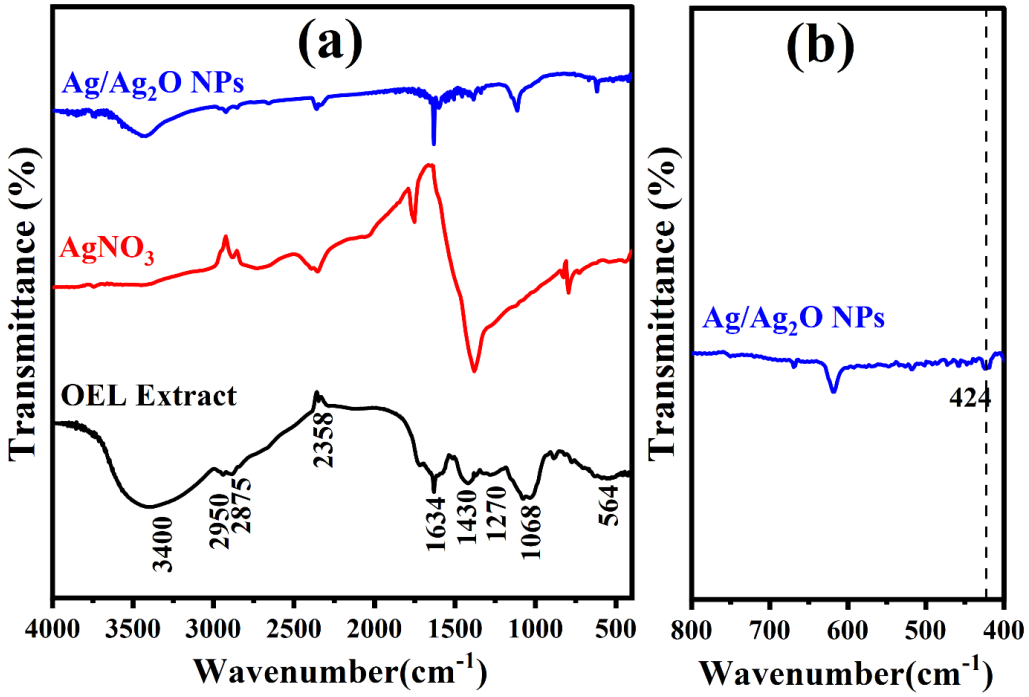

Figure (13): (a). FT-IR graph of synthesized Ag/Ag_2O NPs, $AgNO_3$ and *O. europaea* extract, (b). detailed look at view range (400 to 800 cm^{-1}) of biosynthesized Ag/Ag_2O NPs.

1.2.1.1.3. X-ray diffraction (XRD)

The structural and morphological characteristics of the obtained Ag/Ag_2O powder were analyzed using X-ray diffraction (XRD). Figure (14) displays the XRD patterns with sharp peaks for Ag/Ag_2O. The peak patterns at 2θ values of 26.46°(110), 32.555°(111),, 37.768°(200),, 54.48°(220),, 64.922°(311),, and 68.193° correspond to the (222) planes of silver oxide (Ag_2O) respectively. Other values match the standard data (JCPDS No. 01-076-1393), confirming the cubic crystalline structure of Ag_2O. Additionally, the diffraction peaks at 2θ values of 38.20°, 44.402°, 64.602°, and 77.6° correspond to the (111), (200), (220), and (311) planes of silver (Ag).

Using the Scherrer equation (Vijayaraghavan T *et al.*, 2017), the average crystallite sizes for the two most prominent peaks (38.20° and 32.555°) were determined to be 24 nm for Ag and 26 nm for Ag_2O, respectively

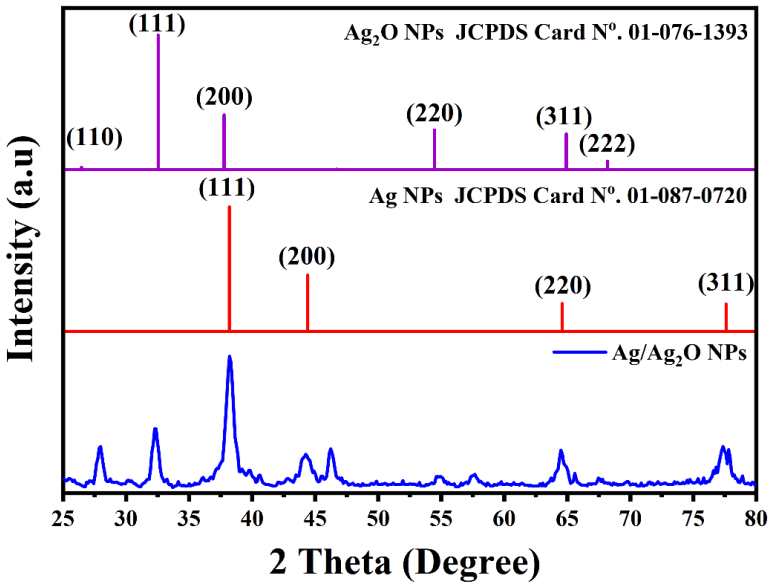

Figure (14): Silver/Silver Oxide Nanoparticles Synthesized XRD Patterns

1.2.1.1.4. Scanning electron microscopy (SEM) and Energy dispersive spectroscopy (EDX)

Figure (15) illustrates the surface morphology of Ag/Ag_2O nanoparticles (NPs), revealing the presence of predominantly spherical or oval-shaped Ag/Ag_2O NPs. The bioactive components in *Olea europaea* leaf extract interact strongly with silver ions, resulting in uniformly spherical and smaller-sized nanoparticles. As shown in Fig. 3b, the middling size distribution of the biosynthesized Ag/Ag_2O NPs is primarily around 45 nm. The image also depicts deformed spherical particles for Ag/Ag_2O NPs larger than 60 nm, which is attributed to either a deficiency or excess of bioactive agents in the *Olea europaea* leaf extract. This imbalance reduces the interaction between the bioreducing agents and the precursor silver, leading to the formation of larger particles.

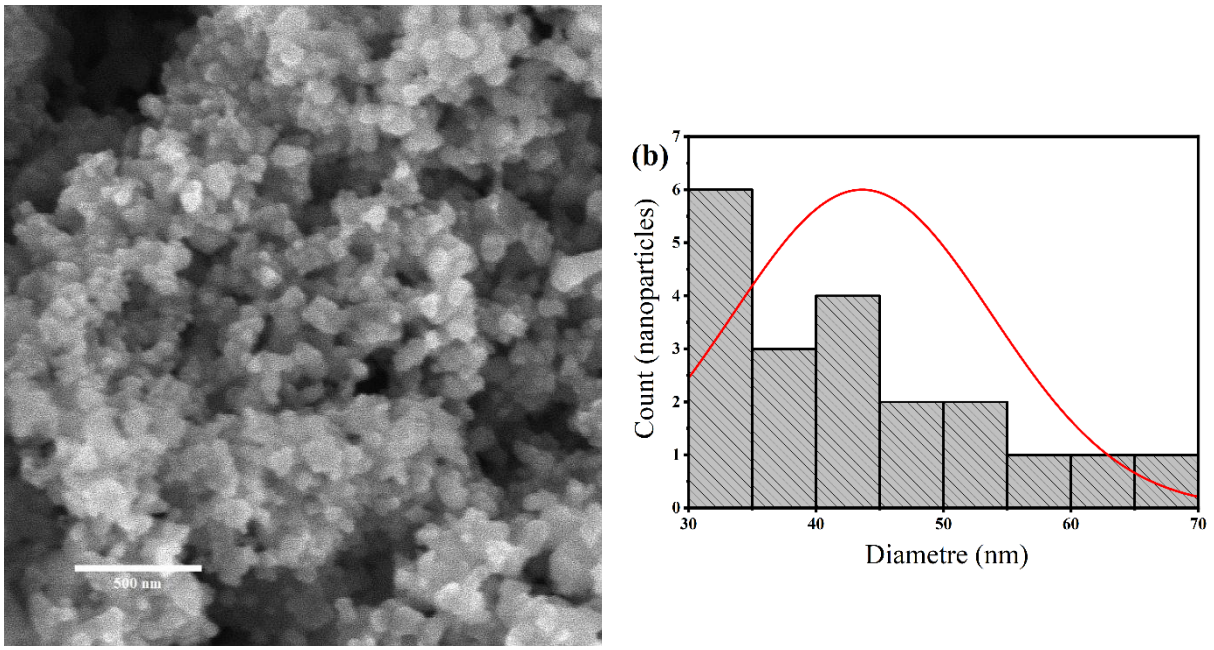

Figure (15): (a) SEM images and (b) particle size distributions of biosynthesis Ag/Ag_2O NPs.

The energy-dispersive X-ray (EDX) analysis of Ag/Ag_2O nanoparticles (NPs) distinctly shows the peaks for silver, chlorine, and oxygen. To ensure the Ag/Ag_2O NPs are uncontaminated, it is important to note that no additional peaks are present in the EDX spectrum, indicating the purity of the silver nanoparticles. Typically, the EDX analysis of Ag/Ag_2O NPs reveals a peak around 3 KeV (Dai and Mumper, 2010), which is attributed to surface plasmon resonance, as illustrated in Figure (16).

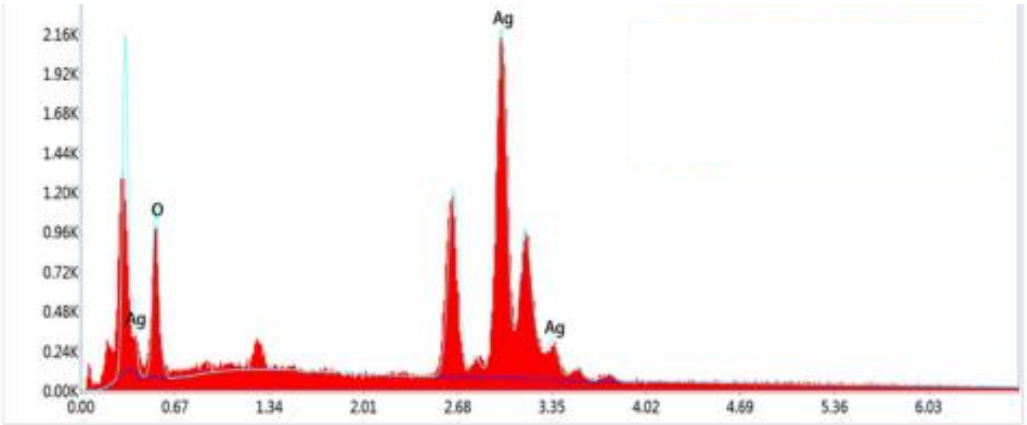

Figure (16): EDX of biosynthesis Ag/Ag_2O NPs.

1.2.2. Green synthesis of Zinc oxyde Nanoparticles

1.2.2.1. Characterization of ZnONPs

1.2.2.1.1. UV-visible spectrophotometer and bandgap energy

In this study, UV-Vis spectroscopy was utilized to explore the characteristics of ZnO nanoparticles (NPs), particularly focusing on determining their energy bandgap and identifying potential modifications. The bandgap indicates the energy needed for an electron to transition from the valence to the conduction bands within a semiconductor. we examined light absorption using UV-Vis spectroscopy.

This absorption prompts electrons to move from the valence to the conduction band, and upon returning to their ground state, they emit energy as light. The energy of the emitted light directly correlates with the bandgap energy. By graphing the absorption coefficient against photon energy and applying Tauc's formula (eq. 1), the bandgap energy of the ZnO NPs nanocomposite was determined (Figure 17 a,b). The analysis revealed a bandgap energy of 3.7 eV. Variations detected in the bandgap energy of the nanocomposites were attributed to the presence of the synthesized ZnO NPs. The efficiency of photodegradation of ZnO NPs is directly affected by their bandgap energy. Remarkably, smaller bandgaps are associated with enhanced photocatalytic performance.

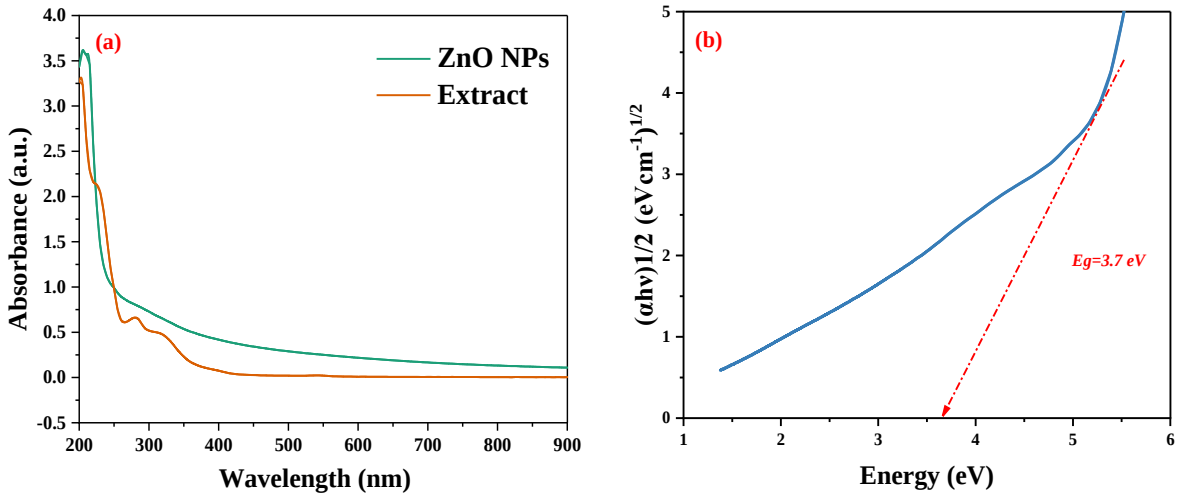

Figure (17): UV-Vis graph (a) of biossynthesized ZnO NPs and *O. europaea* leave extract (b) energy band gap.

1.2.2.1.2. Fourier transforms infrared spectroscopy (FTIR)

The infrared spectroscopy data provided for ZnO and the extract (Figure18) offers valuable insights into molecular vibrations and chemical interactions. The presence of OH groups suggests the existence of hydroxyl functionalities in the sample, at 3572 cm^{-1}. In addition, the peak observed at 2887 cm-1 agrees to CH2 stretching vibrations, indicating the presence of aliphatic hydrocarbons. The presence of unsaturated carbon-carbon bonds(C = C) ascribed to the vibration at 1624 cm^{-1} presented in FTIR graph.. Furthermore, the peak at 1095 cm-1 corresponds to the stretching vibration of C–O groups, implying the involvement of oxygen-containing functional groups. Remarkably, the far-reaching peak around 457 cm-1 indicates the formation of Zn-O bonds, consistent with the characteristic peak predictable for zinc oxide nanoparticles.

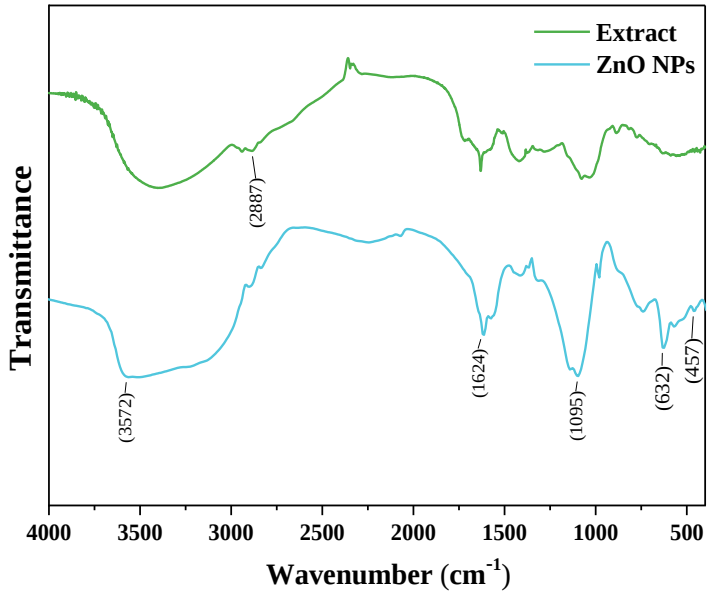

Figure (18): FTIR graphs of (a) *O. europaea* aqueous leaf extract and ZnO nanoparticles.

1.2.2.1.3. X-ray diffraction (XRD)

The objective of the X-ray diffraction (XRD) analysis in this study was to characterize the crystallography and phase formation of ZnO nanoparticles. The XRD profiles, shown in Figure (19), and standard data (JCPDS No.036-1451) revealed a consistent hexagonal crystal structure. The observed reflection planes, identified as (100)- 31.77°, (002)-34.42°, (101)-36.52°, (102)-47.53°, (110)-56.6°, (103)-62.86°, (200)-66.38°, (112)-67.96°, (201)-69.1°, (004)-72.56°, and (202)-76.95°, corresponded to 2θ angles of respectively. The particle size

was determined utilizing the equation of Scherrer, with calculations performed at the (101) plane, acquiescent a ZnO particle size of 18.79 nm.

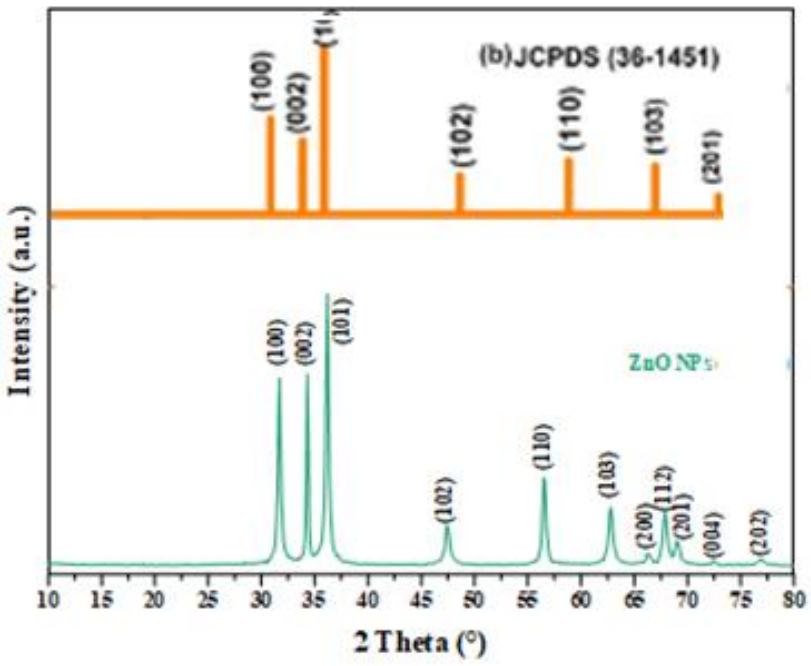

Figure(19): XRD graphs of the biogenic ZnO NPs and JCPDS (36-1451) card.

1.2.2.1.4. Scanning electron microscopy (SEM) and Energy dispersive spectroscopy (EDX)

The morphology of ZnO nanoparticles synthesized through biological resources was evaluated via scanning electron microscopy (SEM). Examination unveiled that these particles displayed consistent shapes with a smooth surface, taking on both spherical and short-rod forms (see Figure 20a). Moreover, SEM images depicted a predominantly spherical morphology for the ZnO nanoparticles. Analysis of particle size distribution histograms (Figure 20b) revealed an average size ranging from 40 to 60 nm.

The energy-dispersive X-ray (EDX) analysis of the ZnO nanoparticles clearly identified peaks corresponding to zinc and oxygen. This analysis also confirmed the absence of any additional peaks, indicating the purity of the zinc oxide nanoparticles. Thus, the pure form of zinc oxide nanoparticles is clearly demonstrated in Figure (21).

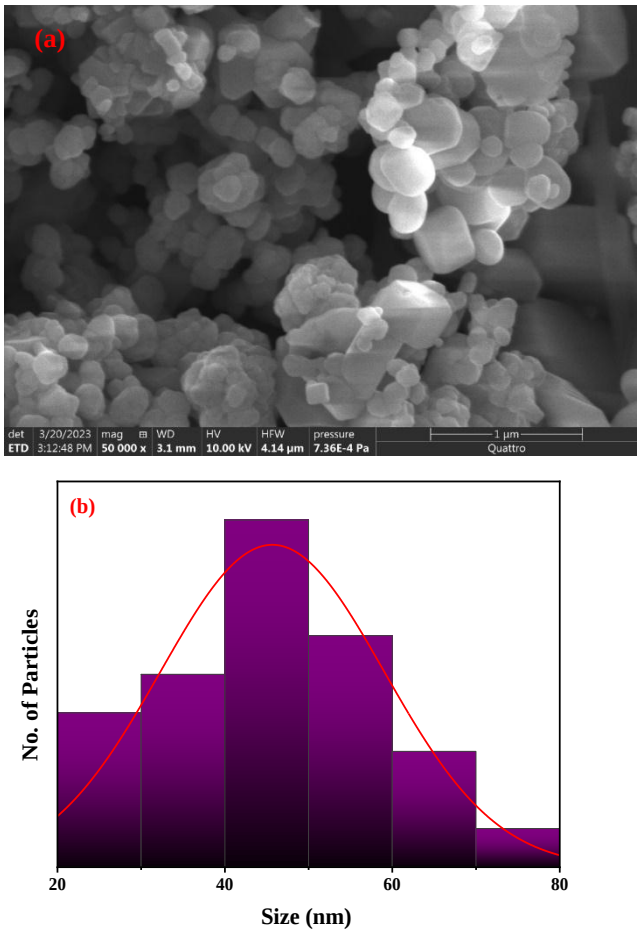

Figure (20): SEM analysis of the biosynthesized: (a) SEM image of ZnO NPs, (b) Size distribution of ZnO NPs

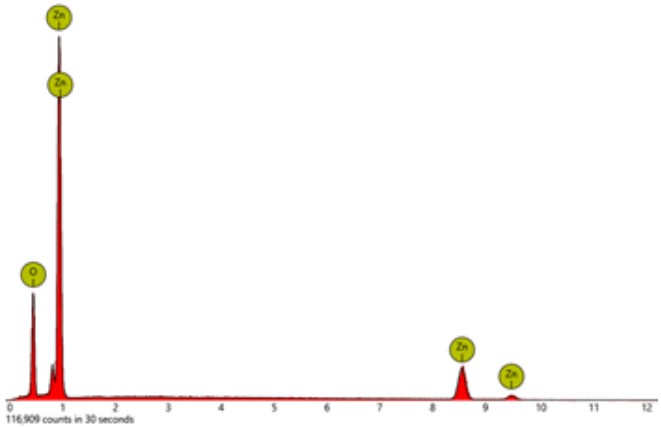

Figure (21): EDX of biosynthesis ZnO NPs.

1.3. *In Vitro* activity of nanoparticles

1.3.1. Antioxidant activity

1.3.1.1. DPPH free-radical scavenging activity (DPPH)

The DPPH radical's IC50 values and percentage inhibition for gallic acid, Ag/Ag_2O NPs, and *Olea europaea* leaf extract are shown in the figures. Ag/Ag_2O NPs (15.1%, 16.2%, and 17.6%) showed poorer scavenging activity than the leaf extract (27.3%, 43.0%, and 46.0%) at lower concentrations. Nonetheless, the scavenging activity was 60.0% and 93.3% for the leaf extract and 67.1% and 95.2% for Ag NPs at doses of 62.5 and 125 µg/mL, respectively. However for ZO NPs showen no reation in this investigation.

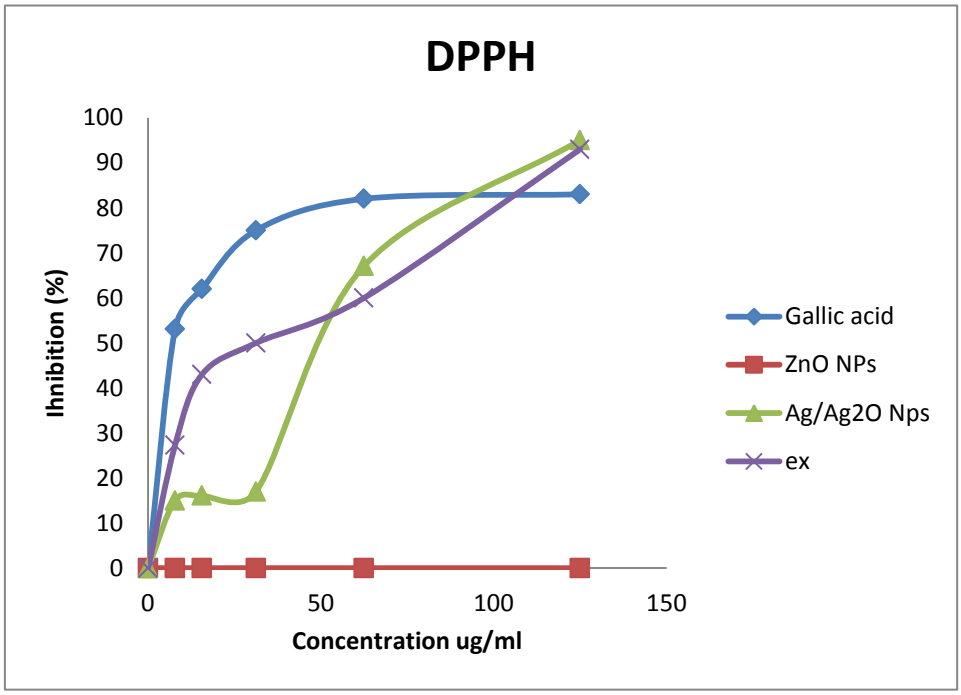

Figure(22): Percent inhibition of DPPH radical of the extract of *Olea europaea* leaf, the Ag/Ag_2O nanoparticles and gallic acid.

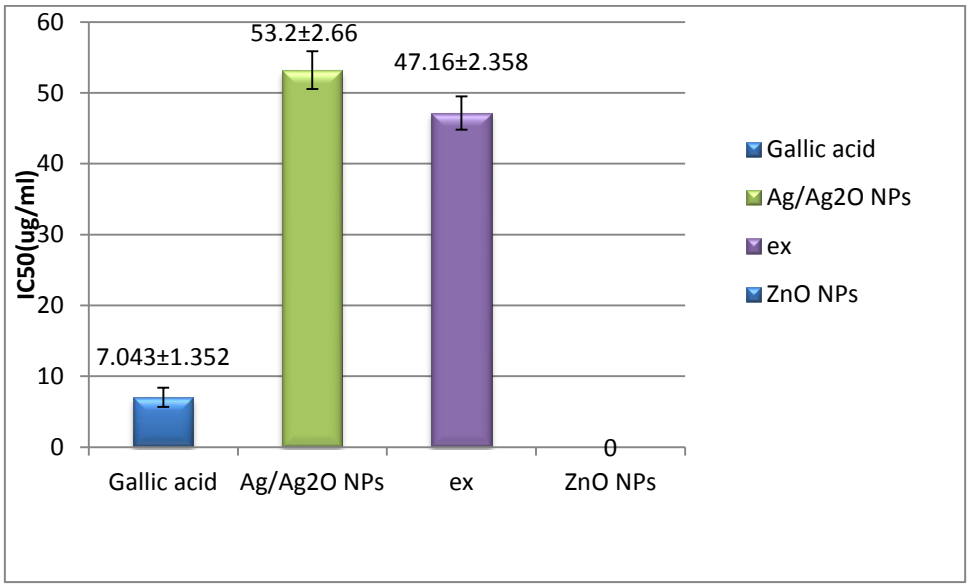

Figure(23): DPPH (IC50, ug/ ml) of the *Olea europaea* leaf extract, the Ag/Ag_2O Nps and gallic acid.

1.3.1.2. Total Antioxidant Capacity assay

In Figure (24) , it has been demonstrated that the increase in total antioxidant capacity (TAC) of Ag/Ag_2O NPs, ZnO NPs, and *Olea europaea* leaf extract is dose-dependent. This suggests that a larger increase in TAC may occur from extract dosages or concentrations that are higher. The results show that each sample has a significant antioxidant capacity. At 200 µg/mL, the extract showed the highest overall antioxidant capacity, measuring 34.31±0.23 mg E GA/g Ex.

The TAC value for the Ag/Ag2O nanoparticles at a greater concentration was 67.73±0.12 mg E GA/g NPs, which was stronger than the ZnO TAC value at the same concentration (31.94±0.24 mg E GA/g NPs).

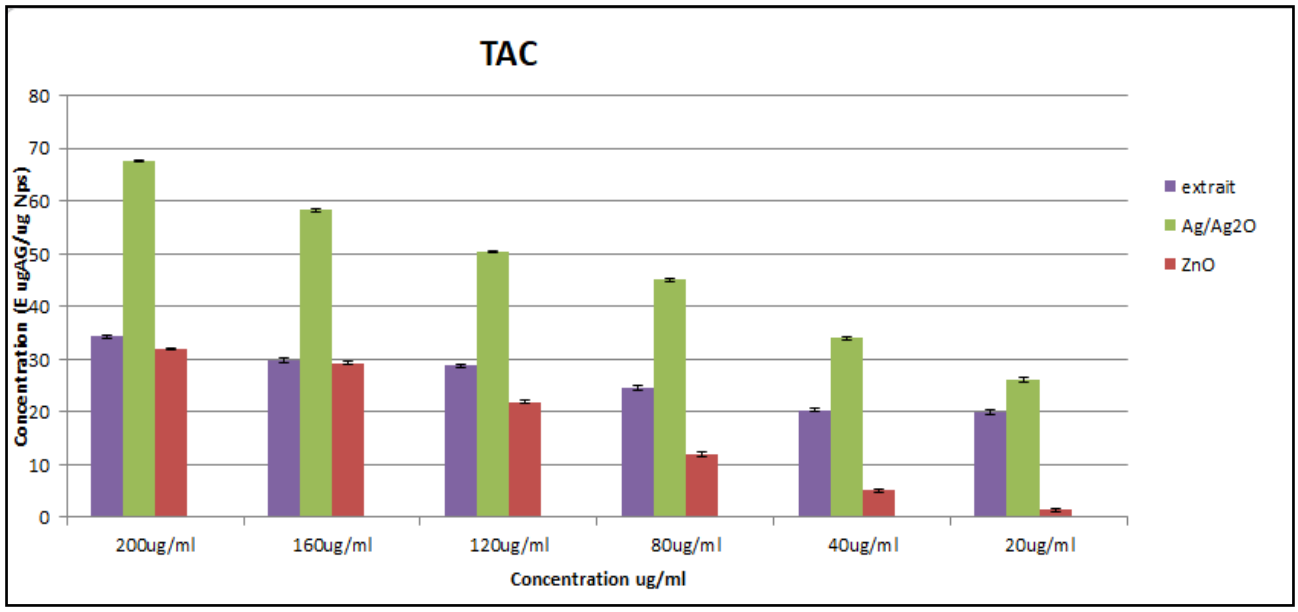

Figure(24): Total antioxidant capacity (TAC, E ug GA/ug NPs) of the Olea Europaea leaf extract, the Ag/Ag_2O Nps and ZnO Nps .

1.3.1.3. Ferric Reducing Power Assay (FRAP)

Figure (25) shows how the semples' antioxidant power to reduce ferric ions increases in a dose-dependent manner. The antioxidant activity of the Olea europaea leaf extract, Ag/Ag_2O NPs, and ZnO NPs at different doses was evaluated in this study using the FRAP assay. Ag/Ag_2O NPs, ZnO NPs, and the extract all showed an increase in reducing activity that was dose-dependent. When compared to normal ascorbic acid, the extract showed antioxidant activity across doses ranging from 20 to 200 µg/mL. With increasing absorbance for Ag/Ag_2O NPs and ZnO, the FRAP value—a measure of the reducing power—increased. The concentration of 200 µg/mL in Ag/Ag_2O NPs showed the greatest.

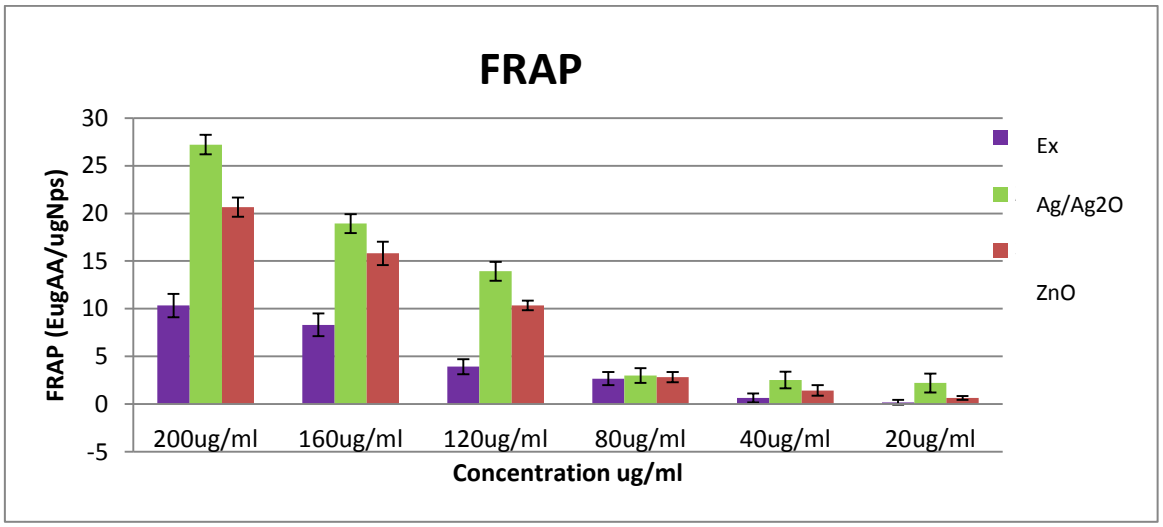

Figure(25): Ferric reducing antioxidant power (FRAP E µg AA/µg NPs) of the *Olea europaea* leaf extract, the Ag/Ag_2O Nps and ZnO Nps .

1.3.2. Antibacterial activity assays

1.3.2.1. Antibacterial test using the agar diffusion method

The biogenerated Ag/Ag_2O NPs in this work were found to have strong antibacterial activity. To assess the antibacterial effects of the generated Ag/Ag_2O NPs, three microorganisms were chosen: *Pseudomonas aeruginosa*, *Escherichia coli*, and *Staphylococcus aureus* (Figure26). It was measured how big the inhibition zones were. *P. aeruginosa* (16 mm) and *S. aureus* (16 mm) had the most powerful antibacterial activity at a greater concentration of Ag/Ag_2O NPs (200 µg/mL) in comparison to the positive control streptomycin (Table 7). *E. coli* (12 mm) was the next most active antibacterial agent.

At 50, 100, and 200 µg/mL, the antibacterial activity was shown to be dose-dependent, with greater concentrations of Ag/Ag_2O NPs corresponding to an increase in the inhibitory zone size. Higher doses of ZnO nanoparticles were less effective in the 10 mm (for *E. coli*) and 10.5 mm (for *P. aeruginosa*) inhibitory zones, respectively

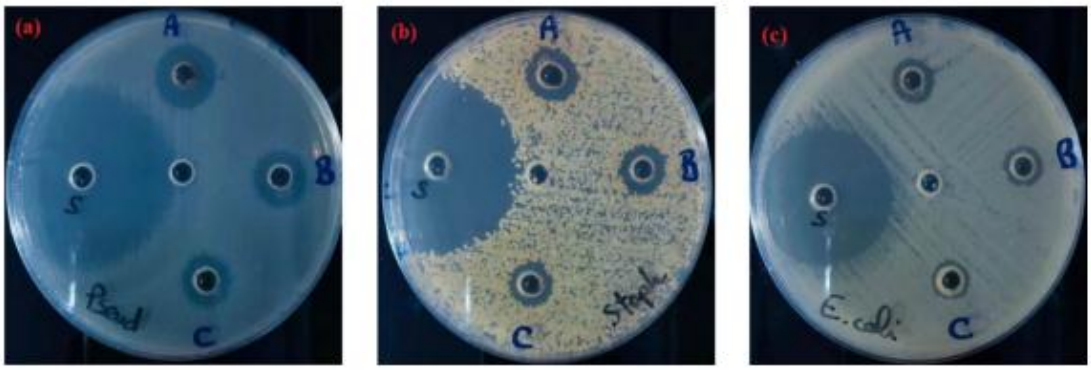

Figure (26): Antibacterial activity of Ag/Ag_2O NPs ((a),(b) and (c) at dose 200 µg/mL, 100 µg/ml and 50 µg/ml respectively , S= streptomycin and negative control DMSO in the center) on human pathogenic bacteria

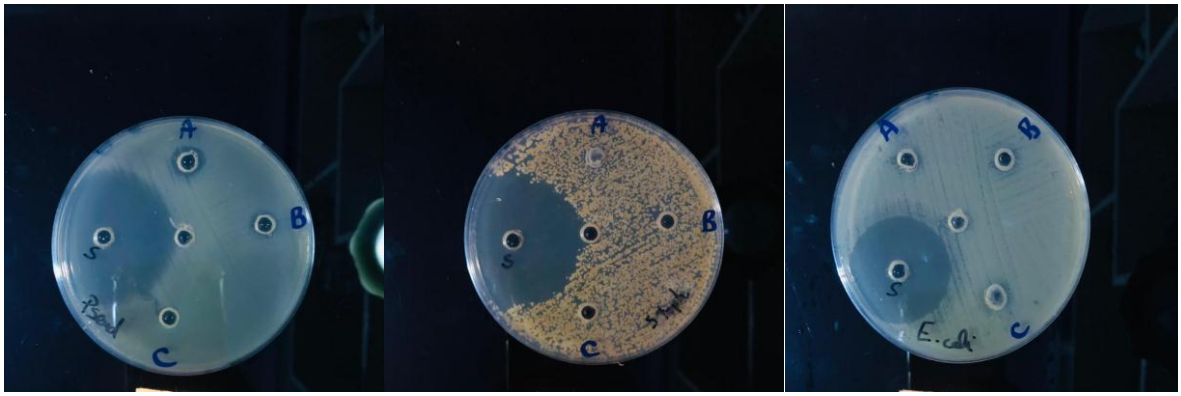

Figure (27): Antibacterial activity of ZnO NPs ((a),(b) and (c) at dose 200 µg/mL, 100 µg/ml and 50 µg/ml respectively , S= streptomycin and negative control DMSO in the center) on human pathogenic bacteria

Table (7): Mean zones of inhibition (mm) produced by plant extract and nanoparticles at diferent concentration

Test	**DMSO**	**Streptomycin**	**Ag/Ag_2O**			**ZnO**		
Dose	/	20 mg/ml	50 Ug/ml	100 Ug/ml	200 Ug/ml	50 Ug/ml	100 Ug/ml	200 Ug/ml
E.coli	NZ	34mm±2.36	10 ±1.26	11 ±1.90	12 ±3.08	8.33 ±1.97	9 ±2.60	10 ±1.58
P.aerugi	NZ	44mm±2.98	12 ±0.98	13 ±2.03	16 ±2.36	NZ	9.33 ±3.6	10.5 ±3.29
S.aureus	NZ	43mm±3.45	12 ±2.55	15 ±1.26	16 ±1.02	NZ	NZ	NZ

1.3.2.2. Antibacterial kinetic study of nanoparticles

The growth patterns of bacteria treated with Ag/Ag_2O and ZnO NPs shown inhibitory effects on the growth and reproduction of *E. coli* and *S. typhimurium* cells. Figures shows the growth curves of *B. cereus* and *S. aureus* cells treated with nanopartilces. After being treated with 200 µg/ml nanopartilces (Ag/Ag_2O and ZnO NPs), nearly all of the bacterial cells in these groups showed retarded growth after the first six hours of growth suppression.

Furthermore, the growth of cells treated with 200 µg/ml Ag/Ag_2O NPs was slightly slower than that of cells in the ZnO Nps group. These results imply that 200 µg/ml ZnO and Ag/Ag_2O Nps had a moderate antibacterial effect, but not enough to stop the rate at which bacteria reproduced. When S. aureus cells were treated with 200 µg/ml ZnO Nps, there was a total suppression of bacterial growth. On the other hand, the bacterial cells treated with 200 µg/ml ZnO started growing again after 18 hours. Cells treated with 200 µg/ml ZnO and Ag/Ag_2O Nps showed all-around reduced bacterial growth curves compared to the control group.

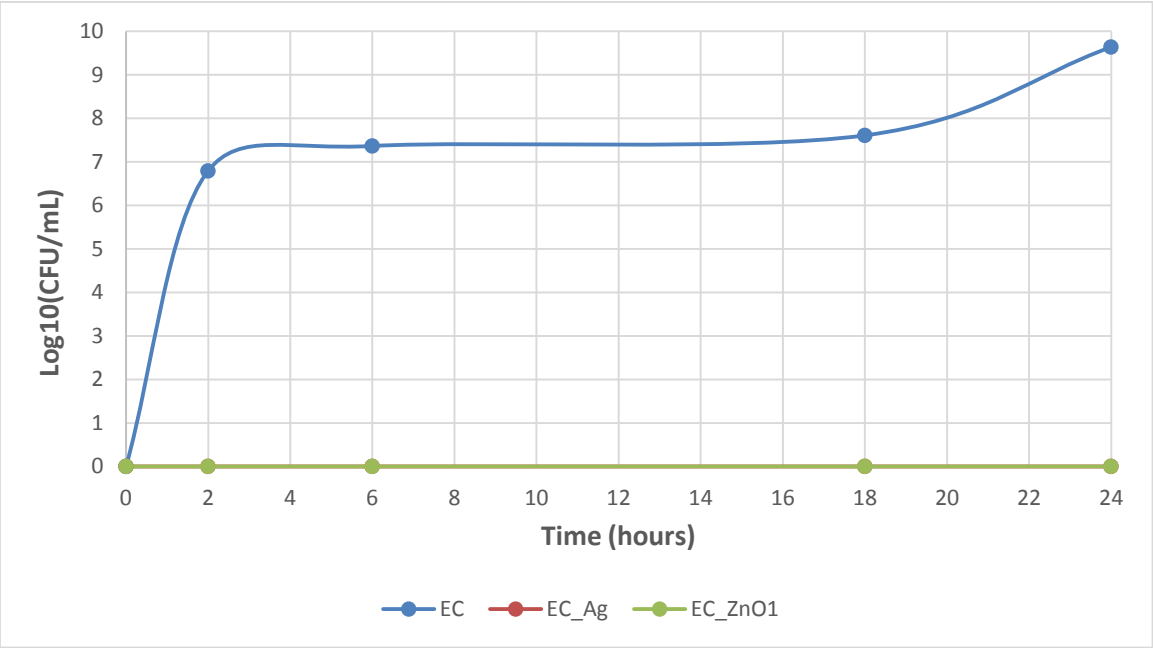

Figure(28): Antibacterial kinetic study of nanoparticles for Escherichia coli (Ec)

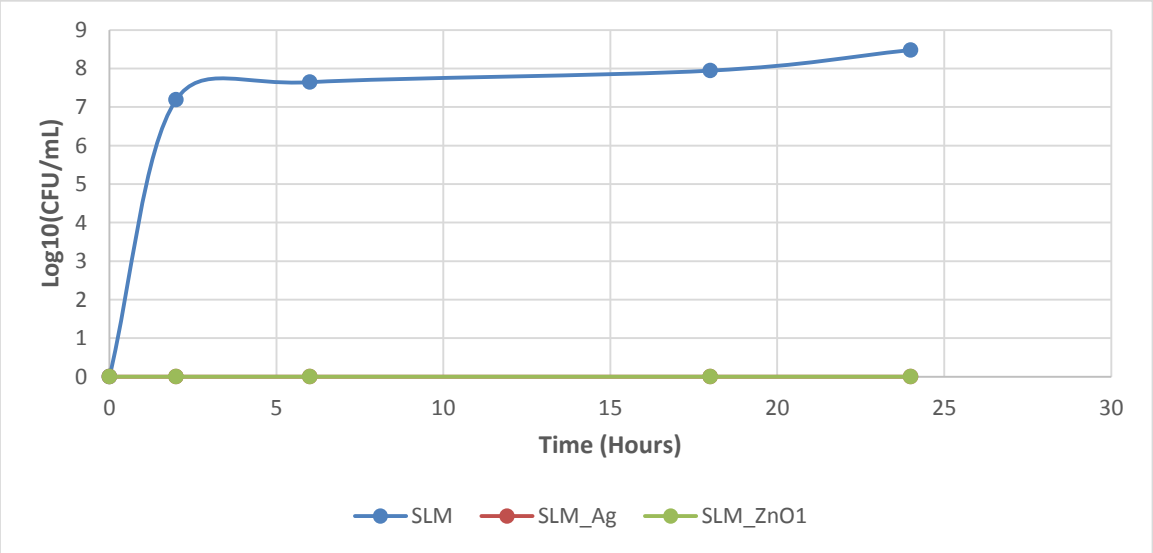

Figure(29): Antibacterial kinetic study of nanoparticles for Salmonella typhimurium (St)

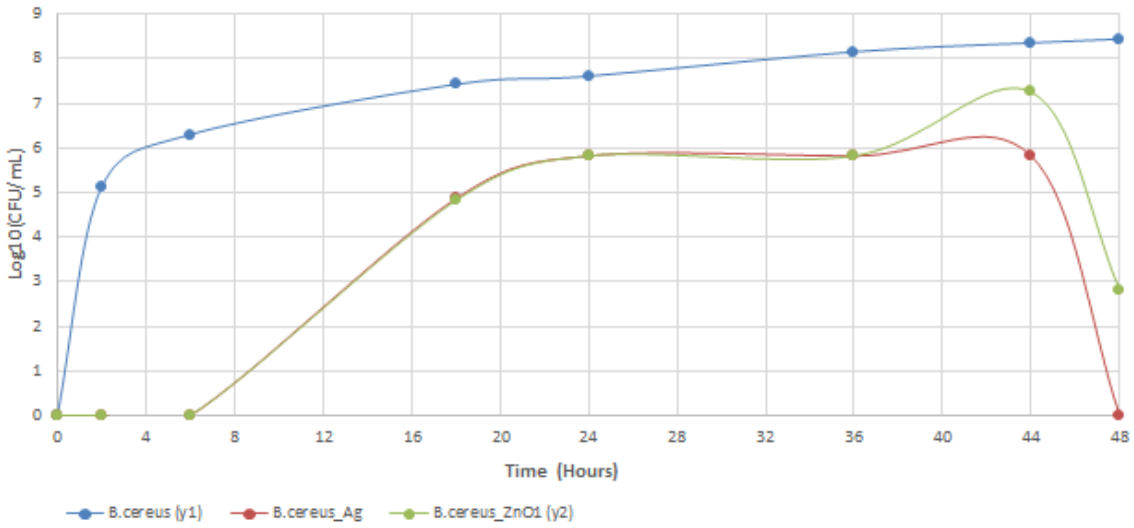

Figure(30): Antibacterial kinetic study of nanoparticles for Bacillus cereus (Bc)

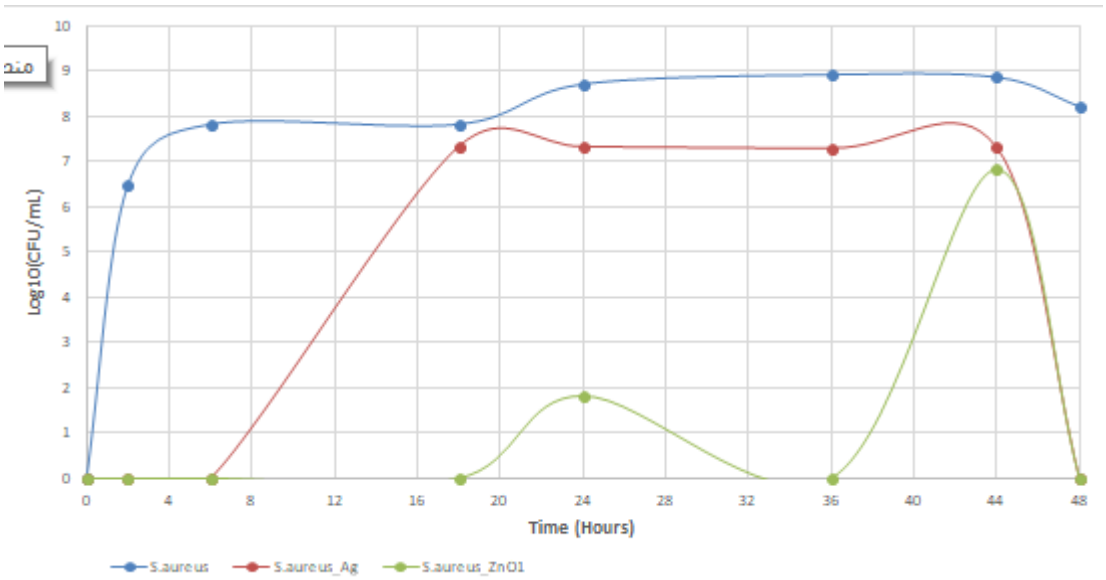

Figure(31): Antibacterial kinetic study of nanoparticles for Methicillin resistant Staphylococcus aureus (MrSa)

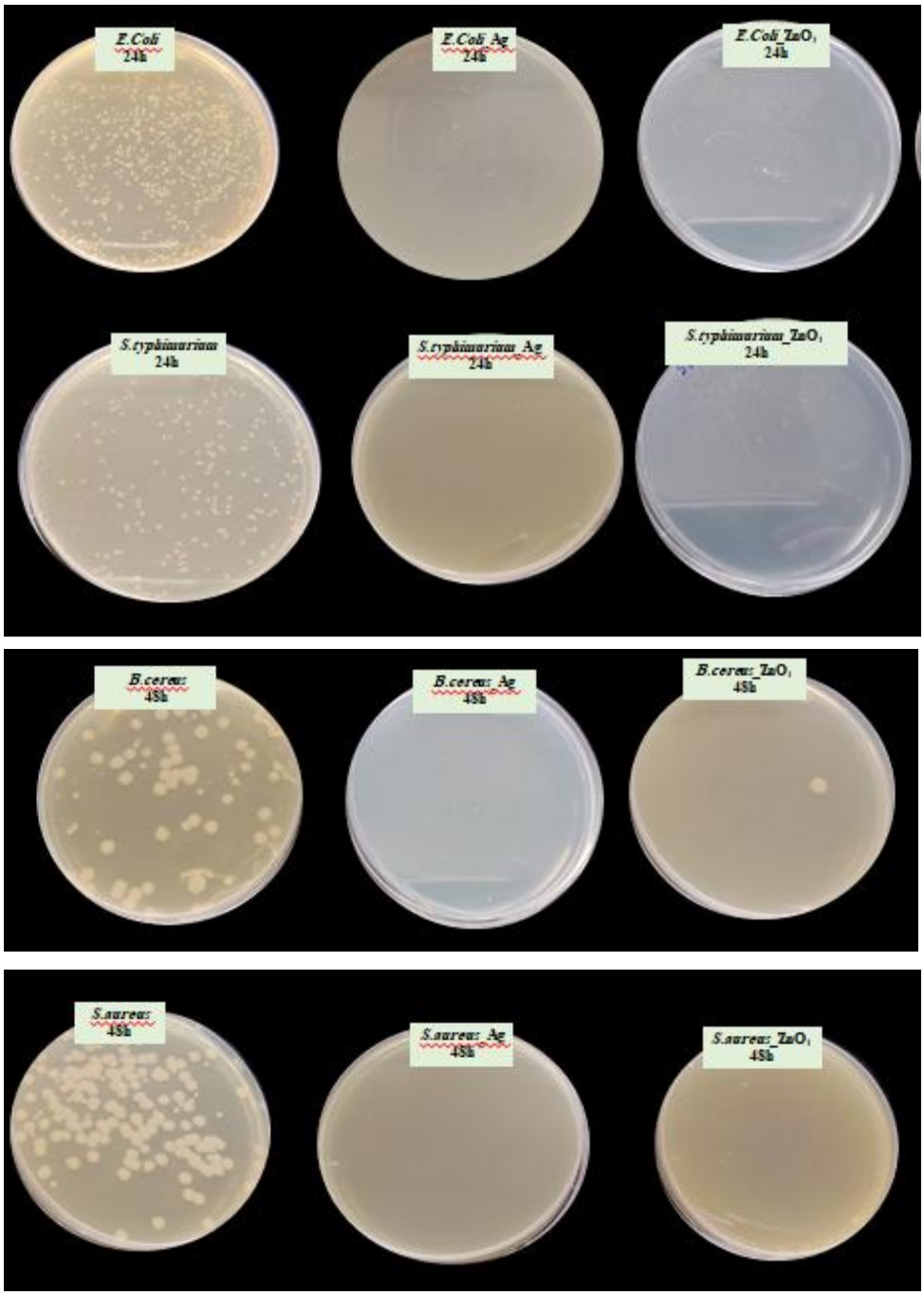

Figure(32): Zone of inhibition of 200 ug/mL dose of Ag/Ag_2O and ZnO NPs against four bacterial strains

1.3.3. Antimutagenic activity

Using 1-nitropyrene (1-NP) (200 ng/tube as the mutagen and the *Salmonella* micro-suspension experiment (YG1024 strain), the antimutagenic activity of the nanoparticles at 50–250 μg/tube was evaluated. When ZnO NPs were biosynthesized using an aqueous extract of *O. europaea* leaves, they showed excellent anti-mutagenicity against S. typhimurium TA98.

At 250 µg/tube, the percent inhibition of ZnO NPs was higher (76.24%) than that of Ag/Ag2O NPS (70%).

Table(8): Antimutagenic activity of the Ag/Ag_2O Nps and ZnO Nps biosynthetised by aqoues extract O. Europaea leaves against 1-NP in *S. typhimurium* TA98.

Test items	**Concentration**	**Revertants TA98**	**Inibition%**	**Revertants TA98**	**Inibition%**
		Ag/Ag_2O NPs		**ZnO NPs**	
Positive control (1-NP)	200 ng/tube	1290±9.8	/	1326±10.2	/
Nanoparticles	50 µg/tube	987±7.5	23.48%	1025±5.4	23.33%
	100 µg/tube	768±3.6	40.46%	735±9.3	45.81%
	150 µg/tube	679±4.1	47.36%	521±7.8	62.40%
	200 µg/tube	429±9.8	66.74%	389±9.9	69.53%
	250 µg/tube	374±3.9	70%	342±4.9	76.27%

1.3.4. Anticoagulant activity of nanoparticles

Similar to the positive control (EDTA), none of the nanoparticles (ZnO and Ag/Ag_2O Nps) were able to prevent coagulation, but the negative control did. All blood samples treated with Ag/Ag_2O Nps retained the biconcave disc form of red blood cells, as shown by microscopic analysis (Figure33). Nonetheless, the pH of Ag/Ag_2O Nps and blood dilution with colloidal Ag/Ag_2O Nps solution may be responsible for a small amount of morphological deformation.

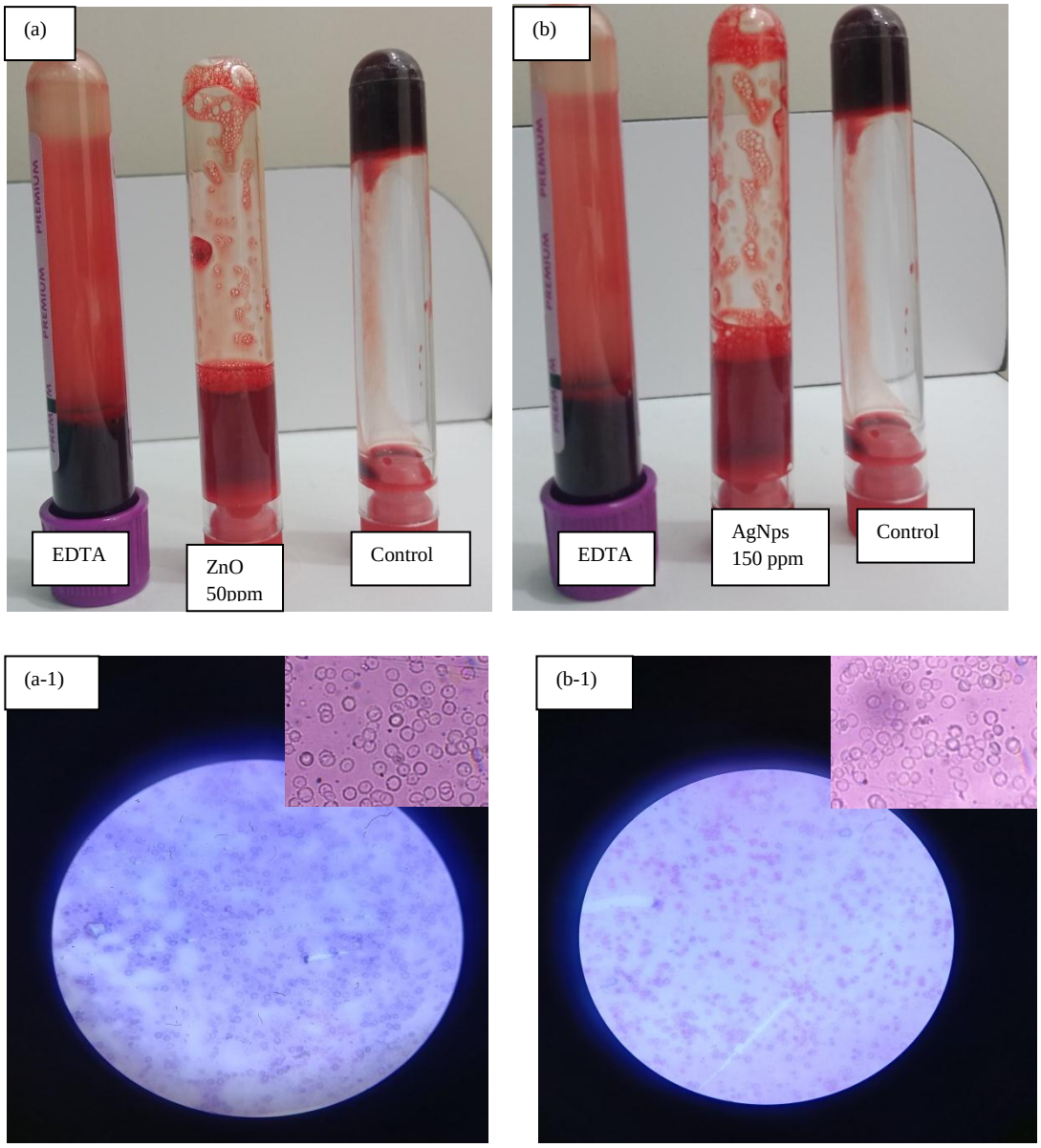

Figure(33): Anticoagulant activity of ZnO and Ag/Ag_2O nanoparticles synthesised using O. europaea (a) Anticoagulant activity of ZnO (b) Anticoagulant activity of and Ag/Ag_2O (a-1) The microscopic examination of the blood sample treated with 50ppm ZnO (b-1) The microscopic examination of the blood sample treated with 50ppm Ag/Ag2O Nps.

1.4. *In vivo* activity of aqueous extract *of O. europaea* and nanoparticles

1.4.1. Toxicity study

The groups who got ZnO NPs at two doses (50 mg/kg and 100 mg/kg body weight) did not have any deaths.

The low-dose Ag/Ag_2O NPs groups (2.5 mg/kg) did not significantly differ from the control group in terms of general health over the 28-day observation period. On the first day

following the 2-hour injection, however, rats treated with the NPs displayed transient symptoms such delayed locomotion, yellowish feces with diarrhea, and dark yellow urine. The next day, these symptoms disappeared (Table 9).

On the other hand, a rat that was given a greater dosage of Ag/Ag_2O NPs (5 mg/kg body weight) passed away 24 hours after the treatment. The majority of the animals in the high-dosage group (5 mg/kg bw i.p.) displayed symptoms that were probably brought on by the dose, including head twitches, diarrhea, loose stools, dark red urine, and alterations in food and water intake. But after four days, these harmful effects progressively went back to normal. These findings led to the estimation that the LD50 of Ag/Ag_2O NPs in rats was higher than 5 mg/kg body weight. Ag/Ag_2O NPs' effects on behavior and physiological states—both neurological and autonomic—declined with time and concentration.

Table (9): Mortality, behavior observations, and clinical signs afterward the acute toxicity using Ag/Ag_2O NPs and ZnO NPs

Dose of Ag/Ag_2O Nps	**Time**	**mortallity**	**Feed/ water**	**Diarrhea**	**Color of urine**	**Lacrimation**	**movements**	**ataxia**	**Head twitches**
0 mg NPs Nps/kg of body weight (control)	1h	0/5	N	-	Clear yellow	-	N	-	-
	2h		N	-	Clear yellow	-	N	-	-
	6h		N	-	Clear yellow	-	N	-	-
	12h		N	-	Clear yellow	-	N	-	-
	24h		N	-	Clear yellow	-	N	-	-
	2d		N	-	Clear yellow	-	N	-	-
	7d		N	-	Clear	-	N	-	-

					yellow				
	14d		N	-	Clear yellow	-	N	-	-
	28d		N	-	Clear yellow	-	N	-	-
2.5 mg Ag/Ag_2O Nps/kg of body weight	1h	0/5	Fasting	-	Clear yellow	-	Slow	-	-
	2h		Fasting	-	Dark yellow	-	Slow	-	-
	6h		AbN	+	Clear yellow	-	AbN	-	-
	12h		AbN	-	Clear yellow	-	AbN	-	-
	24h		AbN	-	Clear yellow	-	N	-	-
	2d		N	-	Clear yellow	-	N	-	-
	7d		N	-	Clear yellow	-	N	-	-
	14d		N	-	Clear yellow	-	N	-	-
	28d		N	-	Clear yellow	-	N	-	-
5 mg Ag/Ag_2O Nps/kg of body	1h	1/5	Fasting	-	Clear yellow	-	Clumsy and invariably slow	+	+

weight	2h		Fasting	++	Dark-red	-	Clumsy and invariably slow	+++	++
	6h		Fasting	+	Dark yellow	-	Slow	++	++
	12h		Fasting	-	yellow	-	Slow	+	++
	24h		AbN	-	yellow	-	AbN	+	+
	2d		AbN	-	yellow	-	AbN	+	-
	7d		AbN	-	Clear yellow	-	N	-	-
	14d		N	-	Clear yellow	-	N	-	-
	28d		N	-	Clear yellow	-	N	-	-
50 mg ZnO Nps/kg of body weight	1h	0/5	Fasting	-	Clear yellow	-	Slow	-	-
	2h		Fasting	-	Dark yellow	-	Slow	-	-
	6h		AbN	+	Clear yellow	-	AbN	-	-
	12h		AbN	-	Clear yellow	-	AbN	-	-
	24h		N	-	Clear yellow	-	N	-	-
	2d		N	-	Clear yellow	-	N	-	-

	7d		N	-	Clear yellow	-	N	-	-
	14d		N	-	Clear yellow	-	N	-	-
	28d		N	-	Clear yellow	-	N	-	-
100 mg ZnO Nps/kg of body weight	1h	0/5	Fasting	-	Clear yellow	-	Clumsy and invariably slow	+	+
	2h		Fasting	++	yellow	-	slow	-	+
	6h		Fasting	-	Dark yellow	-	Slow	-	+
	12h		AbN	-	yellow	-	Slow	+	+
	24h		AbN	-	yellow	-	AbN	-	-
	2d		AbN	-	yellow	-	AbN	-	-
	7d		N	-	Clear yellow	-	N	-	-
	14d		N	-	Clear yellow	-	N	-	-
	28d		N	-	Clear yellow	-	N	-	-

N: Normal , AbN: Abnormal. (-): no signs (+): signs present

1.4.2.Preventive effect of nanoparticles:

1.4.2.1. Hematological parameters analysis

Table 10 shows the outcomes of a hematological profile in rats of the control and treated group given a p.o. dose of 133 mg/kg of metribuzine for 21 days. Comparing the metribuzin-treated animals to the control group, the former showed significantly decreased Hb concentration ($p \leq 0.01$) and PLT ($p \leq 0.05$). The WBC and RBC counts did not differ statistically from the control group. Rats co-treated with nanoparticles did not exhibit significant changes in their haematological parameters. However, Metribuzin revealed that the ZnO nanoparticle treatment group (2.5 mg/Kg) had an increase in Hb conconcentration as compared to the induced-rat group. PLT count decreased ($p \leq 0.001$) in the group receiving the highest dose of Ag/Ag2O NPs, 0.125 mg/kg.bw.

Table(10): Protective effect of ZnO NPs and Ag/Ag_2O NPs on hematological parameters analysis of intoxicated rats with Metribuzin

Group	**WBC 10^3/ul**	**RBC 10^3/ul**	**Hb g/dl**	**PLT 10^3/ul**
Control	10.02± 0.74	8.5 ±0.21	15.94 ±0.17	1405 ±50.6
Metribuzin 133mg/Kg group	12.64 ±3.8	7.62 ±1.6	12.28 ±0.68**	1257 ±42.32*
Metribuzin 133mg/Kg +ZnO NPs 2.5mg/Kg group	10.48± 2.57	8.36 ±0.04	14.38± 0.29b	1349 ±22.7
Metribuzin 133mg/Kg +ZnO NPs 5mg/Kg group	11.1± 1.44	8.29± 0.25	14.24 ±0.61	1326 ±19.54
Metribuzin 133mg/Kg +Ag/Ag_2O NPs 0.062mg/Kg group	11.74 ±1.63	8.8± 0.08	14.04 ±0.4	1299 ±46.9
Metribuzin 133mg/Kg +Ag/Ag_2O NPs 0.125mg/Kg group	13.06 ±2.46	8.30 ±0.12	13.5 ±0.61	233 ±10.98c

1.4.2.2. Biochemical parameters analysis

Significant effect of metribuzin in biochimical parameters, when increase in serum LDL, urea , acid uric, ASAT, ALAT, suggesting hepato-renal failure, on the other hand, ZnO NPs treatement has a benific effect against intoxicated rats with metribuzin.

On the other hand, there was a beneficial effect of ZnO NPs on rats that consumed the pesticide, as the concentration of liver enzymes was diminished by both doses, 2.5 mg/Kg , 5 mg/Kg. There is also another reducing effect of this nanoparticles on blood urea in rats treated with a concentration of 5 mg/Kg b.w.

For the low dose Ag/Ag_2O NPs treatement (0.062mg/Kg), we showed diminution in ASAT and ALAT. Regarding the high concentration (0.125mg/Kg), there was no difference in the effect on liver enzymes, compared to the group exposed to the pesticide, but it caused an increase in the level of creatinine in the blood.

Table(11): Effect of ZnO NPs and Ag/Ag_2O NPs on biochimical markers of metabolisme against intoxicated rats with metribuzin

Group	**GLY 10^{-2} mg/dl**	**CHOL 10^{-2} mg/dl**	**TG 10^{-2} mg/dl**	**HDL 10^{-2} mg/dl**	**LDL 10^{-2} mg/dl**
Control	0.81± 0.1	0.69 ±0.04	0.59± 0.07	0.48 ±0.09	0.092± 0.08
Metribuzin 133mg/Kg group	0.72± 0.12	0.83± 0.18	0.68± 0.09	0.50± 0.07	0.194 ±0.05*
Metribuzin 133mg/Kg +ZnO NPs 2.5mg/Kg group	0.81± 0.09	0.68 ±0.03	0.61± 0.08	0.42± 0.07	0.126± 0.1
Metribuzin 133mg/Kg +ZnO NPs	0.78± 0.06	0.78 ±0.05	0.60 ±0.06	0.52 ±0.17	0.140±0.15

5mg/Kg group					
Metribuzin 133mg/Kg +Ag/Ag_2O NPs 0.062mg/Kg group	0.74± 0.04	0.64 ±0.14	0.47± 0.09[a]	0.41± 0.08	0.136± 0.26
Metribuzin 133mg/Kg +Ag/Ag_2O NPs 0.125mg/Kg group	0.77± 0.03	0.77± 0.05	0.80± 0.61 [b]	0.48± 0.1	0.13± 0.3

Table(12): Effect of ZnO NPs and Ag/Ag_2O NPs on biochimical markers of kidney and liver against intoxicated rats with metribuzin

Group	**UREA 10^{-2} mg/dl**	**CREATININE 10^{-2} mg/dl**	**URIC ACID**	**ASAT U/mL**	**ALAT U/mL**
Control	0.43 ±0.08	4.26± 0.9	32.91± 5.6	222.9 ±45.96	54.1 ±4.75
Metribuzin 133mg/Kg group	0.67 ±0.07[*]	3.73 ±0.34	56.02 ±5.72[*]	357.6 ±50.56[*]	81 ±3.47[**]
Metribuzin 133mg/Kg +ZnO NPs 2.5mg/Kg group	0.55 ±0.04	3.00 ±0.09	38.18± 3.76	257.81±28.24 [a]	63.02±1.49[a]
Metribuzin 133mg/Kg +ZnO NPs 5mg/Kg group	0.43±0.02 [b]	3.63± 0.13	34.94±6.03	238.6 ±23.10 [b]	68.4 ±7.4[a]
Metribuzin	0.55 ±0.06	3.43 ±0.38	46.72 ±8.45	250.6±15.42 [a]	58.4 ±7.1[b]

133mg/Kg +Ag/Ag_2O NPs 0.062mg/Kg group					
Metribuzin 133mg/Kg +Ag/Ag_2O NPs 0.125mg/Kg group	0.59 ±0.04	5.28 ±0.81 [b]	52.54 ±14.26	301.4 ±14.75	87.0 ±2.04

1.4.2.3. Oxidative stress parameters

1.4.2.3.1. Determination of malondialdehyde (MDA) level reduced glutathione level (GSH)

In intoxicated group with metribuzin, a significant imbalance of oxidative stress in the liver, kidney,MDA ($p \leq 0.05$) GSH(($p \leq 0.05$) , MDA ($p \leq 0.01$) GSH(($p \leq 0.05$), respectively. Analysis of parameter of oxidative stress showed that the spleen has no sighnificance for status of spleen .

When using ZnO nanoparticles, for tow doses there is generally a correction in the imbalance of oxidative stress in the studied organs, as the results were as follows: reduction MDA levels in liver and kidney, also advancement GSH contents in kidney, compared to the intoxicated group with metribuzin.

For Ag/Ag_2O NPs at low dose, our results showed that it has beneficial effect on the imbalance of oxidative stress in the liver and kidney. On the contrary, the effect of the higher concentration of Ag/Ag_2O NPs (0.125 mg/Kg b.w) was completely opposite, as it caused increased stress on the liver, kidneys and spleen of the intoxicated rats with metribuzin.

Table(13): Effect of ZnO NPs and Ag/Ag_2O NPs on oxidative stress markers of kidney, liver and spleen against intoxicated rats with metribuzin.

Group	MDA nM/mg P			GSH nM/mg P		
	liver	kideny	spleen	liver	kideny	spleen
Control	1.637±0.92	1.895± 1.00	2.26± 0.83	4.248 ±1.02	2.853 ±0.89	3.940±0.62
Metribuzin 133mg/Kg group	2.606± 0.78 *	3.290±0.21**	2.4 ±0.91	2.366±0.56*	1.670±0.40**	3.319±1.09
Metribuzin 133mg/Kg +ZnO NPs 2.5mg/Kg group	0.968 ±1.03 b	1.799 ±0.67 b	2.870 ±0.62	3.056 ±0.60	2.771 ±0.09	3.79± 0.71
Metribuzin 133mg/Kg +ZnO NPs 5mg/Kg group	1.736 ±0.05	1.863 ±0.79 b	2.260 ±0.91	2.924 ±1.04	3.74 ±0.69 a	2.561± 0.69
Metribuzin 133 mg/Kg +Ag/Ag_2O NPs 0.062mg/Kg group	1.234±0.6 a	1.690± 0.55 b	2.730±0.73	3.621 ±0.82	2.810 ±0.75 a	2.908 ±0.82
Metribuzin 133mg/Kg +Ag/Ag_2O NPs 0.125mg/Kg	2.214± 0.67	2.820 ±1.82	3.02± 0.94 a	1.044± 0.69 b	1.540 ±0.42 a	2.001 ±0.63 a

group						

1.4.2.3.4. Histopathological study of liver, Kidney and spleen

1.4.2.3.4.1. .Histopathological study of liver

Histopathological analysis of rat liver sections in the different experimental groups showing effect of Metribuzin and protective effect of treatment with different doses of ZnO NPs and Ag/Ag_2O NPS. Liver sections of control group showing normal architecture of hepatocytes, and Liver of rat treated with Metribuzin showing dilatation and congestion in the portal vein associated with diffuse kupffer cells proliferation in between the hepatocytes, Liver of rat treated with ZnO NPs (2.5 mg/Kg, 5 mg/Kg) with Metribuzin intoxication showing normal architecture of hepatocytes, Liver of rat treated with Ag/Ag_2O NPs (125 µg/kg) with Metribuzin intoxication showing dilatation and congestion were detected in the central and inflammatory cells infiltration in the portal area, fanelly, the liver of rat treated with Ag/Ag_2O NPs (62.5 µg/kg) with Metribuzin intoxication showing mild dilation of central vein.

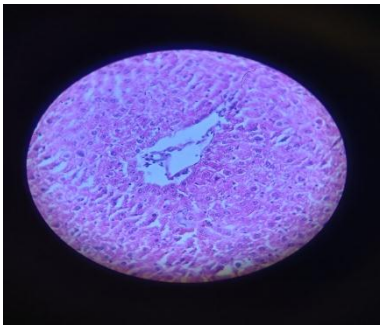

(a)

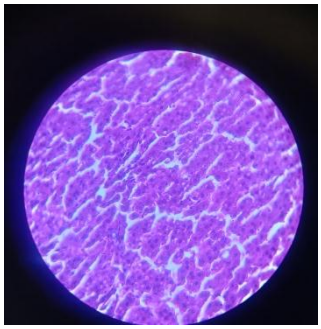

(c)

(e)

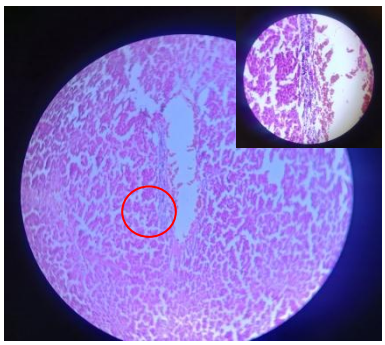

(b)

(d)

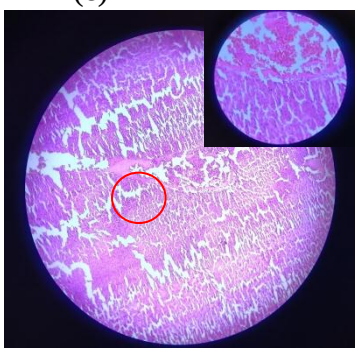

(f)

Figure(34): Photomicrographs of rat liver sections in the different experimental groups . a: control group. b treated group with Metribuzin . c-d: treated group with ZnO NPs (2.5 mg/Kg, 5 mg/Kg) and Metribuzin intoxication . e-: treated group with Ag/Ag_2O NPs (125 µg/kg) and Metribuzin intoxication . f : treated group with Ag/Ag_2O NPs (62.5 µg/kg) and Metribuzin intoxication .

1.4.2.3.4.1. Histopathological study of kidney

Histopathological analysis of rat kidney sections in the different experimental groups showing effect of Metribuzin and protective effect of treatment with different doses of ZnO NPs and Ag/Ag_2O NPs. kidney sections of control group showing normal architecture of kidney cells. For treated group with Metribuzin showing, it was noted that Metribuzin caused a serious damage in the kidney , reveal degenerative changes, atrophy, capsule distortion, and inflammatory cells. the ZnO NPs treatment groups (2.5 mg/Kg, 5 mg/Kg) significantly reduced the extent of the damage and provided significant improvement in glomerular and tubular structure.

Kidney of rat treated with higher dose Ag/Ag_2O NPs (125 µg/kg)+ Metribuzin; showing tubular dilation and cellular infiltrations. Finally, the kidney of rat treated with low dose Ag/Ag_2O NPs (62.5 µg/kg)+ Metribuzin; showing glomeruli and tubules were better preserved with low-dose. However,some tissue injury was observed in them.

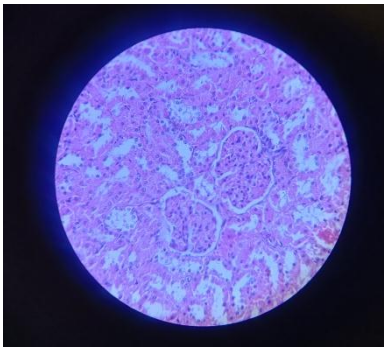

(a)

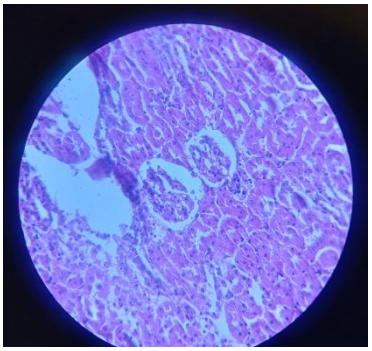

(c)

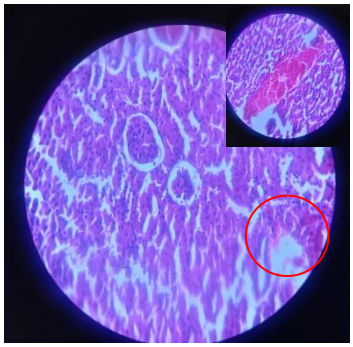

(e)

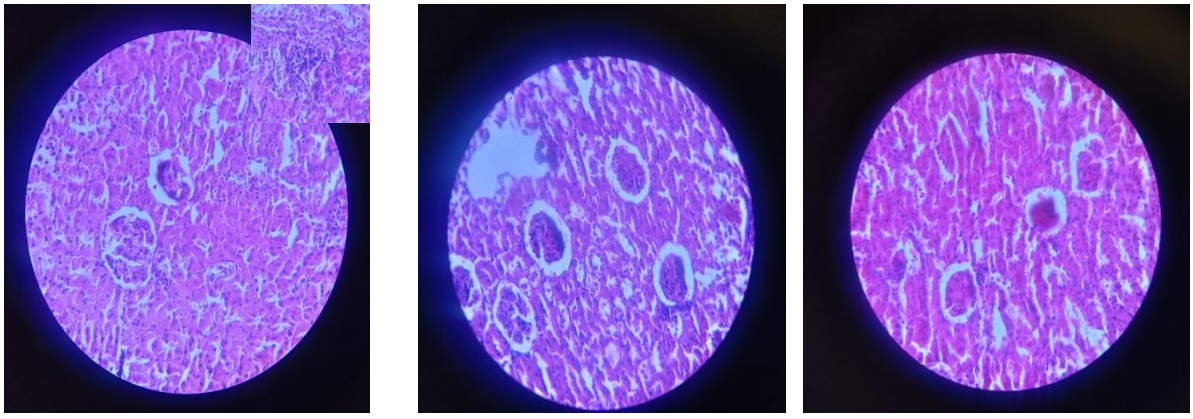

(b) (d) (f)

Figure(35): Photomicrographs of rat Kidney sections in the different experimental groups showing effect of Metribuzin and protective effect of treatment with different doses of ZnO NPs and Ag/Ag_2O NPs. a: control group, b: treated group with Metribuzin , c-d: treated group with ZnO NPs (2.5 mg/Kg, 5 mg/Kg) with Metribuzin intoxication, e-f: treated group with Ag/Ag_2O NPs (125 µg/kg, 62.5 µg/kg) with Metribuzin intoxication

1.4.2.3.4.3. Histopathological study of spleen

Sections of splenic tissues of all rats groups did not show any significant recovery. With the exception of the higher concentration group of Ag/Ag_2O NPs (125 µg/kg,), , Histopathological study displayed deleterious alterations in their spleen tissues where that this dose cause haemorrhagic splenities.

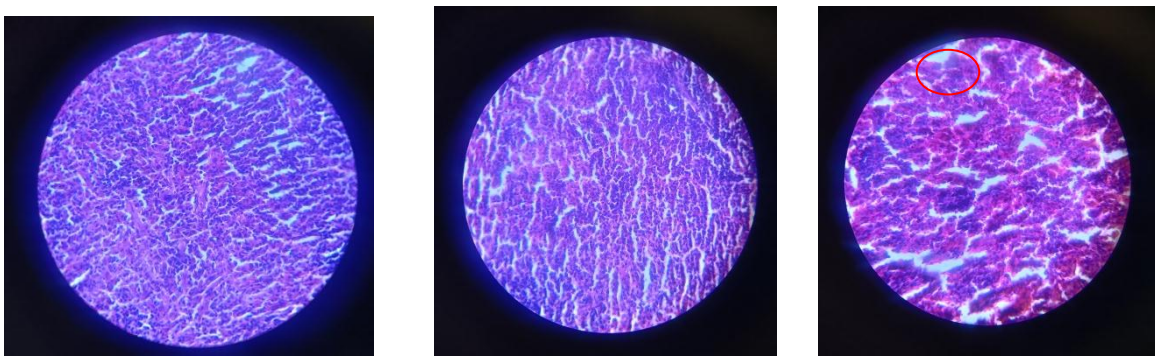

(a) (c) (e)

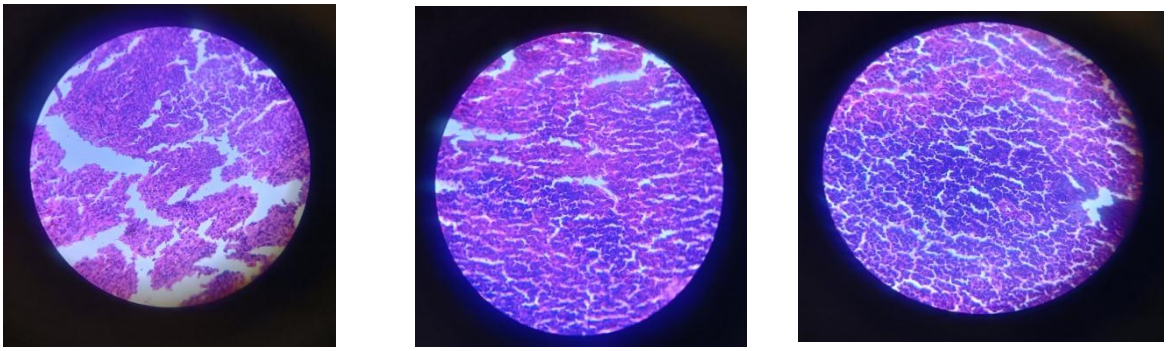

(b) (d) (f)

Figure(36): Photomicrographs of rat spleen sections in the different experimental groups showing effect of Metribuzin and protective effect of treatment with different doses of ZnO NPs and Ag/Ag_2O NPS. a: spleen sections of control group, b: spleen of rat treated with Metribuzin , c-d: spleen of rat treated with ZnO NPs (2.5 mg/Kg, 5 mg/Kg) with Metribuzin intoxication, e-f: spleen of rat treated with Ag/Ag_2O NPs (125 µg/kg, 62.5 µg/kg) with Metribuzin intoxication

CHAPTER III

Discussion

2. Discussion

Natural drugs provide limited hope for health restoration due to their non-targeted action, slow absorption, and, in some cases, reduced effectiveness and prolonged recovery times. Recently, biodegradable nanoparticles have been increasingly employed as treatment delivery vehicles because of their excellent bioavailability, superior encapsulation, and targeted drug efficacy (Singh *et al.*, 2018)

The present study was aimed to biosynthesize the Ag/Ag_2O Nps and ZnO Nps using *Olea europaea* leaf extract and to evaluate antioxidant, antibacterial, anti mutagenic and anti coagulant activities, and to determine their biological actevities and hepato-nephroprotector effect against Metribuzin induced toxicity in a rat model .

Ag/Ag2O Nps and ZnO Nps may be synthesized using Olea europaea leaf extract, which is a wonderful and environmentally friendly substitute for conventional physical and chemical methods. It is also sustainable and adaptable. This approach is environmentally friendly and economical because it avoids the use of hazardous chemicals, uses natural materials, and operates in temperate weather. Further functionalization and stabilization are made possible by the presence of bioactive substances in the leaf extract, and precise control over nanoparticle size and shape is made possible by the bio-inspired synthesis approach. On the other hand, toxic substances, extreme temperatures, and a lack of precision in managing the features of nanoparticles are common in physical and chemical procedures.
(Trang et al., 2021) .

For using this simple and friendly process, we analyse the compounds of *O. europaea* var. Chemllali. Our results of phytochemical screening and determination of some phenolic compounds of aqueous extract of dried leaves of *Olea europaea* revealed the presence of various bioactive compounds, including phenolics, flavonoids, tanins,terpenoids and reducter sugers. The total phenolic content, total flavonoids and condensed tanins were found to be 143.279 ± 1.7 ug GAE/mg extract, 6.764 ± 0.025 ug QCE/mg extract,and 16.333 ± 0.12 ug CTE/mg extract respectively.

The HPLC analysis of olive leaf aqueous extract also allowed the identification of eight phenolic compounds: Chlorogenic Acid, Vanilic acid , Caffiec Acid, Vanilin ,p-Coumaric Acid, Rutin , Naringin, Quercetin, All these compounds were previously reported to occur in

olive leaf. (Benavente-García *et al.*,2000) (Paiva-Martins and Gordon, 2001) (Briante *et al.*,2002) (Bouaziz and Sayadi.,2005)

As well-known antioxidants, phenolic chemicals work to prevent free radicals that cause oxidative injury (Aziz , 2012) . The yield of some chemical groups that are more frequentlyemployed in medicine was calculated in this study using aqueous extract of *O. europaea* leaves.

This study demonstrates the manufacture of biogenic AgNPs with an aqueous extract of *O. europaea* acting as a reducing agent. Important biological components found in the *O. europaea* extract have been employed in green synthesis as capping agents and reductants. Plant material contains polyphenols, which are frequently crucial to these activities. The methods used are straightforward, safe for the environment, and typically involve one pot. High polyphenol extracts function as capping and chelating/reducing agents for nanoparticles (Kharissova *et al.*,2013) .

The reduction of Ag+ ions into Ag0 ions during the creation of biogenic AgNPs was easily observed visually and by UV-Vis spectroscopy. After 30 minutes of incubation, it was seen that the *O. europaea* aqueous extract's color changed from yellow to dark brown, indicating the creation of silver nanoparticles. This was achieved by adding the aqueous extract to the volumetric flask containing the AgNO3 solution. The UV-Vis spectra's absorption peak at 400 nm for all incubation durations further supported its production.
. As a result, the synthesis of biogenic AgNPs took 30 minutes, offering a simple and quick procedure. This was a significant benefit of biological methods over other approaches that used different primary biological material because they are typically synthesized in 30 minutes or less (Padalia *et al*., 2015; Lakshmanan *et al.*, 2018; Chandran *et al.*, 2006). Moreover, Ag-O is represented by the vibration band at 564 cm-1. AgNPs have been identified as the source of the fingerprint region between 1000 and 400 cm−1**(**Tedjani *et al* ., 2022).

Many functional groups found in *Olea europaea* L. extract, such as carbonyl, carboxyl, amide, and phenols, serve as capping and bio-reducing agents for the environmentally friendly production of Ag/Ag_2O (Nanaei *et al*., 2019). These groups are essential to the interactions, binding, and stability of Ag and the extract molecules in the end product (Jose Luis and Du Wessel, 2018).

The average size distribution of biosynthesized Ag/Ag_2O NPs is principally 45 nm. In the image, deformed spherical shaped particles are shown for Ag/Ag_2O NPs greater than 60 nm in size due to *Olea Europaea* leaf extract lacks or contains too many bioactive agents, which leads to reduced interaction between the bioreducing agents and the precursor Ag.

SEM revealed that biogenic Ag/Ag_2O NPs with spherical and oval forms are widely distributed. It was found that the maximal two peaks (38.201 and 32.555) were, respectively, 24 nm for Ag and 26 nm for Ag_2O. Using plant extracts as reducing agents, AgNPs ranging in size from 2 to 75 nm have shown comparable results(Chandran *et al.*, 2006) (Tripathy *et al.*, 2009) (Huang*et al* 2007) (Salari *et al.*,2019) .

Fresh leaf extract of *O.europaea*, which contains reducing and stabilizing agents such flavonoids and terpenoids, was used to create ZnO NPs . The ocular inspection verified the production of ZnO NPs. The leaf mixture's color turned to yellow upon adding Zn(NO3)2.6H2O, signifying the production of ZnO NPs. A powder that was yellowish-white was produced after calcination. This observation was in line with the findings of Khan et al. (2019).

Surface plasmon resonance is responsible for the unique optical properties of NPs, and it is mostly dependent on their size and shape. ZnO NPs exhibited strong absorption between 220-380 nm (Fadillah *et al.*,2021**)**.

FTIR analysis was performed on the green produced zinc oxide nanoparticles (NPs). The broad signal observed at 457 cm-1, which is consistent with the expected characteristic peak for zinc oxide, indicates the production of Zn-O bonds (Handore et al., 2014). This observation is consistent with ZnO being synthesized or present in the material under analysis. All things considered, the infrared spectrum offers insightful information about the molecular makeup and bonding relationships of the ZnO and extract, supporting a thorough comprehension of their chemical characteristics.

ZnO NPs' size and crystalline structure were ascertained by XRD analysis. ZnO was determined to have a particle size of 18.79 nm. Drawing conclusions from the microscopic analysis, a spherical and short rod shape is formed. ZnO nanoparticles have an average size distribution between 40 and 60 nm, according to an analysis of particle size distribution histograms. The presence of zinc and oxygen is confirmed by the EDX peaks, which amply demonstrates the creation of ZnO NPs.

Leaf extracts from Euphorbia sanguinea (Ekennia et al. 2021), S. persica (Alharthi et al.

2020), and Costus woodsonii (Khan et al. 2019) showed similar study.

Antioxidants play a critical role in preventing the damaging effects of free radicals and stopping the domino effect they start. A substance's potential to neutralize reactive species is indicated by its antioxidant activity (He et al., 2017).
The antioxidant activity of the aqueous extract of Olea europaea leaf, Ag/Ag_2O NPs, and ZnO NPs was examined using antioxidant assays, DPPH radical scavenging assay, ferric reducing antioxidant power, and total antioxidant capacity (TAC) in order to assess the antioxydant potential of the nanoparticles.

When compared to Ag/Ag_2O NPs, the leaf extract showed greater scavenging activity at lower concentrations. Nonetheless, the scavenging activity was 60.0% and 93.3% for the leaf extract and 67.1% and 95.2% for Ag NPs at doses of 62.5 and 125 µg/mL, respectively. At increasing concentrations of both nanoparticles, the TAC and FRAP values increased for the nanoparticles. At a concentration of 200 µg/mL, Ag/Ag_2O Nps exhibited the most noteworthy antioxydant activity, surpassing those of ZnO Nps at the same concentration.

In contrast to vitamin C, Nadour et al. assessed the antioxidant capabilities of phenolic compounds found in the O. europaea L chamlali variety. It was discovered that important tests for iron reduction and hydrogen peroxide (H2O2) scavenging were carried out to ascertain the antioxidant properties. Strong reducing powers were shown by all of the drugs that were examined (Nadour et al., 2012).
It's critical to recognize that increased Ag/Ag_2O NP concentrations may have unfavorable effects or cause oxidative stress, which may affect the scavenging activity of these particles. Therefore, it's critical to balance the intended antioxidant effects with any potential cytotoxicity or negative effects linked to increased nanoparticle concentrations (Balkrishna *et al.*,2021) .

Nanoparticles may have a mild antioxidant impact at lower concentrations, most likely by reducing reactive oxygen species (ROS) and oxidative stress. Higher doses of nanoparticles, it is crucial to understand, may cause oxidative stress and adversely impact cellular function. One of the main causes of fatalities and persistent diseases is bacterial infection. Due to their potent effects and low cost, antibiotics have long been the treatment of choice for bacterial illnesses. Nonetheless, a number of investigations have offered concrete proof that the

evolution of bacterial strains resistant to several drugs is a direct result of the extensive use of antibiotics. Indeed, the abuse of antibiotics has recently led to the development of super-bacteria, which are resistant to almost all antibiotics (Hsueh, 2010).

Since nanomaterials act by making direct contact with the bacterial cell wall without having to penetrate the cell, the majority of antibiotic resistance mechanisms do not apply to nanoparticles (NPs). This suggests that NPs may be less likely than antibiotics to encourage bacterial resistance. As a result, intriguing novel NP-based compounds with antibacterial activity have received a lot of attention (Wang *et al.*,2017).

When testing the antibacterial activityof ZnO NPs and Ag/Ag_2O NPs in solid media by well diffusion method, we observe better activity of silver compared to zinc oxid nanoparticles. On the other hand, when studying the kinetics of antibacterial activity in liquid media, we notice that both nanoparticles have a very effective role in eliminating the growth of bacteria or delaying their growth. The lack of ZnO NPs activity in solid media is likely due to The dissolution levels of ZnO NPs. Many reports have confirmed that ZnO tends to dissolve under aqueous, acidic, and biological conditions (Choi *et al.*,2014) (Zheng *et al*.,2011) (Saliani *et al.*,2015) (Yan X *et al.*,2015) .

However, the dosages and physicochemical characteristics of the materials under test had a significant impact on the ZnO dissolution levels. ZnO nanoparticles' density, agglomerate/aggregate size, and specific surface area appear to be the key physicochemical properties influencing the kinetics of dissolution. According to Cardoso et al. (2021), ZnO nanoparticle aggregation/agglomeration and specific surface area have a significant impact on the dissolving kinetics of the particles. Low solubility is also most likely caused by a high ZnO NP concentration.
Ag/Ag_2O NPs' antibacterial activity is dependent on how positively charged Ag+ ions interact with negatively charged bacterial cell walls. This interaction contributes to the antibacterial activity by causing an imbalance in membrane permeability and inhibiting cellular enzymes (Lava *et al.*,2021) .

Because it can release Ag+ ions more gradually and consistently than Ag+ solutions (like AgNO3), the Ag_2O phase, like the Ag phase, can be regarded as a good substitute. Ag+ ions are preferentially released from the (100} facets of the cubic Ag_2O phase due to their increased reactivity compared to the (111) facets. The cubic Ag_2O crystal structure's surface

charges, which are surrounded by the ~100) facets, promote bacterial adsorption and may slightly strengthen the antibacterial effect.

. As such, solid Ag_2O states seem promising as efficient Ag+ solution alternatives in a range of applications. Moreover, the significant release of silver ions into the cell is made possible by Ag/Ag_2O NPs' capacity to adhere to, penetrate, and aggregate within the bacterial cell membrane (Selem et al., 2022).

In line with our findings, a prior work by Skóra et al., (2021) showed that Ag NPs had extremely effective antibacterial action against P. aeruginosa, S. aureus, and E. coli. Furthermore, reactive oxygen species produced by silver nanoparticles alter the structure of DNA and proteins, causing cell death (Sondi and Salopek-Sondi.,2004) (Lee *et al.*, 2003)

It has been proposed that these ions interact with thiol groups in enzymes, like NADH dehydrogenases, to cause disruptions in the respiratory chain, which in turn leads to the death of bacterial cells. Depending on the particular bacteria being targeted, the antibacterial mechanism may change (Mathew et al., 2015).

The ZnO NPs' functionality is responsible for the kinetic antibacterial activity that was detected in this investigation as well. Previous reports have proposed that the bactericidal action of ZnOnanoparticles, which ultimately results in bacterial cell death, may be caused by the negative influence on bacterial cell membranes and the expulsion of cytoplasmic substances. Reactive oxygen species interaction with the cell wall and the production of antimicrobial ions (Zn 2+) are the mechanisms responsible for the inhibition of bacterial activity (Li *et al.*,2011) (Salih and Smail., 2016) .

Zinc oxide nanoparticles are well known for their antibacterial properties, which inhibit the growth of germs by penetrating the cell membrane. Furthermore taken into consideration is the toxicity of nanoparticles, which release harmful ions. Zinc oxide reacts with both alkalis and acids to produce Zn2+ ions because it is an amphoteric substance. Unrestricted Zn2+ ions directly bind to macromolecules like proteins and sugars, stopping all of the bacteria's essential processes (Kelly *et al.*,1998) .

Certain substances, such as antimutagenics, lessen or even completely eradicate the harmful effects of chemicals. The word "antimutagenic" was first used by Novick and Szilard (1952) to describe an agent that has the capacity to reduce the rate or generation of induced or spontaneous mutations. Both artificial and natural variables are included in this group. Two different kinds of anti-mutagenics can be taught, according to Kada et al. (1982). Extracellular desmutagens can inactivate mutagenic chemicals before they reach genetic material.

Conversely, bioantimutagens function inside the cell and aid in the suppression of mutations following DNA damage.

The mutagenicity test, sometimes referred to as the Ames test, is one of the toxicity assessment tests. This assay is approved for the identification of single compounds, mixtures, and environmental materials that have the potential to cause genetic harm and mutate genes. Apart from assessing the synergistic effects of the mixture's constituents, it has also been extensively employed in research to clarify the processes of mutagenesis and antimutagenics agents (Umbuzeiro and Vargas.,2003) The Ames test is based on the use of Salmonella Typhimurium TA98 strains, which are auxotrophic for the amino acid histidine (His−), meaning they are unable to manufacture the histidine required for growth, to induce reverse mutations. The histidine operon, which is intended to identify DNA alterations such frameshifts and base pair substitutions, is mutated in a variety of ways in these strains.

Unless additional mutations develop at the site of existing mutations or in neighboring genes that restore histidine synthesis, they are unable to grow in a minimum culture media without histidine. The test is known as a reversal test because these mutant cells can proliferate and form colonies in the absence of histidine. By counting colonies that proliferate in minimum medium following exposure of a cell population to the chemical under test, the number of revertants can be readily determined (Ames *et al.,* 1973).

Human carcinogenicity is a classification given to nitroaromatic compounds, and 1-NP's presence in food poses a serious threat to public health. The Ames mutagenesis test shows that nitroreduction of 1-NP is an essential process contributing to mutagenesis. Salmonella typhimurium TA98 demonstrates heightened susceptibility to mutagens nitroaromatic. One of the genotoxicity tests now in use, the Salmonella reverse mutation assay is a part of numerous batteries used to evaluate genotoxic danger (Cimino, 2006) .

Illnesses, including cancer, stem from DNA damage that hasn't been sufficiently repaired by the body's own repair mechanism. Genetic mutations are caused by inadequate repair of DNA damage. In somatic cells, repair defects may lead to the development of tumors, while in germ cells, failure to repair raises the risk of genetic disorders in the progeny (Benigni R., 2005). Moreover, metal ions such as silver have the ability to strongly bind with either O or N in the mutagenic chemical complex (Kadriye and Canan 2021) . The best strategy to avoid cancer

and genetic illnesses in daily life is to use anti-mutagenic and anti-carcinogenic drugs (Kim et al.,2000) .

Regarding our results of antimutagenic activity of the Ag/Ag_2O Nps and ZnO Nps biosynthetised by aqoues extract *O. europaea* leaves against 1-NP in S. typhimurium TA98, this study showed strong anti-mutagenic effect of the both nanoparticles at 250 ug/ml concentration against 1-NP (200 ng/plate) ,70 % and 76.4 % respectively, when it increased in a dose-dependent manner .

Sarac and colleagues (2018) recently reported that silver nanoparticles biosynthesised from Streptomyces griseorubens AU2 had anti-mutagenic capabilities. At 250 µg/plate, these nanoparticles shown the highest anti-mutagenic activity against 4-Nitro-o-phenylenediamine (4-NPD: 3 µg/plate) on S. typhimurium TA98. In a different study, Kadriye and Canan (2021) found that biosynthesized silver nanoparticles using Rosa canina waste seed (40 µg/plate) had a high antimutagenic impact (more than 60% suppression) on S. typhimurium TA98 against 4-NPD at 0.1 ml/plate.

Anti-mutagenic substances perform a variety of essential roles and are functional at the cellular level. These include changing the actions of enzymes in charge of detoxifying mutagens, restricting the actions of enzymes in charge of creating mutagen metabolites, ensnaring electrophiles, impeding metabolic activation, scavenging reactive oxygen species, and protecting DNA's nucleophilic sites (Ratnam *et al.*,2006) (Sarac *et al.,* 2018).

In the studies, silver nanoparticles' outstanding nitric oxide scavenging activity was noted in a dose-dependent way (Gonzalez-Ballesteros *et al.*,2019) .

The components of the nanoparticles are biocompatible and can be utilized as anticoagulants because the manufacture of the particles via plant-mediated synthesis is a straightforward process. By mixing the synthesized nanoparticles with recently drawn blood, the anticoagulant qualities of the particles were investigated.

Blood clot was observed in the vial control while there was no blood clot witnessed in the vial of Ag/Ag_2O NPs at 150 ppm concentration, and an other vial containing ZnO NPs 50 ppm, and stable for a longer time. This confirms that the silver nanoparticles and zinc oxide nanoparticles can be used as a blood anticoagulant. This is in accordance with the results obtained by Jeyaraj *et al*., (2013) , El-Waseif *et al.,* (2022) and Ahmed *et al*., (2024)

While this anticoagulant property has potential in nanomedicine for the management of blood clotting disorders, it also highlights the importance of ensuring that when these molecules are

used as drug carriers or coating agents on medical instruments, they do not cause no blood clotting on contact. (Singh *et al.*,2015) .

There is substantial evidence suggesting that nanoparticles can enhance the efficacy of conventional anticoagulant agents, reducing drug concentration, administration frequency, and treatment costs (Lateef *et al.,* 2017) .

Because of changes in lifestyle, cardiovascular illnesses are now a leading cause of mortality and disability globally. The primary ailment is atherosclerosis, which typically takes years to manifest and is not always identified right away. Modifying risk factors lowers mortality and morbidity. Thromboembolic illness has been successfully prevented by anticoagulant medications. The synthesis of plasmin, an enzyme that breaks fibrin bonds and dissolves blood clots, may be stimulated in part by ZnO NPs (Camara e*t al.*,2011) .

Biogenic Ag/Ag_2O NPs and ZnO NPs demonstrated efficacy in this investigation, suggesting potential clinical uses for thrombosis and associated diseases prevention.
Metal nanoparticles constitute valuable tools to improve the effectiveness of current treatments and improve patient compliance with treatments. Therefore, discovering a way to produce nanoparticles with fewer defects related to their physicochemical properties, such as stability, biocompatibility and safety for biochemical applications, represents a major challenge for researchers.

As for studying the toxicity of nanoparticles and their effect on the body of rats, in this experiment the groups that were injected with ZnO NPs (50 and 100 mg/kg) were not severely affected, while the groups treated with Ag/Ag_2O NPs were greatly affected at both concentrations (2.5 and 5 mg/kg).

Rats were selected as the in vivo model of exposure because of their similarity with human metabolic, biochemical and physiological pathways (Singh *et al.,* 2018).

Li *et al.*,(2012) , studied the biodistribution of zinc oxide nanoparticles administered orally or by ip injection to a month and a half-old mice. No obvious adverse effects were detected in mice orally treated with zinc oxide nanoparticles during the tow weeks of study. However, intraperitoneal injection of 2.5 g/kg body weight given to mice showed zinc accumulation in the heart, liver, spleen, lungs, kidneys, and testes. An approximately nine-fold increase in zinc oxide nanoparticles in the liver was observed after 72 hours. Zinc oxide nanoparticles have

been shown to have better biodistribution efficacy to the liver, spleen, and kidneys compared to orally fed mice.. For this reason, this method of injection was chosen in our study.

Zinc oxide nanoparticles are known to be one of those inorganic mineral oxides that meet all the body's requirements and can therefore be safely used as a medicine, as a preservative in packaging and as an antimicrobial agent (Baum *et al.*,2000) (Hiller and Perlmutter ,1971) .

Because zinc is essential for many biological processes, including immune system function, cell division, growth, enzyme activity, DNA synthesis, and protein synthesis, zinc oxide (ZnO) is widely used in the food industry as a Zn supplement, nutrient fortifier, and agricultural fertilizer (Gupta and Yadav, 2014). Zinc is a vital mineral that the body needs to function, and the recommended daily consumption for males and women is 11 mg and 8 mg, respectively (NIH, 2021) .

So, ZnO is generally considered as a material with low toxicity, because zinc is a principle trace element in the human body and is commonly present in foods or added as a nutritional supplement, zinc has a little attention during assessment of toxicity of nanoparticles.

AgNP exposure, however, can have negative effects, such as drug interactions due to AgNPs' inhibitory effect on microsomal enzymes (Kulthong et al., 2012). Following absorption, silver nanoparticles spread widely, have the ability to agglomerate, and may activate the immune system, all of which may have unclear repercussions. The majority of AgNP toxicity research has been done in vitro using particles with sizes ranging from 1 to 100 nm. Although the duration of the animal trials that are now available is somewhat short, data have demonstrated that AgNPs produce histological abnormalities in the skin ,liver, spleen, and muscle (Korani *et al.*,2013) (Moreno *et al.*,2021) .

Previous research like Recordati et al. (2016)study, which discovered enhanced distribution of silver in tissues and acute negative effects linked to the usage of nanoparticles, suggest that the toxicity of the nanoparticles may be due to their small size. These findings are in line with other research that evaluated the short-term and high concentration effects of Ag/Ag_2O NPs in rats and showed increased production of ROS, oxidative stress, hepatotoxicity, serum biochemical changes, and damage to DNA and liver tissue in addition to increased lipid hydroperoxidation (LHP). It is noteworthy that smaller particles have a higher probability of releasing silver ions from their surface compared to larger ones. This phenomenon could perhaps explain the observed indications of oxidative stress and hepatotoxicity. It is unclear,

though, that the toxicity of silver nanoparticles is the only cause of these effects (Recordati *et al.*, 2016) (Cerqueira *et al.*, 2018) .

The most widely used pesticide in Algeria is called metribuzin (4-amino-6-tert-butyl-4,5-dihydro-3-methylthio-1,2,4-triazin-5-one), a herbicide that is used to vegetable crops with the specific goal of controlling grassy and broadleaf weeds. Metribuzin is frequently used on tomatoes, potatoes, peas, lentils, and soybeans (Medjdoub *et al.*,2011) .

The presence of pesticides in food is a great public concern since they may have both acute and chronic effects on health (Hernández *et al.*,2013) .

There is evidence from animal studies that Metribuzin may cause adverse health effects, such as liver enzyme activities, histopathological changes, endocrine modifications , kidney alterationsand fetus toxicity (Porter *et al.*,1993) (USEPA .,2003) .

This is confirmed by our current study, where we found that giving rats a dose of 110 mg/kg p.o of Metribuzin e for 21 days led to damage the liver and kidneys, where a main hematological response of rats to exposure of metribuzin was a decrease of Hb and PLT values compared to the control group.

Pesticides may have an impact on erythroid tissue, which could explain the study's findings of decreased Hb concentration and red blood cell count. Because circulating erythrocytes have a shorter lifespan and less Hb is biosynthesised, anemia is caused by pesticide residue poisoning. (El-Sayed *et al.*,2007). Kadache L et al. (2017) also documented comparable alterations in the haematocrit value, hemoglobin, and erythrocyte counts.

Significant increase in serum ALT, ALP, Acid uric and urea suggesting hepato-renal failure, concomitant reduction in haemoglobin and plattete level,with a significant imbalance of oxidative stress in the liver and kidney, respectively as evidenced by elevated MDA levels, reduced GSH contents, compared to the control group. All this is confirmed by histopathological observations of liver and kidney tissue . A significant increase of marker enzymes in serum is an indication of damage in the liver plasma membrane, due to the oxidation of polyunsaturated fatty acids in the plasma membrane by ROS (Hassan et al., 2014).

This study is also consistent with previous studies (Medila et al., 2021) (Kadeche et al.,2017) .

Glutathione is the primary line of defense against oxidative stress; when groups are exposed to toxicants, their glutathione levels decrease, indicating cellular damage. The therapy groups experienced a reduction in this cellular damage. Our present findings align with earlier research findings(Karthikeyan *et al.*,2012). For instance, Medila *et al.,* (2021) reported a decrease in antioxidant defense due to reduced expression of antioxidants during hepatocellular damage. According to Karthikeyan et al. (2014), animals exposed to toxins saw a decrease in GSH levels, which resulted in cellular damage. The recovery of GSH and GSSG in the therapy groups in our study points to a reduction in liver damage. The therapies' ability to neutralize free radicals and prevent GSH depletion may account for their hepatoprotective qualities (Zeng *et al.*,2014). This last point is confirmed by ours results obtained in this study.

As is known, a lot of work has been done on medicinal implications of Ag/Ag_2O NPs and ZnO NPs , but to the best of our knowledge, this is the first ever piece of work to evaluate the nephro-hepatoprotective efficiency of biosynthesized Ag/Ag_2O NPs and ZnO NPs using *O. eurapaea* leaves aqous extract against metrubizin toxicity in albinos rats.

After 21 days the groups co-treated with zinc oxid nanoparticles, there were a very clear effect in some biochemical parameters and histopathological of liver, kidney and spleen. Where the decrease of PLT count ($p \leq 0.001$) observed in groupe treated with hight dose 125ug/Kg .bw of Ag/Ag2O NPs, this study may be due to the effect of anticoagulante of this nanoparticles , showed in our study previously .

The both ZnO NPs groups (at dose 2.5 and 5 mg/kg) were obtained a notable enhancing effect in preventing the damage caused by the herbicide in rats of control positive group. Where it exhibit significant restoration in above indices towards normal when compared with Metribuzin in toxicated group . Vascular congestion, disruption of glomerulus epithelium, dilated Bowman's capsule appeared in kidney tissues of Metribuzin rats . The distal convoluted tubules were significantly injured by metribuzin, according to the results. On the other hand, green generated ZnONPs cured the kidneys of Metribuzin-treated rats. Significant improvement was seen in kidney tissues with ZnONPs, and ALT and AST levels significantly improved in groups receiving zinc oxide nanoparticles in addition to metribuzin. which demonstrates the nephro-hepatoprotective function of zinc oxide nanoparticles on albino rats' livers when Metribuzin causes toxicity.

Since zinc oxide nanoparticles are innocuous in low doses, they stimulate certain enzymes in man and plants and suppress diseases (Siddiqi *et al.*,2018) (Goma *et al*.,2021) .

As for Ag/Ag_2O NPs co-admenisted 133.33 ug/kg, our study provided evidence that co-administration of Ag/Ag_2O NPs at 62.5 ug/kg b.w to Metribuzin intoxicated, significantly reduced serum liver enzymes level compared with intoxicated rats. This may indicate that at low dose the used agents act as effective hepatoprotective against liver dysfunction caused by pesticides toxicity. The intake of Ag/Ag_2O at 62.5 ug/kg immediately with Metribuzin ingestion presented in this study was beneficial in the prevention of this pestecide induced liver and kidney peroxidation as well as increases the total antioxidant power of hepatocytes.

Our results were supported by the histopathological examination of liver tissues, which clarified that, except the liver structure is becoming again like the control group but with few infiltrations.

On the contrary, our results showed that co-treatment with Ag/Ag_2O NPs at 125 µg/kg combined with 133.33 mg/kg of Metribuzin resulted in hepatocellular changes in the liver. Oxidative stress and hepatotoxicity biomarkers were assessed by measuring MDA, GSH, and the activities of liver enzymes (ASAT/ALAT). It was concluded that the Ag/Ag_2O NPs group at 125 µg/kg may have caused liver alterations, increased infiltration in the central vein. Oxidative stress can lead to liver fibrosis by increasing the activation of stellate cells and collagen synthesis. Moreover, exposure to hepatotoxins can destruction perivenular hepatocytes, which have lower antioxidant defenses (Anjum *et al.*,2023) , the same effect in kidney tissue.

Inspite of that, the high toxicity of silver nanoparticles does not implicate that they should be banned for biomedical applications; however, further toxicological investigations in vivo have to be developed for evaluating menaces of occupational or environmental exposure to nanomaterials.

The impact of nanomaterial size on cytotoxicity and cellular uptake was the subject of numerous earlier investigations (Shan et al., 2014). Controversial reports on the function of AgNP in controlling the inflammatory response have demonstrated that AgNP toxicity affects liver cells by inducing inflammation, which in turn causes various forms of cell death (Lee and Jun.,2019).

As for the spleen, there was no significant effect of the pesticide where keeping the structural integrity of spleen. However, there was a negative effect on the rats treated with the strong dose of Ag/Ag_2O NPs. This confirms the toxicity of silver nanoparticles in high concentrations. It was established that there is a dose-time-and size-dependent relationship

between AgNP and cell toxicity (Ferdous and Nemmar, 2020) . Although Ag NPs are extremely toxic to cancer cells, their use is limited since they are also harmful to normal cells . In continuation, when the toxicity of Ag NPs (10 μg/mL) was examined in human mesenchymal stem cells, DNA injury, impaired functioning, and cell death were detected (AshaRani *et al*.,2009) (Hackenberg *et al.*,2011) .

While for ZnO, it is less toxic because it needs to be in a very high concentration in order to cause toxicity, as indicated by the results of our study of its toxicity, as also indicated by Sharma *et al* study (2012) , where it was used in a high dose of ZnO NPs (300 mg/kg) caused oxidative stress in mice, which resulted in DNA damage, which allowed it to have a wider scope in medical uses safely, as one of the elements needed for the body, as we mentioned previously.

Our results lead us to propose the potential application of biologically produced nanoscale silver or zinc oxide particles for the treatment of nephro-hepatocellular diseases. Extensive research might be conducted to clarify the precise molecular pathways underlying the inhibition of cell development, potentially leading to their application as therapeutic or chemopreventive drugs in the future.

Conclusion

CONCLUSION

Nanotechnology has become an essential and highly effective technology in the fields of pharmaceutical, healthcare, biomedicine and drug delivery. Nanoparticles are being developed for drug delivery to improve drug dissolution rates, leading to improved absorption and bioavailability. Nanoparticle synthesis using biological agents is more environmentally friendly, more cost-effective and a highly focused area of research compared to chemical and physical methods. This approach reduces the use of harmful reagents and solvents, improves the material and energy efficiency of the chemical process, and promotes the design of non-toxic products.

In our study, we used *Olea europaea* leaf extract for nanoparticle synthesis for tow reasons, using a safe, inexpensive and environmentally friendly method to manufacture nanoparticles on the one hand, and in an effort to exploit and valuing natural resources and neglected materials on the other hand, because olive leaves are considered a sort of waste product, this waste product is not profitable; olive leaves are often used as animal feed or simply burned with excess branches gathered.

Our study revealed that olive leaves contain numerous antioxidants that may be to play a significant role in the green synthesis of nanoparticles.

The current study used the aqueous extract of Olea europaea leaves to biosynthesize zinc oxid nanoparticles and to synthesize silver/silver oxide nanoparticles, which were then characterized. The biological activities of eco-friendly produced nanoparticles were assessed in this work both in vitro ,and in vivo against Metribuzin-induced toxicity in Wister rats. Based on the results obtained, we can make the following conclusions:

Through a variety of analyses, including HPLC, Olea europaea has been shown to be exceptionally rich in bioactive components both qualitatively and quantitatively. This has allowed us to discover a new source of bioactive compounds that may be used to treat a wide range of illnesses.

FT-IR, UV-Vis, EDX, XRD, and SEM investigations demonstrated the effective synthesis of zinc oxide and silver/silver oxide nanoparticles. This suggests that the bioactive substances found in Olea europaea leaves are responsible for reducing and encapsulating metal into metal nanoparticles.

In the future, Ag/Ag_2O NPs and ZnO NPs may be used as nanoantibiotics to treat bacterial infections that harm humans since they demonstrate strong antibacterial activity against a variety of microorganisms.

Mutation is an important factor in inducing carcinogenesis. This study reports that a stronger antimutagenic activity of Ag/Ag_2O NPs and ZnO NPs at 250ug/plate concentration, wich used to reduce the exposure of mutation and its inducing agent.

It is possible to interpret the strong antimutagenic activity of both nanoparticles in this study, which increased in a dose-dependent manner against 1-NP in S. typhimurium TA98 as an alteration of the actions of enzymes involved in mutagen detoxification and DNA nucleophilic site protection.
In this study also, there is substantial evidence that Ag/Ag_2O NPs and ZnO NPs can enhance the efficacy of conventional anticoagulant agents.

Thanks to the sub-acute toxicity investigation, the green-synthesized Ag/Ag_2O NPs and ZnO NPs can be safely and effectively used at low concentrations for therapeutic purposes.

Our preventive treatment with Ag/Ag_2O NPs and ZnO NPs has shown improvements in physiological parameters, particularly offering protective effects against pesticide -induced toxicity.

The positive impact of Ag/Ag_2O NPs and ZnO NPs on restoring liver enzymes and biochemical markers demonstrates their effectiveness against pesticide toxicity, which typically causes metabolic imbalances and impairs liver and kidney function. These nanoparticles also exhibit strong hepatoprotective and nephroprotective properties.

Our research indicates that Ag/Ag_2O NPs and ZnO NPs reduce oxidative stress induced by metribuzin by minimizing radical activity, repairing oxidative damage by reducing lipid peroxidation in the liver and kidneys, and enhancing antioxidant defenses. This shows another protective mechanism against diseases related to pesticide exposure.

Furthermore, our treatment demonstrates significant protection at the cellular level, stabilizing cells against oxidative stress-induced damage in the liver and kidneys.

This suggests these nanoparticles could mitigate damage caused by metribuzin and similar substances.

In conclusion, Ag/Ag_2O NPs and ZnO NPs have proven to be highly biologically effective across various levels, offering promising potential for their application in the medical field to address a range of health problems.

Perspective

Considering the importance of these results, they open the door to more thorough research and experimental strategies that should allow us to pinpoint the following:

- O. europaea is a great resource for creating several kinds of nanoparticles.
- The ability of ZnO NPs and Ag/Ag_2O NPs to prevent several chronic diseases, such cancer.
- Possibility of Ag/Ag_2O NPs and ZnO NPs interaction with the reverse transcriptase enzyme to produce COVID-19 and HIV inhibitors.
- The possibility of using these outcomes to launch a start-up following the acquisition of a patent

References

REFERENCES

1) Abbasi, B. H., Nazir, M., Muhammad, W., Hashmi, S. S., Abbasi, R., Rahman, L., & Hano, C. (2019). A comparative evaluation of the antiproliferative activity against Hepg2 liver carcinoma cells of plant-derived silver nanoparticles from basil extracts with contrasting anthocyanin contents. *Biomolecules*, *9*(8), 320.

2) Abdel-Fattah WI, Ali GW. (2018). On the anti-cancer activities of silver nanoparticles. *J Appl Biotechnol Bioen,* 5(1):43–46.

3) Abderrahim, K ., Bouanane, S., Baba Ahmed, Fz ., Merzouk, H. (2020). effects of chlorpyrifos on brain oxidant/antioxidant parameters in pregnant/lactating rats and their offspring. *Revue Agrobiologia*, 10(2): 2036-43

4) Abdollahi, M., Ranjbar, A., Shadnia, S., Nikfar, S., & Rezaie, A. (2004). Pesticides and oxidative stress: a review. *Med Sci Monit*, *10*(6), 141-147.

5) Ago, H. (2015). CVD growth of high-quality single-layer graphene. *Frontiers of Graphene and Carbon Nanotubes: Devices and Applications*, 3-20.

6) Ahmed, N. A., Othman, A. S. (2024). Green fabrication of ZnO nanoparticles via spirulina platensis and its efficiency against biofilm forming pathogens. *Microbial Cell Factories*, *23*(1), 92..

7) Ahn, M.-R., Kumazawa, S., Usui, Y., Nakamura, J., Matsuka, M., Zhu, F., & Nakayama, T. (2007). Antioxidant activity and constituents of propolis collected in various areas of China. *Food Chemistry, 101*(4), 1383-1392.

8) Aiach, A., Ohmann, E., Bodner, U., & Johanningmeier, U. (1992). A herbicide resistant Euglena mutant carrying a Ser to Thr substitution at position 265 in the D1 protein of photosystem II. *Zeitschrift für Naturforschung C*, *47*(3-4), 245-248.

9) Akhgari, M., Abdollahi, M., Kebryaeezadeh, A., Hosseini, R., Sabzevari, O. (2003). Biochemical evidence for free radical induced lipid peroxidation as a mechanism for subchronic toxicity of malathion in blood and liver of rats. *Hum Exp Toxicol*,22:205–211

10) Al-Azzawie, HF., Alhamdani, MS. (2006). Hypoglycemic and antioxidant effect of oleuropein in alloxan-diabetic rabbits. *Life Sci,* 78(12): 1371–1377.

11) Alharthi F. A., Alghamdi A. A., Alothman A. A., Almarhoon Z. M., Alsulaiman M. F. & Al-Zaqri N. (2020) Green Synthesis of Zno Nanostructures Using Salvadora Persica Leaf Extract: Applications for Photocatalytic Degradation of Methylene Blue Dye. *Crystals*, 10(6).

12) Al-Qarawi, AA., Al-Damegh, MA., ElMougy, SA. (2002). Effect of freeze dried extract of Olea europaea on the pituitary-thyroid axis in rats. *Phytother Res*. 16(3):286-7.

13) Alsammarraie, F.K. ., *et al*. (2018).Green synthesis of silver nanoparticles using turmeric extracts and investigation of their antibacterial activities Colloids Surf. *B-Biointerfaces*, 171 , pp. 398-405

14) Altammar, KA. (2023). A review on nanoparticles: characteristics, synthesis, applications, and challenges. *Front Microbiol*. 17;14:1155622. doi: 10.3389/fmicb.2023.1155622.

15) Amato. R D., Falconieri, M., Gagliardi, S, Popovici E, Serra E, Terranova G and Borsella E . (2013). Journal of Analytical and Applied Pyrolysis Synthesis of ceramic nanoparticles by laser pyrolysis : From research to applications J. Anal. Appl. Pyrolysis 104 461–9

16) Ambrose J., Kullappan M., Patil S., Alzahrani K., Banjer H., Qashqari F.I., Raj A.T., Bhandi S., Veeraraghavan V., Jayaraman S., et al. (2022). Plant-Derived Antiviral Compounds as Potential Entry Inhibitors against Spike Protein of SARS-CoV-2 Wild-Type and Delta Variant: An Integrative In SilicoApproach. *Molecules.* 27:1773.

17) Ambrose J., Kullappan M., Patil S., Alzahrani K., Banjer H., Qashqari F.I., Raj A.T., Bhandi S., Veeraraghavan V., Jayaraman S., et al. (2022). Plant-Derived Antiviral Compounds as Potential Entry Inhibitors against Spike Protein of SARS-CoV-2 Wild-Type and Delta Variant: An Integrative In SilicoApproach. *Molecules.* 27:1773.

18) Ames BN, Durston WE, Yamasaki E, Lee FD. .(1973). Carcinogens are mutagens: a simple test system combining liver homogenates for activation and bacteria for detection. *Proc Natl Acad Sci U S A.*;70(8):2281–5

19) Anjum, R., Maqsood, H., Anwar, A., Hussain, S., Kinza, A., Mohsin, S., Aslam, S., Kanwal, S., Ajmal, A., Ahmed, T., Ehtsham, M., Hamid, M. (2023). Evaluation the hepatoprotective effect of quercetin against zinc oxide nanoparticles induced toxicity

in mouse model. *Biol. Clin. Sci. Res. J*: 246. doi: https://doi.org/10.54112/bcsrj.v2023i1.246]

20) Antony J.J., Sivalingam P., Siva D., Kamalakkannan S., Anbarasu K., Sukirtha R., Krishnan M., Achiraman S. (2011). Comparative evaluation of antibacterial activity of silver nanoparticles synthesized using *Rhizophora apiculata* and glucose. *Colloids Surf. B Biointerfaces.* 88:134–140.

21) Anu Mary Ealia, S., & Saravanakumar, M. P. (2017). A review on the classification, characterisation, synthesis of nanoparticles and their application. *IOP Conference Series: Materials Science and Engineering, 263, 032019.* doi:10.1088/1757-899x/263/3/032019

22) Armenda´riz, AH de la Torre, A´ JG Ferna´ndez, and GL Gonza´lez, (2014). Encyclopedia of Toxicology || Metribuzin. *, Elsevier Inc (), 327–329.* doi:10.1016/b978-0-12-386454-3.01194-5

23) Armstrong D, Browne R. (1994). The analysis of free radicals, lipid peroxides, antioxidant enzymes and compounds related to oxidative stress as applied to the clinical chemistry laboratory. Adv Exp Med Biol. 366:43-58. doi: 10.1007/978-1-4615-1833-4_4.

24) AshaRani P. V., Mun G. L. K., Hande M. P., and Valiyaveettil S. (2009). "Cytotoxicity and genotoxicity of silver nanoparticles in human cells," *ACS Nano*, vol. 24, pp. 279–290.

25) Ashe B. (2011). A Detail investigation to observe the effect of zinc oxide and Silver nanoparticles in biological system, M.Sc. (Roll NO-607bm004), National Institute of Technology.

26) Atta-ur-Rahman (2023). Studies in Natural Products Chemistry, vol. 79, Elsevier Science, Amsterdam, The Netherlands.

27) Azhar M.U, Akhtar J.; Akram U.; Anjum N.; Quddusi N. (2011). Pharmacological Activity Of Holy Drug-Zaitoon (Olea Europaea Linn.)-Review a b b c a Ind. J. Unani Med. Vol. IV (Issue-2), pp. 85-91,

28) Aziz FM. (2012); Protective effects of the latex of Ficuscarica L. against lead acetate-induced hepatotoxicity in rats. Jordan J Biol Sci 5:175-82.

29) Aziz, N.H.; Farag, S.E.; Mousa, L.A.A.; Abo-Zaid, M.A. (1998). Comparative antibacterial and antifungal effects of some phenolic compounds. *Microbios 93*, 43–54.

30) Bahadar H, Maqbool F, Niaz K, Abdollahi M. (2016). Toxicity of Nanoparticles and an Overview of Current Experimental Models. Iran Biomed J. 20(1):1-11. doi: 10.7508/ibj.2016.01.001.

31) Baig N., Kammakakam I., Falath W. (2021). Nanomaterials: A review of synthesis methods, properties, recent progress, and challenges. *Mater. Adv.* 2 1821–1871.

32) Balkrishna, A., Kumar, A., Arya, V., Rohela, A., Verma, R., Nepovimova, E., ... & Kuca, K. (2021). Phytoantioxidant functionalized nanoparticles: a green approach to combat nanoparticle- induced oxidative stress. *Oxidative medicine and cellular longevity, 2021*(1), 3155962

33) Bali EB, Ergin V, Rackova L, Bayraktar O, Küçükboyaci N, Karasu Ç. (2014). Olive leaf extracts protect cardiomyocytes against 4-hydroxynonenal- induced toxicity in vitro: comparison with oleuropein, hydroxytyrosol, and quercetin. Planta Med. 80(12): 984–92.

34) Banaszkiewicz T. (2010) .Biomonitoring in the assessment of chemical threats to the environment. In: Skibniewska KA, editor. *Contemporary problems of management and environmental protection.* Olsztyn: Univeristy of Warmia and Mazury; pp. 31–41.

35) Baron JM, Wiederholt T, Heise R, Merk HF, Bickers DR. (2008). Expression and function of cytochrome P450-dependent enzymes in human skin cells. *Curr Med Chem.* 15:2258–64

36) Bartolini G.and Petruccelli R. (2002). *Classification, Origin, Diffusion and History of the Olive*, Food and Agriculture Organization of the United Nations, Rome, Italy,

37) Battinelli L., Daniele C., Cristiani M., Bisignano G., Saija A., and Mazzanti G. (2006). "In vitro antifungal and anti-elastase activity of some aliphatic aldehydes from Olea europaea L. fruit," Phytomedicine, vol. 13, no. 8, pp. 558–563

38) Bauer AW, Kirby WM, Sherris JC, Turck M (1966) Antibiotic susceptibility testing by a standardized single disk method. Am J Clin Pathol 45(4):493–496.

39) Baum MK, Shor-Posner G, Campa A (2000) Zinc status in human immunodeficiency virus infection. J Nutr 130:1421S–1423S

40) Behloul M., Lounici H., Abdi N., Drouiche N., Mameri N. (2017).Adsorption study of metribuzin pesticide on fungus Pleurotus mutilus, Int. Biodeterioration & Biodeg., 119, 687–695

41) Bekro, Y. A., Mamyrbekova, J. A., Boua, B. B., Bi, F. T., & Ehile, E. E. (2007). Etude ethnobotanique et screening phytochimique de Caesalpinia benthamiana (Baill.) Herend. et Zarucchi (Caesalpiniaceae). *Sciences & nature*, *4*(2), 217-225.

42) Ben Salem M, Affes H, Ksouda K, Sahnoun Z, Zeghal K M, Hammami S. (2014). *Pharmacological Activities of Olea europaea Leaves. Journal of Food Processing and Preservation, (), n/a–n/a.* doi:10.1111/jfpp.12341

43) Benavente-García, O.; Castillo, J.; Lorente, J.; Ortuño, A.; Del Rio, J.A. . (2000), Antioxidant activity of phenolics from *Olea europaea* L. leaves. *Food Chem68*, 457–462.

44) Benigni R,) (2005) Structure− activity relationship studies of chemical mutagens and carcinogens: mechanistic investigations and prediction approaches, Chem. Rev. 105 (51767–1800.

45) Bhumi G, Savithramma N. (2014). Biological Synthesis of Zinc oxide Nanoparticles from *Catharanthus roseus* (l.) G. Don. Leaf extract and validation for antibacterial activity. *International Journal of Drug Development and Research*. 6(1):208–214.

46) Bianco A., Ramunno, A. (2006). *The Chemistry of Olea Europaea. Studies in Natural Products Chemistry, 859–903.* doi:10.1016/s1572-5995(06)80042-6

47) Bianco A.; Uccella, N. Biophenolic components of olives. *Food Res. Int* (2000), *33*, 475–485.

48) Bisignano G, Tomaino A, Lo Cascio R, Crisafi G, Uccella N, Saija A. (1999). On the in-vitro antimicrobial activity of oleuropein and hydroxytyrosol. J Pharm Pharmacol. 51(8):971-4. doi: 10.1211/0022357991773258.

49) Bleeke, M.S., Smith, M.T. and Casida, J.E. (1985). Metabolism and toxicity of metribuzin in mouse liver. Pestic. Biochem. Physiol., 23: 123-130.

50) Bolognesi C, Merlo FD. (2011) . Pesticides: human health effects. In: Nriagu JO, editor. *Encyclopedia of environmental health.* Burlington: Elsevier; pp. 438–453.

51) Boskou, D. (1996). History and characteristics of the olive tree. In *Olive Oil Chemistry and Technology*; Ed.; Am. Oil Chem. Soc. Press: Champaign, IL, USA,

52) Boskou, D.; Blekas, G.; Tsimidou, M. (2006). Olive oil composition. In *Olive Oil: Chemistry and Technology*, Ed.; Am. Oil Chem. Soc. Press: Champaign, IL, USA, pp. 1–33.

53) Bott J., Störmer A., Franz R. (2014). *Chemistry of Food, Food Supplements, and Food Contact Materials: from Production to Plate.* ACS Publications. A comprehensive study into the migration potential of nano silver particles from food contact polyolefins; pp. 51–70.

54) Bouaziz, M.; Sayadi, S. (2005). Isolation and evaluation of antioxidants from leaves of a Tunisian cultivar olive tree. *Eur. J. Lipid Sci. Technol., 107,* 497–504.

55) Bracci T., Busconi M., C. Fogher, and L. (2011). Sebastiani, "Molecular studies in olive (*Olea europaea* L.): overview on DNA markers applications and recent advances in genome analysis," *Plant Cell Reports*, vol. 30, no. 4, pp. 449–462,

56) Bradford, M. M. (1976). A rapid and sensitive method for the quantitation of microgram quantities of protein utilizing the principle of protein-dye binding. *Analytical biochemistry*, *72*(1-2), 248-254.

57) Breslin, W.J.,Liberackj, A.B.,Dittenber, D.A., and Quast, J.F.1996. Evaluate developmental and reproductive toxicity of chlorpyrifos in the rat. Fundamental and Applied Toxicology 29: 119- 130.

58) Briante, R.; Patumi, M.; Terenziani, S.; Bismuto, E.; Febbraio, F.; Nucci, R. (2002) *Olea europaea* L. leaf extract and derivatives: antioxidant properties. *J. Agric. Food Chem., 50,* 4934–4940.

59) Broadhurst, R. B., & Jones, W. T. (1978). Analysis of condensed tannins using acidified vanillin. *Journal of the Science of Food and Agriculture*, *29*(9), 788-794.

60) Calvert G.M., Karnik J., Mehler L., Beckman J., Morrissey B., Sievert J., Barrett R., Lackovic M., Mabee L., Schwartz A., Mitchell Y., Moraga-McHaley S. (2008). Acute pesticide poisoning among agricultural workers in the United States, 1998–2005. *Am. J. Ind. Med.* 51:883–898. doi: 10.1002/ajim.20623.

61) Camara RB, Costa LS, Fidelis GP, Nobre LT, Dantas-Santos N, Cordeiro SL, Costa MS, Alves LG, Rocha HA .2011. Heterofucans from the brown

seaweed *Canistrocarpus cervicornis* with anticoagulant and antioxidant activities. Mar Drugs.;9(1):124–38. https://doi.org/10.3390/md9010124..

62) Cárdeno A., Sánchez-Hidalgo M., Rosillo M. A., and De La Lastra C. A. (2013). "Oleuropein, a secoiridoid derived from olive tree, inhibits the proliferation of human colorectal cancer cell through downregulation of HIF-1*α*," *Nutrition and Cancer*, vol. 65, no. 1, pp. 147–156.

63) Cardoso D., Narcy A., Durosoy S., Bordes C., Chevalier Y.(2020). Dissolution kinetics of zinc oxide and its relationship with physicochemical characteristics. *Powder Technol.* 2021;378:746–759. doi: 10.1016/j.powtec...10.049.

64) Carrera-González MP, Ramírez-Expósito MJ, Mayas MD, Martínez-Martos JM. (2013). Protective role of oleuropein and its metabolite hydroxytyrosol on cancer. Trends Food Sci Technol. 31:92–9.

65) Castellano JM, Delgado Hervás T, Guinda Garín MÁ, Gutiérrez-Adánez P, Rada M, Sántos- Lozano JM. (2015). Determination of major bioactive compounds from olive leaf. Food Science and Technology – Zurich. 64(1): 431–8.

66) Cerqueira MA, Vicente AA, Pastrana LM (2018) Chapter 1 - nanotechnology in food packaging: opportunities and challenges. In: Cerqueira MÂPR, Lagaron JM, Pastrana Castro LM, de Oliveira Soares Vicente AAM (eds) Nanomaterials for food packaging. Elsevier, pp 1–11. https://doi.org/10.1016/B978-0-323-51271-8.00001-2

67) Chahardoli A, Karimi N, Sadeghi F, Fattahi A. (2018). Green approach for synthesis of gold nanoparticles from Nigella arvensis leaf extract and evaluation of their antibacterial, antioxidant, cytotoxicity and catalytic activities Art cells. *Nanomed Biotechnol.* 46(3):579–588.

68) Chandran SP, et al. . (2006) . Synthesis of gold nanotriangles and silver nanoparticles using aloevera plant extract. *Biotechnol. Prog*;22:577–583. doi: 10.1021/bp0501423H.

69) Chenikhar H, Djabri B, Salmi A, TaibC, and Rouabhi R, (2018) .Hepatotoxicity Induced by Chlorpyrifos in 'Wistar' Rats. Tunisian Journal of Plant Protection Vol. 13, SI, J. Nanomed. Nanotechnol., 8 (4), 23-30.

70) Choi S.J., Choy J.H. . (2014) Biokinetics of zinc oxide nanoparticles: Toxicokinetics, biological fates, and protein interaction. *Int. J. Nanomed*;9:261–269.

71) Cimino M.C. .(2006). 'Comparative overview of current international strategies and guidelines for genetic toxicology testing for regulatory purposes', *Environ. Mol. Mutagen.*, , 47, (5), pp. 362 –390

72) Colon G, Ward BC, Webster TJ. (2006). Increased osteoblast and decreased *Staphylococcus epidermidis* functions on nanophase ZnO and TiO_2. *J. Biomed. Mater. Res.* 78(3):595–604

73) Colon G, Ward BC, Webster TJ. (2008). Increased osteoblast and decreased *Staphylococcus epidermidis* functions on nanophase ZnO and TiO_2. *J. Biomed. Mater. Res.* 2006;78(3):595–604

74) Cortés-Iza S. C. and Rodríguez A. I., (2018) . "Oxidative stress andpesticide disease: a challenge for toxicology," Revista de laFacultad de Medicina, vol. 66, pp. 261–267,

75) Dai J, Mumper RJ. (2010). Plant phenolics: extraction, analysis and their antioxidant and anticancer properties. Molecules 15(10):7313–7352. https:// doi. org/ 10. 3390/ molec ules1 51073 13

76) Daisy P., Saipriya K. (2012). Biochemical analysis of Cassia fistula aqueous extract and phytochemically synthesized gold nanoparticles as hypoglycemic treatment for diabetes mellitus. *Int. J. Nanomed.* 7:1189–1202. doi: 10.2147/IJN.S26650.

77) Damalas CA, Koutroubas SD. (2016) . Farmers' Exposure to Pesticides: Toxicity Types and Ways of Prevention. Toxics. 8;4(1):1. doi: 10.3390/toxics4010001.

78) Das S., Srivasatava V. C. (2016). Synthesis and characterization of ZnO–MgO nanocomposite by co-precipitation method. *Smart Sci.* 4 190–195.

79) Dbira S, Bedoui A,and Bensalah N. (2014). Investigations on the degradation of triazine herbicides in water by photo-fenton process, American Journal of Analytical Chemistry, 5: 500-517

80) De Laurentis, N., Crescenzo, G., Lai, O.R. And Milillo, M.A. (1997). Investigation on the extraction and concentration of oleuropein and flavonoids in Olea europaea L. based products. Pharm. Pharmacol. Lett. 7, 27–30.

81) Della Rosa RJ, Stannard JN (1964) Acute toxicity as a function of route of administration. Radiat Res Suppl 5:205–215. https:// doi.org/10.2307/3583491

82) DeRosa M.C. (2010). Nanotechnology in fertilizers. Nat. Nanotechnol. 5, 91

83) Dikusar A., Globa P., Belevskii S., Sidel'nikova S. (2009). On limiting rate of dimensional electrodeposition at meso-and nanomaterial manufacturing by template synthesis. *Surf. Eng. Appl. Electrochem.* 45 171–179

84) Dobrucka R, Dugaszewska J. (2016). Biosynthesis and antibacterial activity of ZnO nanoparticles using Trifolium pratense flower extract. *Saudi J Biol Sci*.;23(4):517–523.

85) Durán N, Marcato PD, Alves OL, Souza GIH, De, Esposito E. (2005). Mechanistic aspects of biosynthesis of silver nanoparticles by several Fusarium oxysporum strains. J Nanobiotechnology. 3: 8.

86) Ealia SAM, Saravanakumar MP. (2017). A review on the classification, characterisation, synthesis of nanoparticles and their application. In: IOP Conference Series: Materials Science and Engineering. IOP Publishing; p. 32019.

87) Ecobichon D.J. (2001). Pesticide use in developing countries. *Toxicology.* 160:27–33. doi: 10.1016/S0300-483X(00)00452-2.

88) EFSA. (2010). Conclusion regarding the peer review of the pesticide risk assessment of the active substance - metribuzin. EFSA Scientific Report. 88:1-74. Available at: www.efsa.europa.eu

89) Eidi A., Eidi M., and Darzi R. (2009). "Antidiabetic effect of *Olea europaea* L. in normal and diabetic rats," *Phytotherapy Research*, vol. 23, no. 3, pp. 347–350

90) Ekennia A. C., Uduagwu D. N., Nwaji N. N., Oje O. O., Emma-Uba C. O., Mgbii. S. I., Olowo O. J. & Nwanji O. L. (2021) Green Synthesis of Biogenic Zinc Oxide Nanoflower as Dual Agent for Photodegradation of an Organic Dye and Tyrosinase Inhibitor. Journal of Inorganic and Organometallic Polymers and Materials 31(2), 886–97.

91) Elahi N, Kamali M, Baghersad MH. (2018). Recent biomedical applications of gold nanoparticles: a review. Talanta. 184:537–56.

92) El-Sayed YS, Saad TT, El-Bahr SM. (2007). Acute intoxication of deltamethrin in monosex Nile tilapia, Oreochromis niloticus, with special reference to the clinical, biochemical and haematological effects. *Environ Toxicol Pharmacol.* ;24:212–217

93) El-Waseif AA, Alshehrei F, Al-Ghamdi SB, El-Ghwas DE.2022. Antioxidant and anticoagulant activity of Microbial Nano Cellulose-ZnO-Ag Composite Components. Pak J Biol Sci.;25:531–6.

94) Fadillah R, Y Rati , R Dewi , R Farma and A S Rini. (2021) Optical and structural studies on bio-synthesized ZnO using Citrullus lanatus peel extract. Journal of Physics: Conference Series 1816 012019 . doi:10.1088/1742-6596/1816/1/012019

95) Fakhari S, Jamzad M, Kabiri Fard H (2019) Green synthesis of zinc oxide nanoparticles: a comparison. *Green chemistry letters and reviews* 12, 19-24.

96) Federal Provincial-Territorial Committee on Drinking Water. (2020). Guideline Technical Document: Metribuzin in Drinking Water - For Public Consultation. 1-30

97) Ferdous, Z.; Nemmar, A. (2020), Health Impact of Silver Nanoparticles: A Review of the Biodistribution and Toxicity Following Various Routes of Exposure. Int. J. Mol. Sci. 21, 2375.

98) Ficarra, P., Ficarra, R., De Pasquale, A., Monforte, M.T. And Calabro, M.L. (1991). HPLC analysis of oleuropein and some flavonoids in leaf and bud of Olea europaea L. Farmaco. 46, 803–815

99) Fitsanakis VA, Amarnath V, Moore JT, Montine KS, Zhang J, Montine TJ. (2002). Catalysis of catechol oxidation by metal-dithiocarbamate complexes in pesticides. *Free Radic Biol Med.* 33:1714–1723..

100) Foldbjerg R, Dang DA, Autrup H. (2011). Cytotoxicity and genotoxicity of silver nanoparticles in the human lung cancer cell line, A549. *Archives of toxicology* . 85(7):743–750.

101) Franco R, Li S, Rodriguez-Rocha H, Burns M, (2010) . Panayiotidis MI. Molecular mechanisms of pesticide-induced neurotoxicity: Relevance to Parkinson's disease. *Chem Biol Interact.*;188:289–300.

102) Galloway T, Handy R. (2003). Immunotoxicity of organophosphorous pesticides. *Ecotoxicology.* 2003;12:345–363 van der Oost et al., [180]). van der Oost R, Beyer J, Vermeulen NP. Fish bioaccumulation and biomarkers in environmental risk assessment: a review. *Environ Toxicol Pharmacol.* 2003;13:57–149.

103) Ge, Y., Schimel, J.P., Holden, P.A. (2011). Evidence for negative effects of TiO2 and ZnO nanoparticles on soil bacterial communities. Environ. Sci. Technol. 45, 1659–1664.

104) Ghanbari R, Anwar F, Alkharfy KM, Gilani AH, Saari N. (2012). Valuable nutrients and functional bioactives in different parts of olive (Olea europaea L.)-A review. Int J Mol Sci. 13:3291–340.,

105) Gilani, A.H.; Khan, A.U.; Shah, A.J.; Connor, J.; Jabeen, Q. (2005) Blood pressure lowering effect of olives is mediated through calcium channel blockade. *Int. J. Food Sci. Nutr , 56*, 613–620.

106) Goma, A.A.; Tohamy, H.G.; El-Kazaz, S.E.; Soliman, M.M.; Shukry, M.; Elgazzar, A.M.; Rashed, R.R. (2021), Insight Study on the Comparison between Zinc Oxide Nanoparticles and Its Bulk Impact on Reproductive Performance, Antioxidant Levels, Gene Expression, and Histopathology of Testes in Male Rats. *Antioxidants 10*, 41. https://doi.org/10.3390/antiox10010041

107) Gonzalez-Ballesteros N., ´ M.C. Rodríguez-Argüelles, S. Prado-Lopez, ´ M. Lastra, M. Grimaldi, A. Cavazza, L. Nasi, G. Salviati, F. Bigi. (2019). Macroalgae to nanoparticles: study of Ulva lactuca L. role in biosynthesis of gold and silver nanoparticles and of their cytotoxicity on colon cancer cell lines, Mater. Sci. Eng. C. 97 498–509, https://doi.org/10.1016/j.msec.2018.12.066.

108) Goodner K.I, Jella P, Rouseff R.I: J Agric Food Chem. (2000), 48, 2886. Doi:10.1021/jf990561d

109) Gourama, H.; Bullerman, L.B. (2000). Effects of oleuropein on growth and aflatoxin production by *Aspergillus parasiticus*. *Lebensm. Wiss. Technol* 1987, *20*, 226–228

110) Green.PS (2002),A revision of Olea L (Oleaceae. Kew bellitin). Vol 57,pp 91-140, ISBN,00755974

111) Grohmann F. (1981). "Oleaceae," *Flora of Pakistan*, vol. 59, p. 9.

112) Guerra, F.D., Attia, M.F., Whitehead, D.C., Alexis, F. (2018). Nanotechnology for environmental remediation: materials and applications. Molecules 23, 1760.

113) Gupta PK. (2011). Herbicides and fungicides. In: Gupta RC, editor. *Reproductive and developmental toxicology*. Amsterdam: Academic Press/Elsevier; pp. 503–521.

114) Gupta S., Yadav S. *(* 2014). Bioaccumulation of ZnO-NPs in earthworm *Eisenia fetida* (Savigny) *J. Bioremediation Biodegrad*;5:250–256.

115) Hackenberg S. A., A. Scherzed, M. Kessler et al. (2011). "Silver nanoparticles: evaluation of DNA damage, toxicity and functional impairment in human mesenchymal stem cells," *Toxicology Letters*, vol. 201, no. 1, pp. 27–33

116) Hamza R. Z., Abd El-Azez A. M. and Hussien N. A. (2015). Evaluation of the antioxidant potential for different extracts of al-taif pomegranate (Punica granatum L) induced by atrazine and malathion pesticides in liver of male albino mice, Int. J. Pharm. Sci., 7: 89-94

117) Handore K, Bhavsar S, Horne A, Chhattise P, Mohite K, Ambekar J, Pande N, Chabukswar V (2014) Novel green route of synthesis of ZnO nanoparticles by using natural biodegradable polymer and its application as a catalyst for oxidation of aldehydes. J Macromolecular Sci Part A 51:941–947

118) Harborne . JB, (1973), Phytochemical Methods. A Guide to Modern Techniques of plant analysis, Chapman and Hall Ltd, London, 49-188

119) Hashmi MA, Khan A, Hanif M, Farooq U, Perveen S. (2015); Traditional Uses, Phytochemistry, and Pharmacology of Olea europaea (Olive). Evid Based Complement Alternat Med. *1–29.*541591. doi: 10.1155/2015/541591

120) Hassan S.K., Mousa A.M., Eshak M.G., Farrag A.E.R.H., Badawi A.E.F.M . (2014). Therapeutic and chemopreventive effects of nano Curcumin against diethylnitrosamine induced hepatocellular carcinoma in rats, Int. J. Pharm. Pharm. Sci. 6 (3) 54–62.

121) Hassen I, Casabianca H, Hosni K. . (2015). Biological activities of the natural antioxidant oleuropein: exceeding the expectation – A mini-review. J Funct Foods; 18: 926–40.

122) He L, He T, Farrar S, Ji L, Liu T, Ma X (2017) Antioxidants maintain cellular redox homeostasis by elimination of reactive oxygen species. Cell Physiol Biochem 44(2):532–553. https://doi.org/10. 1159/000485089

123) Henriksen T., Svensmark B., Juhler R.K. (2002). Analysis of Metribuzin and transformation products in soil by pressurized liquid extraction and liquid chromatographic-tandem mass. spectrometry. J. Chromatogr. A., 957(1), 79-87

124) Hernández AF, Lacasaña M, Gil F, Rodríguez-Barrancob M, Pla A, López-Guarnidoa O. (2013); Evaluation of pesticide-induced oxidative stress from a gene–environment interaction perspective. Toxicology 307:95-102.

125) Hiller JM, Perlmutter A (1971) Effect of zinc on viral-host interactions in a rainbow trout cell line, RTG-2. Water Res 5:703–710

126) Horikoshi S., Serpone N. (2013). Microwaves in Nanoparticle Synthesis: Fundamentals and Applications, John Wiley & Sons

127) Hsueh PR. . (2010). New Delhi metallo-β-lactamase-1 (NDM-1): an emerging threat among Enterobacteriaceae. *J Formos Med Assoc*;109(10):685–687

128) Hu, W., Wan, L., Jian, Y., Ren, C., Jin, K., Su, X., Bai, X., Haick, H., Yao, M., Wu, W. (2019). Electronic noses: from advanced materials to sensors aided with data processing. Adv. Mater. Technol. 4, 1800488

129) Huang J, et al. (2007) Biosynthesis of silver and gold nanoparticles by novel sundried *Cinnamomum camphora* leaf. *Nanotechnology.* 18:105104. doi: 10.1088/0957-4484/18/10/105104/pdf

130) Huang X, Jain PK, El-Sayed IH, El-Sayed MA. (2007). Gold nanoparticles: interesting optical properties and recent applications in cancer diagnostics and therapy. Nanomedicine.. https://doi.org/10.2217/17435889.2.5.681.

131) Huertas-Pérez J.F., del Olmo I.M., GarcíaCampaña A.M., González-Casado A., SánchezNavarro A. (2006). Determination of the herbicide metribuzin and its major conversion products in soil by micellar electrokinetic chromatography. J Chromatogr A, 1102(1–2), 280–286

132) Hulteen J C, Treichel D A, Smith M T, Duval M L, Jensen T R and Duyne R P Van 1999 Nanosphere Lithography : Size-Tunable Silver Nanoparticle and Surface Cluster Arrays 3854–63

133) Hussain SM, Hess KL, Gearhart JM, Geiss KT, Schlager JJ. (2005). In vitro toxicity of nanoparticles in BRL 3A rat liver cells. *Toxicology in vitro.* 19(7):975–983.,

134) Hussain I., *et al.* (2016). Green synthesis of nanoparticles and its potential application Biotechnol. Lett., 38 (4) , pp. 545-560

135) Iravani S. (2011). Green synthesis of metal nanoparticles using plants. Green Chem.;13:2638–2650.

136) Jeyaraj M., S. Varadan, K.J.P. Anthony, M. Murugan, A. Raja, S. Gurunathan, (2013). J. Ind. Eng. Chem. 19, 1299–1303].

137) Jose Luis A-T, du Wessel T (2018) The role of UV-visible spectroscopy for phenolic compounds quantification in Winemaking. In: Rosa Lidia S-O, Angel de la Cruz P-C (eds) Frontiers and new trends in the science of fermented food and beverages. IntechOpen, Rijeka, p Ch. 3. https:// doi. org/ 10. 5772/ intec hopen. 79550

138) Joudeh, N., Linke, D. (2022). Nanoparticle classification, physicochemical properties, characterization, and applications: a comprehensive review for biologists. *J Nanobiotechnol* 20, 262. https://doi.org/10.1186/s12951-022-01477-8

139) Kada T, Inoue T, Namiki N .(1982). Environmental desmutagens and antimutagens. In: Klekowski EJ, editor. *Environmental mutagenesis and plant biology*. New York: Praeger;. pp. 137–151.

140) Kadeche, L., E. Bourogaa, M. Saoudi, A. Boumendjel, A. Djeffal, A. E. Feki, and M. .(2017). Messarah. "Ameliorative effects of vanillin against metribuzin-induced oxidative stress and toxicity in rats". *International Journal of Pharmacy and Pharmaceutical Sciences*, vol. 9, no. 1, pp. 56-62, doi:10.22159/ijppsv9i1.14258.

141) Kadriye Ozlem Saygi;Canan Usta; (2021). *Rosa canina waste seed extract-mediated synthesis of silver nanoparticles and the evaluation of its antimutagenic action in Salmonella typhimurium . Materials Chemistry and Physics, (), –* . doi:10.1016/j.matchemphys.2021.12

142) Kah, M., Kookana, R.S., Gogos, A., Bucheli, T.D. (2018). A critical evaluation of nanopesticides and nanofertilizers against their conventional analogues. Nat. Nanotechnol. 13, 677–684.

143) Kammler B H K, Mädler L and Pratsinis S E . (2001). Flame Synthesis of Nanoparticles 24 583–96 .

144) Kaniewski D., Campo E. van, T. Boiy, J.-F. Terral, B. Khadari, and G. Besnard, (2012). "Primary domestication and early uses of the emblematic olive tree:

palaeobotanical, historical and molecular evidence from the Middle East," *Biological Reviews*, vol. 87, no. 4, pp. 885–899,

145) Karakaya S et al., (2015) Olive tree (Olea europaea) leaves: potential beneficial effects on human health. Nutr Rev. 2009 Nov; 67(11): 632–8. Hassen I, Casabianca H, Hosni K. Biological activities of the natural antioxidant oleuropein: exceeding the expectation – A mini-review. J Funct Foods.; 18: 926–40.

146) Karthikeyan R., P. Anantharaman, N. Chidambaram, T. Balasubramanian, S.T. Somasundaram, Padina boergessenii. (2012). ameliorates carbon tetrachloride-induced nephrotoxicity in Wistar rats, J. King Saud Univ. Sci. 24 227–232.

147) Karunakaran G, Sudha KG, Ali S, Cho EB. (2023). Biosynthesis of Nanoparticles from Various Biological Sources and Its Biomedical Applications. Molecules. 2;28(11):4527. doi: 10.3390/molecules28114527.

148) Kelly SA, Havrilla CM, Brady TC, Abramo KH, Levin ED (1998) Oxidative stress in toxicology: established mammalian and emerging piscine model systems. Environ Health Perspect 106:375–384

149) Khan M.., Saadah N. H., Khan M. E., Harunsani M. H., Tan A. L. & Cho M. H. (2019). Potentials of Costus Woodsonii Leaf Extract in Producing Narrow Band Gap ZnO Nanoparticles. Materials Science in Semiconductor Processing 91, 194–200.

150) Khan Y, Panchal S, Vyas N, Butani A, Kumar V. (2007). Olea europaea: a phyto-pharmacological review. Pharmacogn Rev. 1(1): 114–8.

151) Khan ZM, Law FCP. (2005). Adverse effects of pesticides and related chemicals on enzyme and hormone systems of fish, amphibians and reptiles: A review. *Proc Pakistan Acad Sci*;42:315–323.

152) Kharissova, Oxana V.; Dias, H.V. Rasika; Kharisov, Boris I.; Pérez, Betsabee Olvera; Pérez, Victor M. Jiménez (2013). *The greener synthesis of nanoparticles. Trends in Biotechnology, 31(4), 240–248.* doi:10.1016/j.tibtech.2013.01.003

153) Khayyal MT, el-Ghazaly MA, Abdallah DM, Nassar NN, Okpanyi SN, Kreuter MH. (2002). Blood pressure lowering effect of an olive leaf extract (Olea europaea) in L-NAME induced hypertension in rats. Arzneimittelforschung.;52(11):797-802. doi: 10.1055/s-0031-1299970.

154) Kim S.Y. Shon Y.H. Lee J.S. *et al*.: .(2000). 'Antimutagenic activity of soybeans fermented with basidiomycetes in Ames/*Salmonella* test', *Biotechnol. Lett.*, , 22, pp. 1197 –1202

155) Kitous O., Abdi N., Lounici H., Grib H., Drouiche N., Benyoussef E.H., Mameri N. (2016). Modeling of the adsorption of metribuzin pesticide onto electroactivated granular carbon, Desalin. Water Treat., 57, 1865–1873

156) Klaassen C.D. (2013). *Casarett & Doull's Toxicology: The Basic Science of Poisons.* 8th ed. McGraw-Hill Education; Columbus, OH, USA: p. 1454

157) Korani M, S.M. Rezayat, B.S. Arbabi . (2013).Sub-chronic dermal toxicity of silver nanoparticles in guinea pig: special emphasis to heart, bone and kidney toxicities .Iran. J. Pharm. Res., 12 (3) , pp. 511-519

158) Kulthong K, R. Maniratanachote, Y. Kobayashi, T. Fukami, T. Yokoi. (2012). Effects of silver nanoparticles on rat hepatic cytochrome P450 enzyme activity. Xenobiotica, 42 (9) , pp. 854-862

159) Kumar S. Venkateswarlu S., P., Rao V. R., Rao G. N. (2013). Synthesis, characterization and optical properties of zinc oxide nanoparticles. *International Nano Letters, 3,* 1-6.

160) Kumar P. V., Pammi, S., Kollu, P., Satyanarayana, K., & Shameem, U. (2014). Green synthesis and characterization of silver nanoparticles using Boerhaavia diffusa plant extract and their anti bacterial activity. *Industrial Crops and Products, 52,* 562-566.

161) Kumar, *et al.* (2018). Biodegradable hybrid nanocomposites of chitosan/gelatin and silver nanoparticles for active food packaging applications . Food Packag. shelf life, 16 , pp. 178-184

162) Kumar R., *et al.* (2017). Rapid green synthesis of silver nanoparticles (AgNPs) using (Prunus persica) plants extract: exploring its antimicrobial and catalytic activities J. Nanomed. Nanotechnol., 8 (4) , pp. 1-8

163) Lakshmanan G, Sathiyaseelan A, Kalaichelvan PT, Murugesan K. (2018). Plant-mediated synthesis of silver nanoparticles using fruit extract of *Cleome viscosa* L.: assessment of their antibacterial and anticancer activity. *Karbala Int. J. Mod. Sci.* 4:61–68. doi: 10.1016/j.kijoms. 10.007.

164) Laouini SE, Bouafa A, Soldatov AV, Algarni H, Tedjani ML, Ali GAM, Barhoum A (2021) Green synthesized of Ag/Ag2O nanoparticles using aqueous leaves extracts of phoenix dactylifera L. and their azo dye photodegradation. Membranes 11(7):468

165) Lateef, Agbaje; Ojo, Sunday A.; Elegbede, Joseph A.; Azeez, Musibau A.; Yekeen, Taofeek A.; Akinboro, Akeem. (2017). Evaluation of Some Biosynthesized Silver Nanoparticles for Biomedical Applications: Hydrogen Peroxide Scavenging, Anticoagulant and Thrombolytic Activities. *Journal of Cluster Science, 28(3), 1379–1392.* doi:10.1007/s10876-016-1146-0

166) Lateef T. B, Asafa, T. A. Yekeen, A. Akinboro, I. C. Oladipo, E. B. Gueguim-Kana, and L. S. Beukes (2016). Biomedical applications of cocoa bean extract-mediated silver nanoparticles as antimicrobial, larvicidal and anticoagulant agents. J. Clust. Sci.. doi:10.1007/s10876-016-1055-2.,

167) Lava MB, Muddapur UM, Basavegowda N, More SS, More VS. (2021). Characterization, anticancer, antibacterial, anti-diabetic and anti-infammatory activities of green synthesized silver nanoparticles using Justica wynaadensis leaves extract. Mater Today: Proc 46:5942–5947. https://doi.org/10.1016/j.matpr.2020.10.048

168) Lee B, O.; Lee, B. (2010). Antioxidant and antimicrobial activities of individual and combined phenolics in *Olea europaea* leaf extract. *Bioresour. Technol 101,* 3751–3754.

169) Lee HJ, Yeo SY, Jeong SH .(2003). Antibacterial efect of nanosized silver colloidal solution on textile fabrics. J Mater Sci 38(10):2199–2204. https://doi.org/10.1023/A:1023736416361

170) Lee, S.H.; Jun, B.-H. (2019). Silver Nanoparticles: Synthesis and Application for Nanomedicine. Int. J. Mol. Sci. 20(4),p 865.

171) Li CH, Shen CC, Cheng YW, Huang SH, Wu CC, Kao CC, Liao JW, Kang JJ .(2012). Organ biodistribution, clearance, and genotoxicity of orally administered zinc oxide nanoparticles in mice. Nanotoxicology 6:746–756

172) Li M, Zhu L, Lin D. (2011). Toxicity of ZnO nanoparticles to Escherichia coli: mechanism and the influence of medium components. Environ Sci Technol 45:1977–1983 44.

173) Li ZH, Zlabek V, Grabic R, Li P, Randak T. (2010) . Modulation of glutathione-related antioxidant defense system of fish chronically treated by the fungicide propiconazole. *Comp Biochem Physiol C Toxicol Pharmacol*;152:392–398.

174) Li, Q.; Mahendra, S.; Lyon, D.Y.; Brunet, L.; Liga, M.V.; Li, D.; Alvarez, P.J.J. (2008). Antimicrobial nanomaterials for water disinfection and microbial control: Potential applications and implications. *Water Res. 42*, 4591–4602.

175) Lins PG, Marina Piccoli Pugine S, Scatolini AM, de Melo MP. (2018). In vitro antioxidant activity of olive leaf extract (*Olea europaea* L.) and its protective effect on oxidative damage in human erythrocytes. *Heliyon*. 4(9): e00805. .

176) Lu JJ, Bao JL, Wu GS, Xu WS, Huang MQ, Chen XP, Wang YT. (2013) Quinones derived from plant secondary metabolites as anti-cancer agents. Anticancer Agents Med Chem. Mar;13(3):456-63. PMID: 22931417.

177) Lushchak VI, Matviishyn TM, Husak VV, Storey JM, Storey KB. (2018). Pesticide toxicity: a mechanistic approach. *EXCLI J*. 8;17:1101-1136. doi: 10.17179/excli2018-1710.

178) Lushchak VI. . (2011). Adaptive response to oxidative stress: Bacteria, fungi, plants and animals. *Comp Biochem Physiol Part C*;153:175–190.

179) Lyu H., B. Gao , F. He , C. Ding , J. Tang and J. C. Crittenden . (2017) . *ACS Sustainable Chem. Eng.*, , 5 , 9568 —9585

180) Mahdi SS, Vadood R, Nourdahr R. (2012). Study on the antimicrobial effect of nanosilver tray packaging of minced beef at refrigerator temperature. *Glob Vet*. 9:284–9.

181) Mancini Filho J., A. Van Koiij, D.A. Mancini, F.F. Cozzolino, R.P. (1998).Torres, Bull. *Chim. Farm.*, 137,443

182) Mann S, Burkett S L, Davis S A, Fowler C E, Mendelson N H, Sims S D, Walsh D and Whilton N T. (1997). *Sol - Gel Synthesis of Organized Matter* 4756 2300–10 3.1.2.

183) Mansour S.A. and Mossa A.H. (2009). Lipid peroxidation and oxidative stress in rat erythrocytes induced by chlorpyrifos and the protective effect of zinc. *Pestic Biochem Phys*, 93: 34-39..

184) Maron, D.M., Ames, B.N. (1983). Revised methods for the Salmonella mutagenicity test. *Mutat. Res*. 113 (3–4), 173–215

185) Mathew S, Abraham TE, Zakaria ZA (2015) Reactivity of phenolic compounds towards free radicals under in vitro conditions. J Food Sci Technol 52(9):5790–5798. https://doi.org/10.1007/ s13197-014-1704-0

186) Matos, F.d.A. (1997). Introdução à fitoquímica experimental. edições UFC. (Matos, 1997)

187) Médail F., Quézel P., Besnard G., and Khadari B., (2001). "Systematics, ecology and phylogeographic significance of *Olea europaea* L. ssp. *maroccana* (Greuter & Burdet) P. Vargas *et al*., a relictual olive tree in South-west Morocco," *Botanical Journal of the Linnean Society*, vol. 137, no. 3, pp. 249–266,

188) Medila I,Toumi I,Adaika A. (2021) . The protective effect of ephedra alata aqueous extract against metribuzin intoxication on albino wistar rat,The Natural Products Journal, volume 11, issue 4, pages 507-511.

189) Medjdoub, A., Merzouk, S. A., Merzouk, H., Chiali, F. Z., & Narce, M. (2011). *Effects of Mancozeb and Metribuzin on in vitro proliferative responses and oxidative stress of human and rat spleen lymphocytes stimulated by mitogens. Pesticide Biochemistry and Physiology, 101(1), 27–33.* doi:10.1016/j.pestbp.2011.06.002 10.1016/j.pestbp.2011.06.002

190) Meirinhos J., Silva B. M., Valentão P.et al., (2005). "Analysis and quantification of flavonoidic compounds from Portuguese olive (*Olea europaea* L.) leaf cultivars," *Natural Product Research*, vol. 19, no. 2, pp. 189–195.

191) Moreno D.A.N, *et al.*) (2021). Are silver nanoparticles useful for treating second-degree burns. An experimental study in rats Adv. *Pharm. Bull*., 11 1, pp. 130-136.

192) Mukherjee P, Mandal A.A, Senapati S, Sainkar R, Khan MI, Parishcha R, Ajaykumar PV, Alam M, Kumar R, Sastry M. (2001). "Fungus-mediated synthesis of silver nanoparticles and their immobilization in the mycelial matrix: a novel biological approach to nanoparticle synthesis.". *Nano Lett*, 1: p. 515-519. 14.

193) Muñoz-García J., L. Vázquez , R. Cuerno , J. A. Sánchez-García , M. Castro and R. Gago .(2009). *Toward Functional Nanomaterials* , Springer US, New York, NYpp. 323–398

194) Nadour M, Michaud P, Moulti-Mati F. (2012) "Antioxidant activities of polyphenols extracted from olive (*Olea europaea*) of *Chamlal* variety," *Applied Biochemistry and Biotechnology*, vol. 167, no. 6, pp. 1802–1810.

195) Nagajyothi PC, Cha SJ, Yang IJ, et al. (2015). Antioxidant and anti-inflammatory activities of zinc oxide nanoparticles synthesized using *Polygala tenuifolia* root extract. *J Photochem Photobiol B*. 146:10–17.

196) Nam J. H., M. J. Jang , H. Y. Jang , W. Park , X. Wang , S. M. Choi and B. Cho . (2020). Room temperature sputtered electrocatalyst WSe_2 nanomaterials for hydrogen evolution reaction . *J. Energy Chem.*, , 47 , 107 —111

197) Nanaei M, Nasseri MA, Allahresani A, Kazemnejadi M. (2019). Phoenix dactylifera L. extract: antioxidant activity and its application for green biosynthesis of Ag nanoparticles as a recyclable nanocatalyst for 4-nitrophenol reduction. SN Appl Sci 1(8):853. https:// doi. org/ 10. 1007/ s42452- 019- 0895-4

198) National Institutes of Health (NIH) .(2021). Zinc: Fact Sheet for Health Professionals. [(accessed on 7 December2021)]; Available online: https://ods.od.nih.gov/factsheets/Zinc-HealthProfessional/

199) Nesheim O.N., Fishel F.M., Mossler M. (2014).*Toxicity of Pesticides. PI-13.* University of Florida (UF), Institute of Food and Agricultural Sciences (IFAS) Extension; Gainesville, FL, USA: p. 6.

200) Niaounakis, M.; Halvadakis, C.P. (2006). Characterization of Olive Processing Waste. In *Waste Management Series*, 2nd ed; Elsevier: Amsterdam, the Netherlands,; Volume 5, Chapter 2; pp. 23–64.

201) Nie M., K. Sun and D. D. Meng . (2009). Formation of metal nanoparticles by short-distance sputter deposition in a reactive ion etching chamber. *J. Appl. Phys.*, 106 , 054314

202) Nieves-Puigdoller K, Bjornsson BT, McCormick SD. (2007). Effects of hexazinoneand atrazine on the physiology and endocrinology of smolt development in Atlantic salmon. *Aquat Toxicol*;84:27–37.

203) Novick A, Szilard L. . .(1952). Anti-mutagens. *Nature*;170:926–927.

204) OEHHA (2001). Evidence on the developmental and reproductive toxicity of metribuzin. California Environmental Protection Agency, Office of Environmental Health Hazard Assessment, Reproductive and Cancer Hazard Assessment Section. Available at: https://oehha.ca.gov/proposition-65/chemicals/metribuzin.

205) Oraiza, M. (1986). Studies on product of browning reaction prepared from glucosamine. *Japanese J Nutr*, *44*, 307-315.

206) Osman, A.I., Zhang, Y., Farghali, M. *et al*. (2024). Synthesis of green nanoparticles for energy, biomedical, environmental, agricultural, and food applications: A review. *Environ Chem Lett* 22, 841–887 https://doi.org/10.1007/s10311-023-01682-3

207) Othman SH, Abd Salam NR, Zainal N, Kadir Basha R, Talib RA. (2014). Antimicrobial activity of TiO2 nanoparticle-coated film for potential food packaging applications. Int J Photoenergy.; 945930. https://doi.org/10.1155/2014/945930

208) Padalia H, Moteriya P, Chanda S. (2014). Green synthesis of silver nanoparticles from marigold flower and its synergistic antimicrobial potential. *Arab. J Chem.* 2015;8:732–741. doi: 10.1016/j.arabjc.11.015.

209) Padmavathy N, Vijayaraghavan R. (2008). Enhanced bioactivity of ZnO nanoparticles—an antimicrobial study. *Sci. Technol. Adv. Mater.* 9(3):035004..

210) Paiva-Martins, F.; Gordon, M.H. (2001). Isolation and characterization of the antioxidant component 3,4-dihydroxyphenylethyl-4-formyl-3-formylmethyl-4-hexenoate from olive (*Olea europaea*) leaves. *J. Agric. Food Chem*, *49*, 4214–4219.

211) Panizzi L. i, Scarpati M. L., (1960). Costituzione oleuropeina, glucoside amaro e ad azione amaro ipotensiva dell' olivo, Gazz. Chim. Ital 90:1449-1485

212) Park E.-J. , *et al.* (2010). Repeated-dose toxicity and inflammatory responses in mice by oral administration of silver nanoparticles . Environ. Toxicol. Pharmacol., 30 (2) , pp. 162-168

213) Patil A.P. , K.H. Kapadnis, S. Elangovan. (2021). Antibacterial applications of biosynthesized AgNPs: a short review . Mater. Sci. Res. India, 18 (2) pp. 143-153

214) Patil N., Bhaskar R., Vyavhare V., Dhadge R., Khaire V., Patil Y. (2021). Overview on methods of synthesis of nanoparticles. *Int. J. Curr. Pharm. Res.* 13 11–16

215) Penghui Nie, Yu Zhao, Hengyi Xu, (2023). Synthesis, applications, toxicity and toxicity mechanisms of silver nanoparticles: A review, Ecotoxicology and Environmental Safety, Volume 253, 114636, https://doi.org/10.1016/j.ecoenv.2023.114636.

216) Peralbo-Molina Á., Priego-Capote F., and Castro M. D. L. (2012). "Tentative identification of phenolic compounds in olive pomace extracts using liquid chromatography-tandem mass spectrometry with a quadrupole-quadrupole-time-of-flight mass detector," *Journal of Agricultural and Food Chemistry*, vol. 60, no. 46, pp. 11542–11550

217) Pereira A. P., Ferreira I. C. F. R., Marcelino F. et al. (2007). "Phenolic compounds and antimicrobial activity of olive (Olea europaea L. Cv. Cobranc¸osa) leaves," Molecules, vol. 12, no. 5, pp. 1153– 1162,

218) Pérez J. Hernández A., Trujillo J. M., López H. (2005). "Iridoids and secoiridoids from *Oleaceae*," *Studies in Natural Products Chemistry*, vol. 32, pp. 303–363,

219) Pérez-Bonilla M., Salido S.,. van Beek T. A et al. (2006)., "Isolation and identification of radical scavengers in olive tree (*Olea europaea*) wood," *Journal of Chromatography A*, vol. 1112, no. 1-2, pp. 311–318,

220) Pfost D, Vardeny Z, Tauc J (1985) Pfost, vardeny, and tauc respond. Phys Rev Lett 54(3):251–251. https:// doi. org/ 10. 1103/ PhysR evLett. 54. 251

221) Pimpin A and Srituravanich, Pimpin A and Srituravanich W . (2012). Review on Micro- and Nanolithography Techniques and their Applications,. 16 –37

222) Porter W.P., S.M. Green, S.M. Debbink, I. (1993). Carlson, Groundwater pesticides: interactive effects of low concentrations of carbamates, aldicarb and methomyl and the triazine metribuzin on thyroxine and somatotropin levels in white rats, J. Toxicol. Environ. Health 40 15–34.

223) Poudyal, H., Campbell, F. And Brown, L. (2010). Olive leaf extract attenuates cardiac, hepatic and metabolic changes in high carbohydrate-, high fat-fed rats. J. Nutr. 140, 946–953.

224) Pourmand A, Abdollahi M. (2012). Current opinion on nanotoxicology. *Daru journal of pharmaceutical sciences.* 20(1):95.

225) Prasad Yadav T., Manohar Yadav R. and Pratap Singh D.(2012). *Nanosci. Nanotechnol.*, , 2 , 22 —48

226) Prashant Mohanpuria; Nisha K. Rana; Sudesh Kumar Yadav 2008). *Biosynthesis of nanoparticles: technological concepts and future applications. , 10(3), 507–517.* doi:10.1007/s11051-007-9275-x

227) Qidwai, A., Pandey, M., Kumar, R. *et al.* (2017). Comprehensive evaluation of pharmacological properties of *Olea europaea* L. for Cosmeceuticals prospects. *Clin Phytosci* 3, 12 https://doi.org/10.1186/s40816-017-0050-y

228) Raja, S., Ramesh, V., Thivaharan, V. (2015). *Antibacterial and anticoagulant activity of silver nanoparticles synthesised from a novel source–pods of Peltophorum pterocarpum. Journal of Industrial and Engineering Chemistry, 29, 257–264.* doi:10.1016/j.jiec.2015.03.033] ,

229) Raimondi F., Scherer G.G., Kötz R., Wokaun A. (2005). "Nanoparticles in Energy Technology: Examples from Electrochemistry and Catalysis," Angewandte Chemie International Edition, vol. 44, no. 15, p. 2190–2209

230) Ranjbar A., Pasalar P., Sedighi A., Abdollahi M. (2002). Induc-tion of oxidative stress in paraquat formulating workers,"Toxicology Letters, vol. 131, no. 3, pp. 191–194,

231) Rasmussen JW, Martinez E, Louka P, Wingett DG. (2010). Zinc oxide nanoparticles for selective destruction of tumor cells and potential for drug delivery applications. *Expert Opin. Drug Deliv.* 7(9):1063–1077

232) Ratnam D.V., Ankola D.D., Bhardwaj V., Sahana D.K., Kumar M.N.V.R. (2006). Role of antioxidants in prophylaxis and therapy: A pharmaceutical perspective, J. Control. Release 113 (3) 189–207.

233) Raveendran P, Fu J, Wallen SL. (2003). Completely "green" synthesis and stabilization of metal nanoparticles. J Am Chem Soc;125:13940–13941.

234) Recordati C, De Maglie M, Bianchessi S, Argentiere S, Cella C, Mattiello S, Cubadda F, Aureli F, D'Amato M, Raggi A, Lenardi C, Milani P, Scanziani E. (2016). Tissue distribution and acute toxicity of silver after single intravenous administration in mice: nano-specific and size-dependent effects. Part Fibre Toxicol 13(1):12. https://doi.org/10.1186/s12989-016-0124-x

235) Robertson A., Tirado C., Lobstein T., Jermini M., Knai C., Jensen J.H., Ferro-Luzzi A., James W.P.T. (2004). *Food and Health in Europe: A New Basis for Action, European Series, No. 96.* WHO Regional Publications; Geneva, Switzerland: p. 385In

236) Roy R, Kumar S, Tripathi A, Das M, Dwivedi PD. (2014). Interactive threats of n anoparticles to the biological system. Immunol Lett. 158(1–2):79–87.

237) Ryan D and Robards K . (1998). "Phenolic compounds in olives," *Analyst*, vol. 123, no. 5, pp. 31R–44R.

238) Ryan D., Robards K, Prenzler P., Jardine D., T. Herlt, and M. Antolovich, (1999). "Liquid chromatography with electrospray ionisation mass spectrometric detection of phenolic compounds from *Olea europaea*," *Journal of Chromatography A*, vol. 855, no. 2, pp. 529–537,

239) Ryan D., Robards K. (1998), "Phenolic compounds in olives," *Analyst*, vol. 123, no. 5, pp. 31R–44R,

240) Ryan, D., Prenzler, P.D.; Lavee, S.; Antolovich, M.; Robards, K. (2003), . Quantitative changes in phenolic content during physiological development of the olive (*Olea europaea*) cultivar Hardy's Mammoth. *J. Agric. Food Chem 51,* 2532–2538.

241) Salari S, Bahabadi SE, Samzadeh-Kermani A, Yosefzaei F. (2019). In-vitro evaluation of antioxidant and antibacterial potential of green synthesized silver nanoparticles using *Prosopis farcta* fruit extract. *Iran. J. Pharm. Res*;18:430–445

242) Saleh S.M., Alminderej F. M., Ali R., Abdallah O.I. (2020). Optical sensor film for metribuzin pesticide detection. Spectrochimica Acta Part A: Molecular and Biomolecular Spectroscopy, 229, 117971

243) Saliani M., Jalal R., Kafshdare G.E. . (2015). Effects of pH and temperature on antibacterial activity of Zinc Oxide nanofluid against *Escherichia coli* O157: H7 and *Staphylococcus aureus*. *Jundishapur. J. Microbiol*;8:e17115. doi: 10.5812/jjm.17115.

244) Salih SJ, Smail AK .(2016). Synthesis, characterization and evaluation of antibacterial efficacy of zinc oxide nanoparticles. Pharm Biol Evaluations 3:327–333

245) Samova L. I., Shode F. O., Ramnanan P., Nadar A. (2003). Antihypertensive, antiatherosclerotic and antioxidantactivity of triterpenoids isolated from Oleaeuropaea, subspecies Africana leaves, J. Ethnopharmacol., 84:299–305

246) Samova. L. I., Shode F. O., and Mipando M. (2004). "Cardiotonic and antidysrhythmic effects of oleanolic and ursolic acids, methyl maslinate and uvaol," Phytomedicine, vol. 11, no. 2-3, pp. 121–129

247) Santhoshkumar J, Venkat Kumar S, Rajeshkumar S. (2017). Synthesis of zinc oxide nanoparticles using plant leaf extract against urinary tract infection pathogen. *Resource-Efficient Technologies*.;3(4):459–465.

248) Santhoshkumar J, Venkat Kumar S, Rajeshkumar S. (2017). Synthesis of zinc oxide nanoparticles using plant leaf extract against urinary tract infection pathogen. *Resource-Efficient Technologies*. 3(4):459–465.

249) Saraç, N., Baygar, T., Uğur, A. (2018). in vitro mutagenic and anti- mutagenic properties of green synthesised silver nanoparticles. IET Nanobiotechnology, 12(2), 230-233. https://doi.org/10.1049/iet-nbt.2017.0016.

250) Saraç, N; Şen, B . (2014). Antioxidant, mutagenic, antimutagenic activities, and phenolic compounds of *Liquidambar orientalis Mill*. var. orientalis. Industrial Crops and Products, 53(), 60-64. doi:10.1016/j.indcrop.2013.12.01

251) Saratale R.G, *et al.* (2018). Exploiting antidiabetic activity of silver nanoparticles synthesized using Punica granatum leaves and anticancer potential against human liver cancer cells (HepG2) Artif. Cells, Nanomed., Biotechnol., 46 (1) , pp. 211-222

252) Sarwar M. (2013). "The theatrical usefulness of olive *Olea europaea* L.(Oleaceae family) nutrition in human health: a review," *Sky Journal of Medicinal Plant Research*, vol. 2, no. 1, pp. 1–4.

253) Sato H., C. Genet, A. Strehle et al. (2007). "Anti-hyperglycemic activity of a TGR5 agonist isolated from Olea europaea," Biochemical and Biophysical Research Communications, vol. 362, no. 4, pp. 793–798

254) Savournin C., Baghdikian B., Elias R., Dargouth-Kesraoui F., K. Boukef, and G. (2001). Balansard, "Rapid high -performance liquid chromatography analysis for the quantitative determination of oleuropein in *Olea europaea* leaves," *Journal of Agricultural and Food Chemistry*, vol. 49, no. 2, pp. 618–621

255) Sedef N El, Karakaya S, (2009), Olive tree (*Olea europaea*) leaves: potential beneficial effects on human health, *Nutrition Reviews*, Volume 67, Issue 11, 1 November Pages 632–638, https://doi.org/10.1111/j.1753-4887.2009.00248.x

256) Seil J.T, Taylor E.N., Webster T.J. (2009). Reduced activity of *Staphylococcus epidermidis* in the presence of sonicated piezoelectric zinc oxide nanoparticles, in *2009 IEEE 35th Annual Northeast Bioengineering Conference*, Boston, MA, USA, 3–5 April 2009, pp. 1–2.

257) Seil JT, Webster TJ. (2012). Antimicrobial applications of nanotechnology: methods and literature. *Int. J. Nanomed.* ;7:2767–2781.

258) Selem E, Mekky AF, Hassanein WA, Reda FM, Selim YA. (2022) Antibacterial and antibiofilm effects of silver nanoparticles against the uropathogen Escherichia coli U12. Saudi J Biol Sci 29(11):103457. https://doi.org/10.1016/j.sjbs.2022.103457

259) Servili M, Baldioli M, Selvaggini R, Macchioni A, Montedoro G. (1999). Phenolic compounds of olive fruit: one- and two-dimensional nuclear magnetic resonance characterization of Nüzhenide and its distribution in the constitutive parts of fruit. J Agric Food Chem. 47(1): 12–8.

260) Servili M, Esposto S, Fabiani R, Urbani S, Taticchi A, Mariucci F, et al. . (2009). Phenolic compounds in olive oil: antioxidant, health and organoleptic activities according to their chemical structure. *Inflammopharmacology*; 17(2): 76–84.

261) Shan Mc, D.; Ray, P.C.; Yu, H. (2014), Molecular toxicity mechanism of nanosilver. J. Food Drug Anal. 22, 116–127.

262) Shankar SS, Ahmad A, Pasricha R, Sastry M. (2003). Bioreduction of chloroaurate ions by Geranium leaves and its endophytic fungus yields gold nanoparticles of different shapes, J. Mater. Chem., 13(7), 1822−1826.

263) Sharma V., P. Singh, A. K. Pandey, and A. Dhawan. (2012). "Induction of oxidative stress, DNA damage and apoptosis in mouse liver after sub-acute oral exposure to zinc oxide nanoparticles," *Mutation Research*, vol. 745, no. 1-2, pp. 84–91

264) Shenashen M. A., El-Safty S. A., Elshehy E. A. (2014). Synthesis, morphological control, and properties of silver nanoparticles in potential applications. *Part. Part. Syst. Char.* 31 293–316.

265) Shrivastava S, T. Bera, S. K. Singh, G. Singh, P. Ramachandrarao, and D. Dash (2009). Characterization of antiplatelet properties of silver nanoparticles. ACS Nano 3, 1357–1364.

266) Shu M. X. L., (1996). "Olea," *Flora of China*, vol. 15, pp. 295–298,

267) Siddiqi KS, Ur Rahman A, Tajuddin, Husen A. (2018). Properties of Zinc Oxide Nanoparticles and Their Activity Against Microbes. Nanoscale Res Lett. May 8;13(1):141. doi: 10.1186/s11671-018-2532-3.

268) Simoneaux, B. (2008). *The Triazine Herbicides || Plant Uptake and Metabolism of Triazine Herbicides. , (), 73–99.* doi:10.1016/B978-044451167-6.50010-6

269) Sindona G.. De Nino A, Di Donna L., Mazzotti F., Muzzalupo E., Perri E., Tagarelli A. (2005)., Absolute method for the assay of oleuropein in olive oils by atmospheric pressure chemical ionization tandem mass spectrometry. Anal.Chem. 77:5961-5964

270) Singh A, Dar MY, Joshi B, Sharma B, Shrivastava S, Shukla S. (2018). Phytofabrication of Silver nanoparticles: Novel Drug to overcome hepatocellular ailments. Toxicol Rep. Mar 1;5:333-342.

271) Singh P., Kim Y. J., Yang D. C. (2015). A strategic approach for rapid synthesis of gold and silver nanoparticles by Panax ginseng leaves. Artif. Cells Nanomed. Biotechnol. 44, 1949–1957.

272) Singh R, Dutt S, Sharma P, Sundramoorthy AK, Dubey A, Singh A, Arya S. (2023). Future of Nanotechnology in Food Industry: Challenges in Processing, Packaging, and Food Safety. Glob Chall. 21;7(4):2200209. doi: 10.1002/gch2.202200209.

273) Singhal, R. Bhavesh, K. Kasariya, A. Sharma R., and Singh R. P. (2011). ”Biosynthesis of silver nanoparticles using Ocimum sanctum (Tulsi) leaf extract and screening its antimicrobial activity,” J Nanoparticle Res, vol. 13

274) Sirelkhatim A, Mahmud S, Seeni A, Kaus NHM, Ann LC, Bakhori SKM, Hasan H, Mohamad D. (2015). Review on Zinc Oxide Nanoparticles: Antibacterial Activity and Toxicity Mechanism. Nanomicro Lett.;7(3):219-242. doi: 10.1007/s40820-015-0040-x.

275) Skóra B, Krajewska U, Nowak A, Dziedzic A, Barylyak A, KusLiśkiewicz M. (2021). Noncytotoxic silver nanoparticles as a new antimicrobial strategy. Sci Rep 11(1):13451. https://doi.org/10. 1038/s41598-021-92812-w

276) Slinkard K., Singleton, V. L. (1977). Total phenol analysis: automation and comparison with manual methods. *American journal of enology and viticulture*, *28*(1), 49-55.

277) Sofowara A. (1989).Medicinal plants and Traditional medicine in Africa, Spectrum Books Ltd, Ibadan, Nigeria, 1993, 191-289. [11]GE Trease ; WC Evans, Pharmacognosy, , 11, 45-50

278) Soler-Rivas C, Espín JC, Wichers HJ. (2000) Oleuropein and related compounds. J Sci Food Agric.; 80(7): 1013–23

279) Sondi I, Salopek-Sondi B. (2004). Silver nanoparticles as antimicrobial agent: a case study on E. coli as a model for Gram-negative bacteria. J Colloid Interface Sci 275(1):177–182. https://doi.org/ 10.1016/j.jcis.2004.02.012

280) Speerschneider P, Dekant W. (1995). Renal tumorigenicity of 1,1-dichloroethene in mice: The role of male-specific expression of cytochrome P450 2E1 in the renal bioactivation of 1,1-dihloroethene. *Toxicol Appl Pharmacol.* 130:48–56.

281) Spring H, S.K. (1995). "Diversity of magnetotactic bacteria.". Syst Appl Microbiol, 18(2): p. 147-153

282) Sudjana AN, D'Orazio C, Ryan V, Rasool N, Ng J, Islam N, Riley TV, Hammer KA. (2009). Antimicrobial activity of commercial Olea europaea (olive) leaf extract. Int J Antimicrob Agents. 33(5):461-3. doi: 10.1016/j.ijantimicag.2008.10.026.

283) Sulaiman GM, Tawfeeq AT, Naji AS. (2018). Biosynthesis, characterization of magnetic iron oxide nanoparticles and evaluations of the cytotoxicity and DNA damage of human breast carcinoma cell lines, Art cells. *Nanomed Biotechnol.* 46(6):1215–1229..

284) Sundaraselvan G, Quine SD. (2017). Green synthesis of zinc oxide nanoparticle using seed extract of Murraya Koenigii and their antimicrobial activity against some human pathogens. *Journal of nanoscience and technology*.;3(4):289–292.

285) Swarnalatha L., Rachel C., Ranjan S., Baradwaj P. (2012). Evaluation of invitro antidiabetic activity of *Sphaeranthus amaranthoides* silver nanoparticles. *Int. J. Nanomater. Biostruct.* 2:25–29

286) Tahir R, Bilal M, Iqbal H, et al. (2017). Green biosynthesis of silver nanoparticles using leaves extract of Artemisia vulgaris and their potential biomedical applications. Colloids Surf B Biointerf 158:408–415.

287) Tang J, Xiong L, Wang S, Wang J, Liu L, Li J, Yuan F, Xi T. (2009). Distribution, translocation and accumulation of silver nanoparticles in rats. *Journal of nanoscience and nanotechnology.* 9(8):4924–4932..

288) Tasioula-Margari, M.; Ologeri, O. (2001). Isolation and characterization of virgin olive oil phenolic compounds by HPLC/UV and GC/MS. *J. Food Sci 66*, 530–534

289) Tedjani ML, Khelef A, Laouini SE, Bouafia A, Albalawi N .(2022). Optimizing the antibacterial activity of iron oxide nanoparticles using central composite design. J Inorg Organomet Polym Mater 32(9):3564–3584. https:// doi. org/ 10. 1007/ s10904- 022- 02367-0

290) Trang NLN, Hoang V-T, Dinh NX, Tam LT, Le VP, Linh DT, Cuong DM, Khi NT, Anh NH, Nhung PT, Le A-T .(2021). Novel eco-friendly synthesis of biosilver nanoparticles as a colorimetric probe for highly selective detection of Fe (III)

ions in aqueous solution. J Nanomater 2021:5527519. https://doi.org/10.1155/2021/5527519

291) Tripathy, A., Raichur, A. M., Chandrasekaran, N., Prathna, T. C., & Mukherjee, A. (2010). Process variables in biomimetic synthesis of silver nanoparticles by aqueous extract of Azadirachta indica (Neem) leaves. *Journal of Nanoparticle Research*, *12*, 237-246.

292) Tsuji, B. T.; Yang, J. C.; Forrest, A.; Kelchlin, P. A.; Smith, P. F. (2008). *In vitro pharmacodynamics of novel rifamycin ABI-0043 against Staphylococcus aureus. Journal of Antimicrobial Chemotherapy, 62(1), 156–160.* doi:10.1093/jac/dkn133 .

293) Umbuzeiro G.A., Vargas V.M.F,.(2003). Teste de mutagenicidade com Salmonella typhimurium (teste de Ames) como indicador de mutagenicidade em potencial para mamíferos, in: Ribeiro, L.R., Salvadori, D.M.F., Marques, E.K. Mutagênese Ambiental. Ulbra, Canoas. pp. 81-112.

294) USEPA, Health. (2003). Effects Support Document for Metribuzin. Office of Water, EPA Report 822-R-03-004, p. 84.

295) Usman M, Farooq M, Wakeel A, Nawaz A, Cheema SA, Rehman H, et al. (2020). Nanotechnology in agriculture: current status, challenges and future opportunities. Sci Total Environ. 721: 137778.

296) Van der Oost R, Beyer J, Vermeulen NP. . (2003) . Fish bioaccumulation and biomarkers in environmental risk assessment: a review. *Environ Toxicol Pharmacol*13:57–149.

297) Vander Oost R, Beyer J, Vermeulen NP. (2003). Fish bioaccumulation and biomarkers in environmental risk assessment: a review. *Environ Toxicol Pharmacol.* 13:57–149.

298) Vijayaraghavan T, Sivasubramanian R, Hussain S, Ashok A .(2017). A facile synthesis of LaFeO3-based perovskites and their application towards sensing of neurotransmitters. ChemistrySelect 2(20):5570–5577. https:// doi. org/ 10. 1002/ slct. 20170 0723

299) Vijayaram S, Razafindralambo H, Sun YZ, Vasantharaj S, Ghafarifarsani H, Hoseinifar SH, Raeeszadeh M. (2024). Applications of Green Synthesized Metal

Nanoparticles - a Review. Biol Trace Elem Res.;202(1):360-386. doi: 10.1007/s12011-023-03645-9

300) Vishwakarma V, Samal SS, Manoharan N. (2010). Safety and risk associated with nanoparticles-a review. *Journal of minerals and materials characterization and engineering.* 9(5):455.

301) Visioli F, Bellomo G, Montedoro G, Galli C. (1995). Low density lipoprotein oxidation is inhibited in vitro by olive oil constituents. Atherosclerosis. 117:25–32.

302) Wang L, Hu C, Shao L. (2017) The antimicrobial activity of nanoparticles: present situation and prospects for the future. Int J Nanomedicine. Feb 14;12:1227-1249. doi: 10.2147/IJN.S121956. PMID: 28243086; PMCID: PMC5317269.

303) Wasef, L., Nassar, A.M.K., El-Sayed, Y.S. *et al*.(2021). The potential ameliorative impacts of cerium oxide nanoparticles against fipronil-induced hepatic steatosis. *Sci Rep* 11, 1310 https://doi.org/10.1038/s41598-020-79479-5

304) Weckbecker, G., & Cory, J. G. (1988). Ribonucleotide reductase activity and growth of glutathione-depleted mouse leukemia L1210 cells in vitro. *Cancer letters*, *40*(3), 257-264.

305) Yaki, K. (1976). A simple fluorometric assay for lipoprotein in blood plasma. *Biochem Med*, *15*, 212-217.

306) Yan X., Rong R., Zhu S., Guo M., Gao S., Wang S., Xu X. .(1979). Effects of ZnO nanoparticles on dimethoate-induced toxicity in mice. *J. Agric. Food Chem.* 2015;63:8292–8298. doi: 10.1021/acs.jafc.5b0

307) Zeng Q., D. Shao, W. Ji, J. Li, L. Chen, J. Song, (2014) . The nanotoxicity investigation of optical nanoparticles to cultured cells in vitro, Toxicol. Rep. 1 137–144

308) Zhao, X., Liu, W., Cai, Z., Han, B., Qian, T., Zhao, D. (2016). An overview of preparation and applications of stabilized zero-valent iron nanoparticles for soil and groundwater remediation. *Water research*, *100*, 245-266.

309) Zheng X., Wu R., Chen Y. (2000). Effects of ZnO nanoparticles on wastewater biological nitrogen and phosphorus removal. *Environ. Sci. Technol.* 2011;45:2826–2832. doi: 10.1021/es 744.

310) Zheng Z., Zhang X., Carbo D., Clark C., Nathan C.-A., Lvov Y. (2010). Sonication-assisted synthesis of polyelectrolyte-coated curcumin nanoparticles. *Langmuir* 26 7679–7681.

Annex

Annex 01: Calibration curve for estimation of phytochemicals compounds

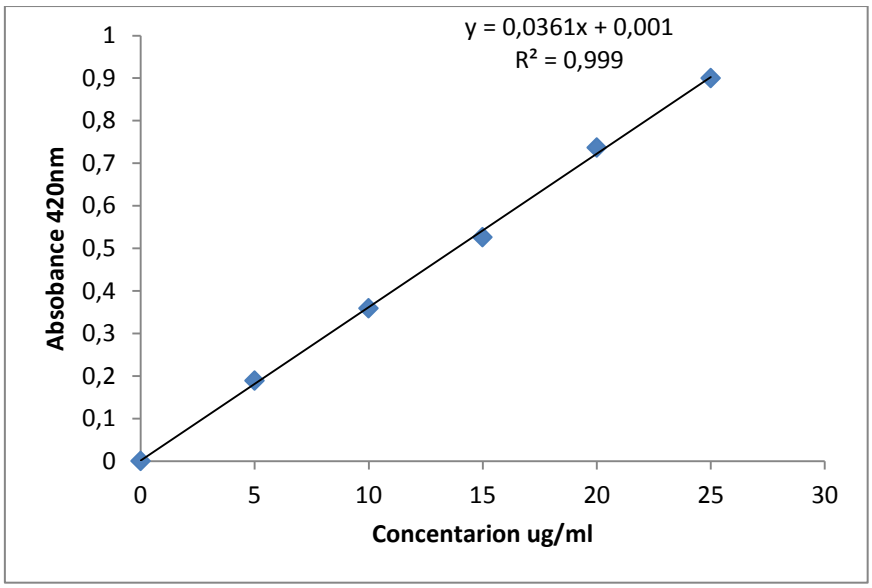

Figure: Calibration curve of Quercitin for determination of total flavonoids content.

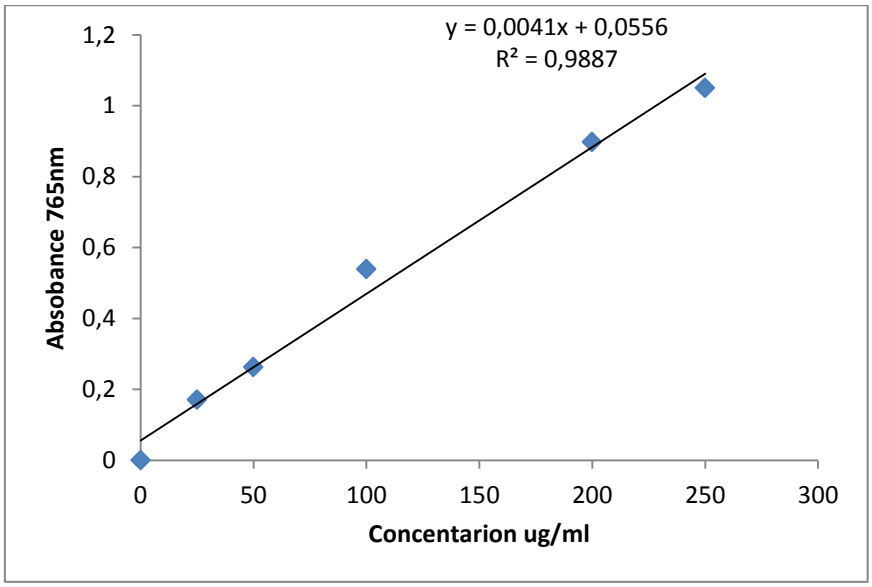

Figure: Calibration curve of Gallic acid for determination of total phenolic content.

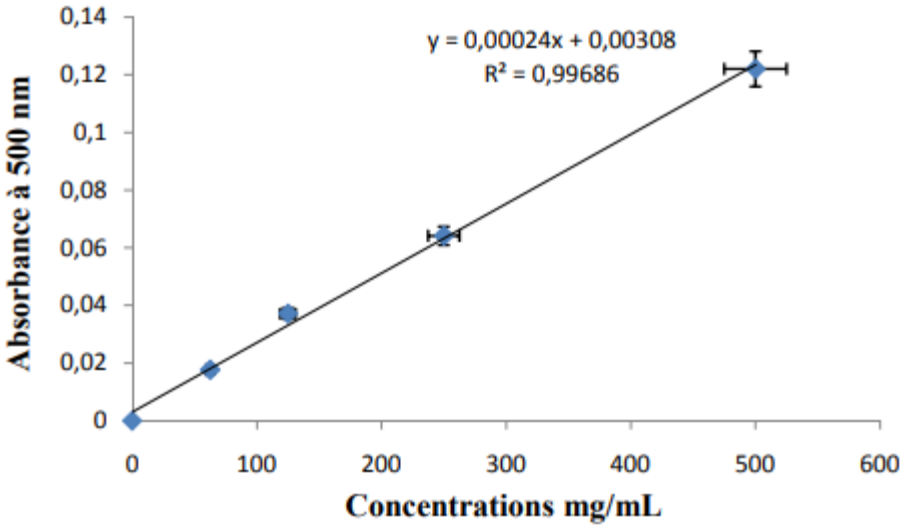

Figure: Calibration curve of Catechin for determination of condensed tannins content.

Annex 02: Calibration curve for determination of capacity antioxidant

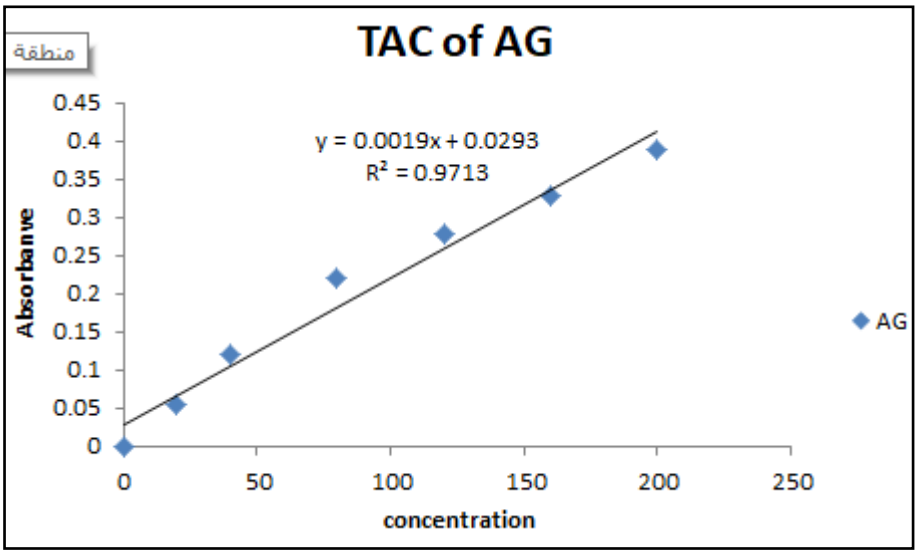

Figure: Calibration curve of Gallic acid for determination of total antioxidant capacity

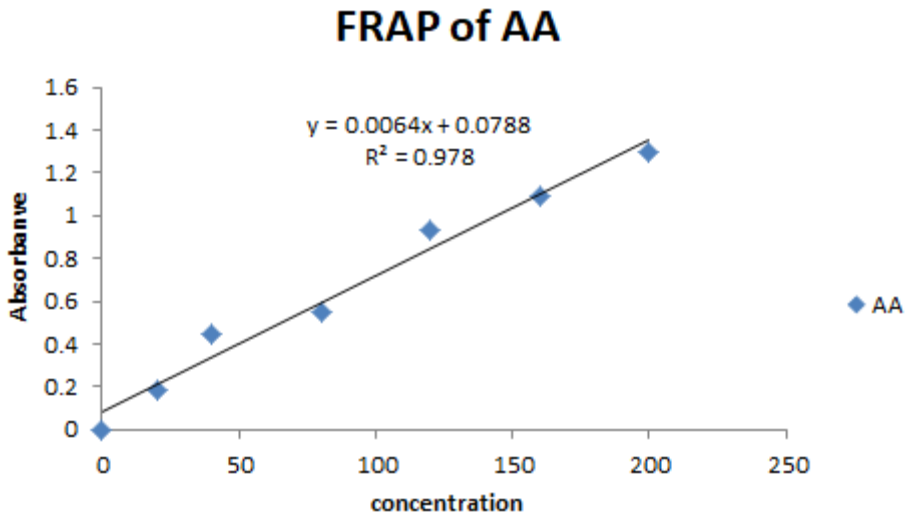

Figure: Calibration curve of Ascorbic Acid for determination of reducing power capacity

Annex 04: Biochemical parameters analysis

SPINREACT

CE GLUCOSE -HK

Glucose-HK

Hexokinase. Enzymatic - UV

Quantitative determination of glucose
IVD

Store at 2-8 °C

PRINCIPLE OF THE METHOD

Hexoquinase (HK) catalyzes the phosphorylation of glucose to glucose-6-phosphate (G6P) by ATP. The formed glucose-6-phosphate is reduced to 6-phosphogluconate in the presence of glucose-6-phosphate dehydrogenase (G6P-DH) with the subsequent reduction of NAD to NADH:

$$\text{Glucose} + \text{ATP} \xrightarrow{\text{HK}} \text{Glucose-6-phosphate} + \text{ADP}$$

$$\text{G6P} + \text{NAD}^+ \xrightarrow{\text{G6P-DH}} \text{6-Phosphogluconate} + \text{NADH} + \text{H}^+$$

The increase in concentration of NADH is proportional to the glucose concentration in the sample[1,2].

CLINICAL SIGNIFICANCE

Glucose is a major source of energy for most cells of the body; insulin facilitates glucose entry into the cells.
Diabetes is a disease manifested by hyperglycemia; patients with diabetes demonstrate an inability to produce insulin[1,5,6].
Clinical diagnosis should not be made on a single test result; it should integrate clinical and other laboratory data.

REAGENTS

R 1 Buffer	TRIS pH 7,5	4 mmol/L
	ATP	2,1 mmol/L
	Mg^{2+}	0,8 mmol/L
R 2 Enzymes	NAD^+	2 mmol/L
	Hexoquinase (HK)	1000 U/L
	Glucose-6-phosphate (G6P-DH)	1000 U/L
GLUCOSE CAL	Glucose aqueous primary standard 100 mg/dL	

PREPARATION

Working reagent (WR): Dissolve (→) the contents of one vial of R 2 Enzymes in one bottle of R 1 Buffer.
Cap and mix gently to dissolve contents.
The reagent is stable after reconstitution 1 month in the refrigerator (2-8ºC) or 7 days at room temperature (15-25ºC).

STORAGE AND STABILITY

All the components of the kit are stable until the expiration date on the label when stored tightly closed at 2-8ºC, protected from light and contaminations prevented during their use.
Do not use reagents over the expiration date.
Signs of reagent deterioration:
- Presence of particles and turbidity.
- Blank absorbance (A) at 340 nm ≥ 0,30.

4. Mix and incubate for 5 min. at 37ºC or 10 min. at room temperature (15-25ºC).
5. Read the absorbance (A) of the samples and calibrator, against the Blank.

CALCULATIONS

$$\frac{(A)\text{Sample} - (A)\text{Blank}}{(A)\text{Standard} - (A)\text{Blank}} \times 100\ (\text{Standard conc.}) = \text{mg/dL glucose in the sample}$$

Conversion factor: mg/dL x 0,0555= mmol/L.

QUALITY CONTROL

Control sera are recommended to monitor the performance of assay procedures: SPINTROL H Normal and Pathologic (Ref. 1002120 and 1002210).
If control values are found outside the defined range, check the instrument, reagents and calibrator for problems.
Each laboratory should establish its own Quality Control scheme and corrective actions if controls do not meet the acceptable tolerances.

REFERENCE VALUES[1]

Serum or plasma:

60 – 110 mg/dL ≅ 3,33 – 6,10 mmol/L

These values are for orientation purpose; each laboratory should establish its own reference range.

PERFORMANCE CHARACTERISTICS

Measuring range: From *detection limit* of 0,16 mg/dL to *linearity limit* of 600 mg/dL.
If the results obtained were greater than linearity limit, dilute the sample 1/2 with NaCl 9 g/L and multiply the result by 2.
Precision:

	Intra-assay (n=20)		Inter-assay (n=20)	
Mean (mg/dL)	98	251	99	253
SD	1,05	4,15	1,51	2,42
CV (%)	1,07	1,66	1,52	0,96

Sensitivity: 1 mg/dL = 0,0036 A.
Accuracy: Results obtained using SPINREACT reagents (y) did not show systematic differences when compared with other commercial reagents (x).
The results obtained using 50 samples were the following:
Correlation coefficient $(r)^2$: 0,99
Regression equation: y=1,0146x + 5,5029.
The results of the performance characteristics depend on the analyzer used.

INTERFERENCES

Hemoglobin up to 19 g/L and bilirubin up to 100 mg/L, do not interfere[1].
A list of drugs and other interfering substances with glucose determination has been reported by Young et. al[3,4].

NOTES

1. GLUCOSE CAL: Proceed carefully with this product because due its nature it can get contaminated easily

SPINREACT

CE CREATININE -J

Creatinina

Jaffé. Colorimétrico - cinético

Determinación cuantitativa de creatinina

IVD

Conservar a 2-8ºC

PRINCIPIO DEL MÉTODO

El ensayo de la creatinina esta basado en la reacción de la creatinina con el picrato de sodio descrito por Jaffé.

La creatinina reacciona con el picrato alcalino formando un complejo rojizo. El intervalo de tiempo escogido para las lecturas permite eliminar gran parte de las interferencias conocidas del método.

La intensidad del color formado es proporcional a la concentración de creatinina en la muestra ensayada[1].

SIGNIFICADO CLÍNICO

La creatinina es el resultado de la degradación de la creatina, componente de los músculos y puede ser transformada en ATP, fuente de energía para las células.

La producción de creatinina depende de la modificación de la masa muscular. Varía poco y los niveles suelen ser muy estables.

Se elimina a través del riñón. En una insuficiencia renal progresiva hay una retención en sangre de urea, creatinina y ácido úrico.

Niveles altos de creatinina son indicativos de patología renal[1,2]

El diagnóstico clínico debe realizarse teniendo en cuenta todos los datos clínicos y de laboratorio.

REACTIVOS

R 1 Reactivo Pícrico	Ácido pícrico	17,5 mmol/L
R 2 Reactivo Alcalinizante	Hidróxido sódico	0,29 mol/L
CREATININE CAL	Patrón primario acuoso de Creatinina	2 mg/dL

PRECAUCIONES

R1/ R2: H314-Provoca quemaduras graves en la piel y lesiones oculares graves.

CAL: H290-Puede ser corrosivo para los metales.

Seguir los consejos de prudencia indicados en la FDS y etiqueta del producto.

PREPARACIÓN

Reactivo de trabajo (RT): Mezclar volúmenes iguales de R1 Reactivo Pícrico y de R2 Reactivo Alcalinizante.

Estabilidad del reactivo de trabajo: 15 días a 2-8ºC o 7 días a temperatura ambiente (15-25ºC).

CONSERVACIÓN Y ESTABILIDAD

Todos los componentes del kit son estables, hasta la fecha de caducidad indicada en la etiqueta, cuando se mantienen los frascos bien cerrados a 2-8ºC, protegidos de la luz y se evita su contaminación. No usar reactivos

4. Mezclar y poner en marcha el cronómetro.
5. Leer la absorbancia (A_1) al cabo de 30 segundos y al cabo de 90 segundos (A_2) de la adición de la muestra.
6. Calcular: $\Delta A = A_2 - A_1$.

CÁLCULOS

$$\frac{\Delta A \text{ Muestra} - \Delta A \text{ Blanco}}{\Delta A \text{ Patrón} - \Delta A \text{ Blanco}} \times 2 \text{ (Conc. Patrón)} = \text{mg/dL de creatinina en la muestra}$$

Factor de conversión: mg/dL x 88,4 = µmol/L.

CONTROL DE CALIDAD

Es conveniente analizar junto con las muestras sueros control valorados: SPINTROL H Normal y Patológico (Ref. 1002120 y 1002210).

Si los valores hallados se encuentran fuera del rango de tolerancia, revisar el instrumento, los reactivos y el calibrador.

Cada laboratorio debe disponer su propio Control de Calidad y establecer correcciones en el caso de que los controles no cumplan con las tolerancias.

VALORES DE REFERENCIA[1]

Suero o plasma:

Hombres	0,7 - 1,4 mg/dL	≙ 61,8 - 123,7 µmol/L
Mujeres	0,6 - 1,1 mg/dL	≙ 53,0 - 97,2 µmol/L

Orina: 15-25 mg/Kg/24 h

Hombres	10 - 20 mg/Kg/24 h
Mujeres	8 - 18 mg/Kg/24 h

Estos valores son orientativos. Es recomendable que cada laboratorio establezca sus propios valores de referencia.

CARACTERÍSTICAS DEL MÉTODO

Rango de medida: Desde el *límite de detección* de 0,000 mg/dL hasta el *límite de linealidad* de 35 mg/dL.

Si la concentración es superior al límite de linealidad, diluir la muestra 1/2 con ClNa 9 g/L y multiplicar el resultado final por 2.

Precisión:

	Intraserie (n=20)		Interserie (n=20)	
Media (mg/dL)	0,92	3,43	0,96	3,50
SD	0,03	0,07	0,04	0,09
CV (%)	2,76	1,90	3,97	2,51

Sensibilidad analítica: 1 mg/dL = 0,0407 ΔA/min.

Exactitud: Los reactivos de SPINREACT (y) no muestran diferencias sistemáticas significativas cuando se comparan con otros reactivos comerciales (x).

Los resultados obtenidos con 50 muestras fueron los siguientes:

Coeficiente de correlación $(r)^2$: 0,99584

Ecuación de la recta de regresión: y= 0,953x + 0,075

Las características del método pueden variar según el analizador utilizado.

SPINREACT

CE UREA-UV

Urea-UV

Ureasa -GLDH. Cinético UV

Determinación cuantitativa de urea
IVD

Conservar a 2-8ºC

PRINCIPIO DEL METODO

La ureasa cataliza la hidrólisis de la urea, presente en la muestra, en amoniaco (NH_3) y anhídrido carbónico (CO_2).

El amoniaco formado se incorporan al α-cetoglutarato por acción de la glutamato deshidrogenasa (GLDH) con oxidación paralela de NADH a NAD^+:

$$\text{Urea} + H_2O + 2\,H^+ \xrightarrow{\text{Ureasa}} 2\,NH_3 + CO_2$$

$$2\,NH_3 + \alpha\text{-Cetoglutarato} + NADH \xrightarrow{\text{GLDH}} H_2O + NAD^+ + \text{L-Glutamato}$$

La disminución de la concentración de NAD^+ en el medio es proporcional a la concentración de urea de la muestra ensayada[1].

SIGNIFICADO CLINICO

La urea es el resultado final del metabolismo de las proteínas; se forma en el hígado a partir de su destrucción.

Puede aparecer la urea elevada en sangre (uremia) en dietas con exceso de proteínas, enfermedades renales, insuficiencia cardiaca, hemorragias gástricas, hipovolemia y obstrucciones renales [1,4,5].

El diagnóstico clínico debe realizarse teniendo en cuenta todos los datos clínicos y de laboratorio.

REACTIVOS

R 1 Tampón	TRIS pH 7,8	80 mmol/L
	α-Cetoglutarato	6 mmol/L
R 2 Enzimas	Ureasa	3750 U/L
	Glutamato deshidrogenasa (GLDH)	6000 U/L
	NADH	0,32 mmol/L
UREA CAL	Patrón primario acuoso de Urea	50 mg/dL

PREPARACION

Reactivo de trabajo (RT): Disolver (➞) el contenido de un vial de R 2 Enzimas en un frasco de R 1 Tampón.

Tapar y mezclar suavemente hasta disolver su contenido.

Estabilidad: 6 semanas a 2-8ºC o 7 días a 15-25ºC.

CONSERVACION Y ESTABILIDAD

Todos los componentes del kit son estables, hasta la fecha de caducidad indicada en la etiqueta, cuando se mantienen los frascos bien cerrados a 2-8ºC, protegidos de la luz y se evita su contaminación. No usar reactivos fuera de la fecha indicada.

Indicadores de deterioro de los reactivos:

- Presencia de partículas y turbidez.
- Absorbancia (A) del blanco a 340 nm < 1,00.

MATERIAL ADICIONAL

- Espectrofotómetro o analizador para lecturas a 340 nm.

CALCULOS

$$\frac{\text{(A1-A2) Muestra - (A1-A2) Blanco}}{\text{(A1-A2) Patrón - (A1-A2) Blanco}} \times 50\ (\text{Conc. Patrón}) = \text{mg/dL de urea en la muestra}$$

mg/dL urea x 0,466 = mg/dL de urea BUN (Blood Urea Nitrogen)[1]

Factor de conversión: mg/dL x 0,1665 = mmol/L.

CONTROL DE CALIDAD

Es conveniente analizar junto con las muestras sueros control valorados: SPINTROL H Normal y Patológico (Ref. 1002120 y 1002210).

Si los valores hallados se encuentran fuera del rango de tolerancia, revisar el instrumento, los reactivos y el calibrador.

Cada laboratorio debe disponer su propio Control de Calidad y establecer correcciones en el caso de que los controles no cumplan con las tolerancias.

VALORES DE REFERENCIA[1]

Suero: de 15 a 45 mg/dL (2,49-7,49 mmol/L)

Orina: de 20 a 35 gr/24 horas

Estos valores son orientativos. Es recomendable que cada laboratorio establezca sus propios valores de referencia.

CARACTERISTICAS DEL METODO

Rango de medida: Desde el *límite de detección* de 1,241 mg/dL hasta el *límite de linealidad* de 530 mg/dL.

Si la concentración es superior al límite de linealidad, diluir la muestra 1/2 con ClNa 9 g/L y multiplicar el resultado final por 2.

Precisión:

	Intraserie (n=20)		Interserie (n=20)	
Media (mg/dL)	40,7	130	40,5	128
SD	0,88	1,02	1,19	2,07
CV (%)	2,16	0,78	2,94	1,61

Sensibilidad analítica: 1 mg/dL = 0,00080 ΔA.

Exactitud: Los reactivos SPINREACT (y) no muestran diferencias sistemáticas significativas cuando se comparan con otros reactivos comerciales (x).

Los resultados obtenidos con 50 muestras fueron los siguientes:

Coeficiente de correlación $(r)^2$: 0,998.

Ecuación de la recta de regresión: y= 1,5759x + 1,1577.

Las características del método pueden variar según el analizador utilizado.

INTERFERENCIAS

Como anticoagulante se recomienda la heparina. En ningún caso deben utilizarse sales de amonio o fluoruro[1].

Se han descrito varias drogas y otras substancias que interfieren en la determinación de la urea[2,3].

NOTAS

SPINREACT

CE URIC ACID

Ácido úrico

Uricasa -POD. Enzimático colorimétrico

Determinación cuantitativa de ácido úrico
IVD

Conservar a 2-8ºC

PRINCIPIO DEL MÉTODO

El ácido úrico es oxidado por la uricasa a alantoína y peróxido de hidrógeno ($2H_2O_2$) que en presencia de peroxidasa (POD), 4-aminofenazona (4-AF) y 2-4 Diclorofenol Sulfonato (DCPS) forma un compuesto rosáceo:

$$\text{Ácido úrico} + 2H_2O + O_2 \xrightarrow{\text{Uricasa}} \text{Alantoína} + CO_2 + 2H_2O_2$$

$$2H_2O_2 + \text{4-AF} + \text{DCPS} \xrightarrow{\text{POD}} \text{Quinonaimina} + 4H_2O$$

La intensidad de quinonaimina roja formada es proporcional a la concentración de ácido úrico presente en la muestra ensayada[1,2].

SIGNIFICADO CLÍNICO

El ácido úrico y sus sales son el producto final del metabolismo de las purinas. En una insuficiencia renal progresiva hay una retención en sangre de urea, creatinina y ácido úrico.
Niveles altos de ácido úrico son indicativos de patología renal y generalmente se asocia con la gota[1,5,6].
El diagnóstico clínico debe realizarse teniendo en cuenta todos los datos clínicos y de laboratorio.

REACTIVOS

R 1 Tampón	Fosfatos pH 7,4	50 mmol/L
	2-4 Diclorofenol Sulfonato (DCPS)	4 mmol/L
R 2 Enzimas	Uricasa	60 U/L
	Peroxidasa (POD)	660 U/L
	Ascorbato oxidasa	200 U/L
	4 - Aminofenazona (4-AF)	1 mmol/L
URIC ACID CAL	Patrón primario acuoso de Ácido úrico	6 mg/dL

PREPARACIÓN

Reactivo de trabajo (RT): Disolver (→) el contenido de un vial de R 2 Enzimas en un frasco de R 1 Tampón. Tapar y mezclar suavemente hasta disolver su contenido. Estabilidad: 1 mes en nevera (2-8ºC) o 10 días a temperatura ambiente.

CONSERVACIÓN Y ESTABILIDAD

Todos los componentes del kit son estables, hasta la fecha de caducidad indicada en la etiqueta, cuando se mantienen los frascos bien cerrados a 2-8ºC, protegidos de la luz y se evita su contaminación. No usar reactivos fuera de la fecha indicada.

Indicadores de deterioro de los reactivos:

- Presencia de partículas y turbidez.
- Absorbancia (A) del blanco a 520 nm ≥ 0,16.

MATERIAL ADICIONAL

- Espectrofotómetro o analizador para lecturas a 520 nm.
- Cubetas de 1 cm de paso de luz.

CÁLCULOS

Suero o plasma

$$\frac{\text{(A) Muestra - (A) Blanco}}{\text{(A) Patrón - (A) Blanco}} \times 6\ (\text{Conc. Patrón}) = \text{mg/dL de ácido úrico en la muestra}$$

Orina 24 h

$$\frac{\text{(A) Muestra - (A) Blanco}}{\text{(A) Patrón - (A) Blanco}} \times 6 \times \text{vol. (dL) orina/24h} = \text{mg/24 h de ácido úrico}$$

Factor de conversión: mg/dL x 59,5= µmol/L.

CONTROL DE CALIDAD

Es conveniente analizar junto con las muestras sueros control valorados: SPINTROL H Normal y Patológico (Ref. 1002120 y 1002210).
Si los valores hallados se encuentran fuera del rango de tolerancia, revisar el instrumento, los reactivos y el calibrador.
Cada laboratorio debe disponer su propio Control de Calidad y establecer correcciones en el caso de que los controles no cumplan con las tolerancias.

VALORES DE REFERENCIA[5]

Suero o plasma:

Mujeres	2,5 - 6,8 mg/dL	= 149 – 405 µmol/L
Hombres	3,6 - 7,7 mg/dL	= 214 – 458 µmol/L
Orina:	250 - 750 mg/24 h	= 1,49 - 4,5 mmol/24 h

Estos valores son orientativos. Es recomendable que cada laboratorio establezca sus propios valores de referencia.

CARACTERÍSTICAS DEL MÉTODO

Rango de medida: Desde el *límite de detección* de 0,00 mg/dL hasta el *límite de linealidad* de 40 mg/dL.
Si la concentración es superior al límite de linealidad, diluir la muestra 1/2 con NaCl 9 g/L y multiplicar el resultado final por 2.

Precisión:

	Intraserie (n=20)		Interserie (n=20)	
Media (mg/dL)	4,74	10,55	4,73	10,50
SD	0,02	0,03	0,13	0,29
CV (%)	0,50	0,30	2,67	2,77

Sensibilidad analítica: 1 mg/dL = 0,02930 A.
Exactitud: Los reactivos SPINREACT (y) no muestran diferencias sistemáticas significativas cuando se comparan con otros reactivos comerciales (x).
Los resultados obtenidos con 50 muestras fueron los siguientes:
Coeficiente de correlación $(r)^2$: 0,97137.
Ecuación de la recta de regresión: y=1,162x + 0,14156.
Las características del método pueden variar según el analizador utilizado.

INTERFERENCIAS

No se han observado interferencias con bilirrubina hasta 170 µmol/L, hemoglobina hasta 130 mg/dL y ácido ascórbico hasta 570 µmol/L[2].
Se han descrito varias drogas y otras substancias que interfieren en la

CE CHOLESTEROL

Cholestérol

CHOD-POD. Enzymatique chlorimétrique

Détermination quantitative de cholestérol
IVD

Conserver à 2-8°C

PRINCIPE DE LA METHODE

Le cholestérol présent dans l'échantillon donne lieu à un composé coloré, suivant la réaction suivante:

$$\text{Cholestérol ester} + H_2O \xrightarrow{CHE} \text{Cholestérol} + \text{Acides gras}$$

$$\text{Cholestérol} + O_2 \xrightarrow{CHOD} \text{4-Cholestènone} + H_2O_2$$

$$2\,H_2O_2 + \text{Phénol} + \text{4-Aminophénazone} \xrightarrow{POD} \text{Quinonimine} + 4H_2O$$

L'intensité de la couleur formée est proportionnelle à la concentration de cholestérol présent dans l'échantillon testé[1, 2].

SIGNIFICATION CLINIQUE

Le cholestérol est une substance grasse présente dans toutes les cellules de l'organisme. Le foie produit naturellement tout le cholestérol dont il a besoin pour former les membranes cellulaires et pour produire certaines hormones. La détermination du cholestérol est l'un des outils les plus importants pour diagnostiquer et classifier les lipémies. L'augmentation du niveau de cholestérol est l'un des facteurs de risques cardiovasculaires possibles[5, 6].
Le diagnostic clinique doit tenir compte des données cliniques et de laboratoire.

REACTIFS

R 1 Tampon	PIPES pH 6,9 phénol	90 mmol/L 26 mmol/L
R 2 (Remarque 2) Enzymes	Cholestérol estérase (CHE) Cholestérol oxydase (CHOD) Peroxydase (POD) 4 - Aminophénazone (4-AF)	300 U/L 300 U/L 1250 U/L 0,4 mmol/L
CHOLESTEROL CAL	Patron primaire de détection du cholestérol 200 mg/dL. Contient Triton X-114 10-15%.	

PRÉCAUTIONS

CAL : H225- Liquide et vapeurs très inflammables. H318- Provoque des lésions oculaires graves. H412- Nocif pour les organismes aquatiques, entraîne des effets néfastes à long terme.
Suivez les conseils de prudence donnés en SDS et étiquette.

PREPARATION

Réactif de travail (RT): Dissoudre (→) le contenu d'une capsule d'enzymes R 2 dans un 1 flacon de tampon R 1.
Refermer et mélanger doucement jusqu'à ce que le contenu soit dissout

4. Mélanger et incuber pendant exactement 5 minutes à 37°C ou 10 min. at température ambiante.
5. Lire l'absorbation (A) du patron et l'échantillon, en comparaison avec le blanc du réactif. La couleur reste stable pendant au moins 60 minutes.

CALCULS

$$\frac{(A)\text{Échantillon} - (A)\text{Blanc}}{(A)\text{Etalon} - (A)\text{Blanc}} \times 200\ (\text{étalon conc.}) = \text{mg/dL de cholestérol dans l'échantillon}$$

Facteur de conversion: mg/dL x 0,0258= mmol/L.

CONTROLE DE QUALITE

Il est conseillé d'analyser conjointement les échantillons de sérum dont les valeurs ont été contrôlées: SPINTROL H Normal et pathologique (Réf. 1002120 et 1002210).
Si les valeurs se trouvent en dehors des valeurs tolérées, analyser l'instrument, les réactifs et le calibreur.
Chaque laboratoire doit disposer de son propre contrôle de qualité et déterminer les mesures correctives à mettre en place dans le cas où les vérifications ne correspondraient pas aux attentes.

VALEURS DE REFERENCE

Evaluation du risque[5, 6]:

Moins de 200 mg/dL	Normal
200-239 mg/dL	Modéré
≥ 240	Elevé

Ces valeurs sont données à titre d'information. Il est conseillé à chaque laboratoire de définir ses propres valeurs de référence.

CARACTERISTIQUES DE LA METHODE

Gamme de mesures: Depuis la limite de détection de 0 mg/dL jusqu'à la limite de linéarité de 900 mg/dL.
Si la concentration de l'échantillon est supérieure à la limite de linéarité, diluer 1/2 avec du ClNa 9 g/L et multiplier le résultat final par 2.
Précision:

	Intra-série (n=20)		Inter-série (n=20)	
Moyenne (mg/dL)	90,4	187	92,8	193
SD	1,15	1,01	1,98	2,39
CV (%)	1,27	0,54	2,14	1,24

Sensibilité analytique: 1 mg/dL = 0,00152 A.
Exactitude: Les réactifs SPINREACT (y) ne montrent pas de différences systématiques significatives lorsqu'on les compare à d'autres réactifs commerciaux (x).
Les résultats obtenus avec 50 échantillons ont été les suivants:
Coefficient de corrélation $(r)^2$: 0,99541.
Equation de la Coubre de régression: y=0,95293x – 3,020.
Les caractéristiques de la méthode peuvent varier suivant l'analyseur employé.

INTERFERENCES

Aucune interférence d'hémoglobine n'a été constaté jusqu'à 5 g/L et bilirubine

SPINREACT

CE TRIGLYCERIDES

Triglycérides

GPO-POD. Enzymatique colorimétrique

Détermination quantitative de triglycérides
IVD

Conserver à 2-8°C

PRINCIPE DE LA METHODE

Les triglycérides incubés avec de la lipoprotéinlipase (LPL) libèrent du glycérol et des acides gras libres. Le glycérol est phosphorilasé par du glycérophosphate déshydrogénase (GPO) et de l'ATP en présence de glycérol kinase (GK) pour produire du glycérol-3-phosphate (G3P) et de l'adénosine-5-di phosphate (ADP). Le G3P est alors transformé en dihydroxiacétone phosphate (DAP) et en peroxyde d'hydrogène (H_2O_2) par le GPO.
Au final, le peroxyde d'hydrogène (H_2O_2) réagit avec du 4-aminophénazone (4-AF) et du p-chlorophénol, réaction catalysée par la peroxydase (POD), ce qui donne une couleur rouge:

$$\text{Triglycérides} + H_2O \xrightarrow{LPL} \text{Glycérol} + \text{Acides gras libres}$$

$$\text{Glycérol} + ATP \xrightarrow{Glycérolkinase} G3P + ADP$$

$$G3P + O_2 \xrightarrow{GPO} DAP + H_2O_2$$

$$H_2O_2 + 4\text{-AF} + \text{p-Chlorophénol} \xrightarrow{POD} \text{Quinone} + H_2O$$

L'intensité de la couleur formée est proportionnelle à la concentration de triglycérides présents dans l'échantillon testé [1, 2, 3].

SIGNIFICATION CLINIQUE

Les triglycérides sont des graisses qui fournissent à la cellule son énergie. Tout comme le cholestérol, ils sont transportés vers les cellules de l'organisme par les lipoprotéines du sang.
Un régime fort en graisses saturés ou en carbohydrates peut élever les niveaux de triglycérides.
Leur augmentation est relativement neutre. Diverses maladies, telles que certaines dysfonctions hépatiques (cirrhose, hépatite, obstruction biliaire) ou diabètes mellitus, peuvent être associées à des hausses de triglycérides [3, 6, 7].
Le diagnostique clinique doit tenir compte des données cliniques et de laboratoire.

REACTIFS

R 1 Tampon	GOOD pH 7,5 p-Chlorophénol	50 mmol/L 2 mmol/L
R 2 Enzymes	Lipoprotéine lipase (LPL) Glycérol kinase (GK) Glycérol-3-oxydase (GPO) Peroxydase(POD) 4 – Aminophénazone (4-AF) ATP	150000 U/L 500 U/L 2500 U/L 440 U/L 0,1 mmol/L 0,1 mmol/L
TRIGLYCERIDES CAL	Patron primaire de détection de triglycérides 200 mg/dL	

PREPARATION

Réactif de travail (RT): Dissoudre (→) le contenu d'une capsule d'enzymes R 2 et un flacon de tampon R 1.
Réf: 1001310 Réactif de travail (RT): Reconstituer (→) le contenu d'une capsule d'enzymes R 2 dans 10 ml de tampon R 1.

	Blanc	Modèle	Echantillon
RT (mL)	1,0	1,0	1,0
Modèle [Remarque 1, 2] (µL)	--	10	--
Echantillon (µL)	--	--	10

4. Mélanger et incuber 5 minutes a 37°C ou 10 min. à température ambiante.
5. Lire l'absorbation (A) du patron et l'échantillon, en comparaison avec le blanc du réactif. La couleur reste stable pendant au moins 30 minutes.

CALCULS

$$\frac{(A)\text{Echantillon}}{(A)\text{Modèle}} \times 200\ (\text{modèle conc.}) = \text{mg/dL de triglycéride dans l'échantillon}$$

Facteur de conversion: mg/dL x 0,0113 = mmol/L.

CONTROLE DE QUALITE

Il est conseillé d'analyser conjointement les échantillons de sérum dont les valeurs ont été contrôlées: SPINTROL H Normal et pathologique (Réf. 1002120 et 1002210).
Si les valeurs se trouvent en dehors des valeurs tolérées, analyser l'instrument, les réactifs et le calibreur.
Chaque laboratoire doit disposer de son propre contrôle de qualité et déterminer les mesures correctives à mettre en place dans le cas où les vérifications ne correspondraient pas aux attentes.

VALEURS DE REFERENCE

Hommes: 40 – 160 mg/dL
Femmes: 35 – 135 mg/dL

Ces valeurs sont données à titre d'information. Il est conseillé à chaque laboratoire de définir ses propres valeurs de référence.

CARACTERISTIQUES DE LA METHODE

Gamme de mesures: Depuis la limite de détection de 0,000 mg/dL jusqu'à la limite de linéarité de 2200 mg/dL.
Si la concentration de l'échantillon est supérieure à la limite de linéarité, diluer 1/2 avec du ClNa 9 g/L et multiplier le résultat final par 2.
Précision:

	Intra-série (n=20)		Inter-série (n=20)	
Moyenne (mg/dL)	103	219	103	217
SD	0,41	0,93	3,74	7,80
CV (%)	0,39	0,43	3,62	3,59

Sensibilité analytique: 1 mg/dL = 0,00137 A.
Exactitude: Les réactifs SPINREACT (y) ne montrent pas de différences systématiques significatives lorsqu'on les compare à d'autres réactifs commerciaux (x).
Les résultats obtenus avec 50 échantillons ont été les suivants:
Coefficient de corrélation (r): 0,99760.
Equation de la Coubre de régression: y=0,905x +10,77.
Les caractéristiques de la méthode peuvent varier suivant l'analyseur employé.

INTERFERENCES

Aucune interférence n'a été relevée avec bilirubine jusqu'à 170 µmol/L et hémoglobine jusqu'à 10 g/L. [2].
Différentes drogues ont été décrites ainsi que d'autres substances qui peuvent interférer lors de la détermination de la triglycérides [4,5].

SPINREACT

CE GPT (ALT)-LQ

GPT (ALT)

NADH. Cinétique UV. IFCC rec. liquide

Détermination quantitative d'alanine amino transférase
GPT (ALT)
IVD

Conserver à 2-8°C

PRINCIPE DE LA METHODE

L'alanine amino transférase (ALT) initialement appelée transaminase glutamique pyruvique (GPT) catalyse le transfert réversible d'un groupe animique d'alanine vers l'alpha-cétoglutarate à formation de glutamate et de pyruvate. Le pyruvate produit est réduit en lactate en présence de lactate déshydrogénase (LDH) et NADH:

$$\text{Alanine} + \alpha\text{-Cétoglutarate} \xrightarrow{\text{ALT}} \text{Glutamate} + \text{Pyruvate}$$

$$\text{Pyruvate} + \text{NADH} + \text{H}^+ \xrightarrow{\text{LDH}} \text{Lactate} + \text{NAD}^+$$

La vitesse de réduction de la concentration en NADH au centre, déterminée photométriquement, est proportionnelle à la concentration catalytique d'ALT dans l'échantillon[1].

SIGNIFICATION CLINIQUE

L'ALT est une enzyme intracellulaire, qui se trouve principalement dans les cellules du foie et des reins.
Son meilleur avantage est le diagnostic de maladies du foie.
On l'observe en grandes quantités dans le cadre de maladies hépatiques, telles que l'hépatite, les maladies du muscles et des infarctus du cœur, étant donné que la valeur de l'ALT reste dans les limites standards et augmente dans les niveaux de AST[1, 4,5].
La diagnostique clinique doit être réalisée en prenant en compte les données cliniques et de laboratoire.

REACTIFS

R 1 Tampon	TRIS pH 7,8	100 mmol/L
	Lactate déshydrogénase (LDH)	1200 U/L
	L-Alanine	500 mmol/L
R 2 Substrats	NADH	0,18 mmol/L
	α-Cétoglutarate	15 mmol/L

PRECAUTIONS

R1 : H290- Peut être corrosif pour les métaux.
Suivez les conseils de prudence donnés en SDS et étiquette.

PREPARATION

Réactif de travail (RT):
Mélanger: 1 vol. de (R2) Substrats + 4 vol. (R1) Tampon.
Stabilité: 21 jours à 2-8°C ou 72 heures à température ambiante (15-25°C).

CONSERVATION ET STABILITE

Tous les composants du kit sont stables jusqu'à la date de péremption indiquée sur l'étiquette, et si les flacons sont maintenus hermétiquement fermés à 2-8°C, à l'abri de la lumière et des sources de contamination. Ne pas utiliser les réactifs en dehors de la date indiquée.
Indices de détérioration des réactifs:
- Présence de particules et turbidité.

CALCULS

ΔA/min x 1750 = U/L d'ALT

Unités: L'unité internationale (UI) correspond à la quantité d'enzymes qui converti 1 μmol de substrats par minute, dans des conditions standard. La concentration est exprimée en unité/litre (U/L).

Facteurs de conversion de températures
Les résultats peuvent se transformer à d'autres températures, en multipliant par:

Température de mesure	Facteur de conversion à		
	25°C	30°C	37°C
25°C	1,00	1,32	1,82
30°C	0,76	1,00	1,39
37°C	0,55	0,72	1,00

CONTROLE DE QUALITE

Il est conseillé d'analyser conjointement les échantillons de sérum dont les valeurs ont été contrôlées: SPINTROL H Normal et pathologique (Réf. 1002120 et 1002210).
Si les valeurs se trouvent en dehors des valeurs tolérées, analyser l'instrument, les réactifs et le calibreur.
Chaque laboratoire doit disposer de son propre contrôle de qualité et déterminer les mesures correctives à mettre en place dans le cas où les vérifications ne correspondraient pas aux attentes.

VALEURS DE REFERENCE[4, 5]

	25°C	30°C	37°C
Hommes	Jusqu'à 22 U/L	29 U/L	40 U/L
Femmes	Jusqu'à 18 U/L	22 U/L	32 U/L

Chez les nouveau-nés en bon état de santé, on a détecté des valeurs presque doublés par rapport à celle relevées chez les adultes, état donné leur maturité hépatique, ces valeurs redeviennent normales dans les trois mois.
Ces valeurs sont données à titre d'information. Il est conseillé à chaque laboratoire de définir ses propres valeurs de référence.

CARACTERISTIQUES DE LA METHODE

Gamme de mesures: Depuis la *limite de détection* de 0 U/L, jusqu'à la *limite de linéarité* de 400 U/L.
Si la concentration de l'échantillon est supérieure à la limite de linéarité, diluer 1/10 avec du ClNa 9 g/L et multiplier le résultat final par 10.
Précision:

	Intra-série (n= 20)		Inter-série (n= 20)	
Moyenne (U/L)	42,0	116	41,1	115
SD	0,47	0,42	0,76	1,61
CV (%)	1,11	0,36	1,85	1,40

Sensibilité analytique: 1 U/L = 0,00052 *ΔA* /min
Exactitude: Les réactifs SPINREACT (y) ne montrent pas de différences systématiques significatives lorsqu'on les compare à d'autres réactifs commerciaux (x).
Les résultats obtenus avec 50 échantillons ont été les suivants:
Coefficient de corrélation $(r)^2$: 0,99597.
Equation de la Coubre de régression: y=1,1209x + 1,390.
Les caractéristiques de la méthode peuvent varier suivant l'analyseur employé.

SPINREACT

CE GOT (AST)

GOT (AST)

NADH. Cinétique UV. IFCC rec.

Détermination quantitative d'aspartate amino transférase GOT (AST)
IVD

Conserver à 2-8°C

PRINCIPE DE LA METHODE

L'aspartate amino transférase (AST), initialement appelée transaminase glutamate oxaloacétique (GOT) catalyse le transfert réversible d'un groupe animique de l'aspartate vers l'alpha-cétoglutarate à formation de glutamate et d'oxalacétate. L'oxalacétate produit est réduit en malate en présence de déshydrogénées (MDH) et NADH:

$$\text{Aspartate} + \alpha\text{-Cétoglutarate} \xrightarrow{\text{AST}} \text{Glutamate} + \text{Oxalacétate}$$

$$\text{Oxalacétate} + \text{NADH} + \text{H}^+ \xrightarrow{\text{MDH}} \text{Malate} + \text{NAD}^+$$

La vitesse de réduction de la concentration en NADH au centre, déterminée photo numériquement, est proportionnelle à la concentration catalytique d'AST dans l'échantillon[1].

SIGNIFICATION CLINIQUE

L'AST est une enzyme intracellulaire, qui se trouve en grandes quantités dans les muscles du cœur, les cellules du foie, les cellules du muscle squelettique et en plus faibles quantités dans les autres tissus.
Bien qu'un niveau élevé d'AST dans le sérum ne soit pas caractéristique d'une maladie hépatique, elle s'emploie principalement pour les diagnostics et le suivi, avec d'autres enzymes telles que l'ALT et l'ALP. Elle s'utilise également dans le cadre du contrôle post-infarctus, chez les patients souffrant de troubles musculaires du squelette et dans certains autres cas[1, 4,5].
Le diagnostic clinique doit être réalisé en prenant en compte les données cliniques et les données de laboratoire.

REACTIFS

R 1 Tampon	TRIS pH 7,8	80 mmol/L
	L-aspartate	200 mmol/L
R 2 Substrats	NADH	0,18 mmol/L
	Lactate déshydrogéné (LDH)	800 U/L
	Malate déshydrogénisé (MDH)	600 U/L
	α-cétoglutarate	12 mmol/L

PREPARATION

Réactif de travail (RT):
Réf: 1001160 Dissoudre (→) une tablette de substrats R2 dans une dose (ampoule) R1.
Réf: 1001161 Dissoudre (→) une tablette de substrats R2 dans 15 mL de R1.
Réf: 1001162 Dissoudre (→) une tablette de substrats de R2 dans 50 mL de R1.
Refermer et mélanger doucement, jusqu'à ce que le contenu soit totalement dissout.
Stabilité: 21 jours à 2-8°C ou 72 heures à température ambiante (15-25°C).

CONSERVATION ET STABILITE

5. Lire l'absorbation (A) initiale de l'échantillon, mettre en route le chronomètre et lire l'absorbation à chaque minute pendant 3 minutes.
6. Calculer la moyenne de l'augmentation d'absorbation par minute (ΔA/min).

CALCULS

ΔA/min x 1750 = U/L de AST

Unités: L'unité internationale (UI) correspond à la quantité d'enzymes qui converti 1 µmol de substrats par minute, dans des conditions standard. La concentration est exprimée en unité/litre (U/L).

Facteurs de conversion de températures

Les résultats peuvent se transformer à d'autres températures, en multipliant par:

Température de mesure	Facteur de conversion à		
	25°C	30°C	37°C
25°C	1,00	1,37	2,08
30°C	0,73	1,00	1,54
37°C	0,48	0,65	1,00

CONTROLE DE QUALITE

Il est conseillé d'analyser conjointement les échantillons de sérum dont les valeurs ont été contrôlées: SPINTROL H Normal et pathologique (Réf. 1002120 et 1002210).
Si les valeurs se trouvent en dehors des valeurs tolérées, analyser l'instrument, les réactifs et le calibreur.
Chaque laboratoire doit disposer de son propre contrôle de qualité et déterminer les mesures correctives à mettre en place dans le cas où les vérifications ne correspondraient pas aux attentes.

VALEURS DE REFERENCE[1]

	25°C	30°C	37°C
Hommes	Jusqu'à 19 U/L	26 U/L	38 U/L
Femmes	Jusqu'à 16 U/L	22 U/L	31 U/L

Ces valeurs sont données à titre d'information. Il est conseillé à chaque laboratoire de définir ses propres valeurs de référence.

CARACTERISTIQUES DE LA METHODE

Gamme de mesures: Depuis la limite de détection 0 U/L jusqu'à la limite de linéarité 360 U/L.
Si la concentration de l'échantillon est supérieure à la limite de linéarité diluer 1/10 avec du ClNa 9 g/L et multiplier le résultat final par 10.

Précision:

	Intra-série (n= 20)		Inter-série (n= 20)	
Moyenne (U/L)	55,5	165	55,0	162
SD	1,30	3,44	0,92	2,52
CV (%)	2,35	2,07	1,68	1,55

Sensibilité analytique: 1 U/L = 0,00051 ΔA /min
Exactitude: Les réactifs SPINREACT (y) ne montrent pas de différences systématiques significatives lorsqu'on les compare à d'autres réactifs commerciaux (x).
Les résultats obtenus avec 50 échantillons ont été les suivants:
Coefficient de corrélation $(r)^2$: 0,98277.
Equation de la Coubre de régression: y= 0,9259x - 5,1685.
Les caractéristiques de la méthode peuvent varier suivant l'analyseur employé.

ABSTRACT

The primary aim of this study is to biosynthesize Ag/Ag_2O NPs and ZnO NPs using *O. europaea* var. Chemllali leaves aqueous extract. Additionally, the biological effects of these nanoparticles will be assessed both in vitro and in vivo. Qualitative, quantitative analysis and HPLC analysis was used for the identification of specific phenolic components of the extract. However, Ag/Ag_2O NPs and ZnO NPs have been green synthesized and characterized using more then one technique (UV, FTIR, XRD, and SEM-EDX). Furthermore, antioxidant, antibacterial, antimutagenic, anticoagulant activities have been used to evaluate the in vitro activities. For in vivo study using Wistar male rats, to evaluate the extent of toxicity of these nanoparticles, and to assess protective effect of this nanoparticles against metrubizin toxicity. Some biochemical and hematological indicators, also histopathological and oxidative stress parameter of liver, kidney and spleen were mesured. Phytochemical analysis revealed the presence of many seconder metabolites in aquous extract, also quantified of the total phenolic, flavonoids and condensed tanins content. Another analyze by HPLC,we have identified eight phenolic compounds; when quercetin (1945.90 µg/g) was the most abundant element. After characterization of biogenic nanopartilces, we confirmed that Ag/Ag_2O NPs and ZnO NPs were biosynthesized. The average size distribution of Ag/Ag_2O NPs is principally 45 nm, and 18.79 nm for ZnO NPs size. For antioxidant activities of the *O.europaea* leaf extract, Ag/Ag_2O NPs and ZnO Nps is shown to be dose-dependent, as the scavenging activity, TAC and FRAP, the most notable antioxydant activities were observed with 200 µg/mL of Ag/Ag_2O Nps. The antibacterial activity in solid agar was found also to be dose-dependent of Ag/Ag_2O NPs against *S.aureus*, *E.coli*, and *P. aeruginosa*, while the ZnO nanoparticles at higher dose was less effective. However, antibacterial kinetic study in liquid medium revealed inhibitory effects of nanoparticles on bacterial growth of *E. coli* and *S. typhimurium* cells at 200ug/ml, but the growth of *B. cereus* and *MS-S. aureus* cells was suppressed in the initial hours, with almost all bacterial cells exhibiting retarded growth after this period. This tow nanoparticles biosynthetised showed strong anti-mutagenicity against *S. typhimurium* TA98, when the percent inhibition of ZnO NPs was stronger (76.24%) then Ag/Ag_2O NPS (70%) at 250 µg/plat. All nanoparticles (ZnO and Ag/Ag_2O NPs) prevented coagulation similarly to the positive control (EDTA). Toxicity study of nanoparticles revealed no mortality for ZnO NPs (50 mg/kg and 100 mg/kg b.w) and Ag/Ag_2O NPs (2.5 mg/Kg) for single dose during the 28-days. In contrast, one rat that received a higher dose of 5 mg/kg b.w of Ag/Ag_2O NPs died after 24 h, and we showed signs of toxicity in this group. Moreover, the findings in metribuzin-treated rats induced for 21 days significant changes in hematological, biochemical parameters and imbalance in oxidative stress status and deterioration of the liver, the kidney and the spleen structure compared to the control group. However, the treatment with ZnO NPs (2.5 mg/Kg , 5 mg/Kg) mitigated most of toxic effects and the restored most of previous parameters. As for Ag/Ag_2O NPs, most of the effects of low concentration (0.062mg/Kg) were generally beneficial. On the other hand, the effect of high concentration (0.125mg/Kg) was hopeless and even toxic, as demonstrated by the analyzes and histological images of the organs studied. En conclusion, this work realizes the potential for green synthesis of nanoparticles from *O. europaea* (ZnO NPs and Ag/Ag_2O NPs), as these particles have shown to be highly biological efficient and varied among them, While Ag/Ag_2O NPs was toxic to a certain degree.

Key words: *O.europaea* , ZnO NPs, Ag/Ag_2O NPs, antibacterial, antimutagenic, toxicity ,protective effect

الملخص

الهدف الأساسي من هذه الدراسة هو التخليق الحيوي لـ Ag/Ag_2O NPs و ZnO NPs باستخدام المستخلص المائي أوراق نبات الزيتون *O.europaea*. بالإضافة إلى ذلك، سيتم تقييم التأثيرات البيولوجية لهذه الجسيمات النانوية. تم استخدام التحليل النوعي والكمي وتحليل HPLC لتحديد المكونات الفينولية المحددة للمستخلص. وبعدها، تم التصنيع الحيوي للجزئيات النانوية للفضة/أوكسيد ثنائي الفضة Ag/Ag_2O NPs و أوكسيد الزنك ZnO NPs، قد وتم فحص خصائصها باستخدام أكثر من تقنية (UV، FTIR، XRD، و-SEM EDX). علاوة على ذلك، تم إختبار مدى نشاطيتها في المختبر المضادة الأكسدة، والمضادة الجراثيم، والمضادة الطفرات، وكذا المضادة لتخثر الدم. و قد تم أيضا إجراء دراسة على الجسم الحي باستخدام ذكور فئران ويستار، لتقييم مدى سمية هذه الجسيمات النانوية، وتقييم التأثير الوقائي لهذه الجسيمات النانوية ضد سمية المبيد ميتروبيزين. حيث تم قياس بعض المؤشرات البيوكيميائية والدموية وكذلك مؤشرات الإجهاد التأكسدي وفحص لأنسجة الكبد والكلى والطحال. كشف التحليل الكيميائي النباتي عن وجود العديد من المستقلبات الثانوية في المستخلص المائي، كما تم قياس كمية الفينول الكلي والفلافونويدات والتانينات المكثفة. وتحليل آخر بواسطة HPLC، حيث حددنا ثمانية مركبات فينولية؛ من بينها الكيرسيتين (1945.90 ميكروغرام / غرام) هو العنصر الأكثر وفرة. بعد التخليق الأخضر الجسيمات النانوية، أكدنا أن Ag/Ag_2O NPs وZnO NPs قد تم تصنيعهما حيويًا. وبلغ متوسط حجم توزيع Ag/Ag2O NPs 45 نانومتر، و18.79 نانومتر لحجم ZnO NPs. بالنسبة للأنشطة المضادة للأكسدة لمستخلص أوراق O.europaea، Ag/Ag_2O NPs وZnO Nps تبين أن مدى النشاطية يعتمد على زيادة الجرعة، حيث لوحظ نشاط الكسح، TAC وFRAP، الأقوى في تركيز 200 ميكروغرام/مل من Ag/ Ag2O NPs.وكذلك وجد أن النشاط المضاد للبكتيريا في الأجار الصلب يعتمد أيضًا على زيادة الجرعة لـ Ag/Ag2O NPs ضد *S.aureus* و*E.coli* و*P. aeruginosa*، بينما كانت جزيئات أكسيد الزنك النانوية عند الجرعة الأعلى أقل فعالية. ورغم ذلك، كشفت الدراسة الحركية المضادة للبكتيريا في الوسط السائل عن تأثيرات مثبطة للجسيمات النانوية على النمو البكتيري لخلايا *E. coli* و *S. typhimurium* عند 200 ميكروغرام/مل، ولكن نمو *B. cereus* و *MS-S. aureus*. تم قمع الخلايا البكترية في الساعات الأولى، حيث أظهرت جميع الخلايا البكتيرية تقريبًا نموًا متأخرا بعد هذه الفترة. كما أظهرت هذه الجسيمات النانوية المصنعة حيويًا مقاومة قوية للطفرات ضد *S. typhimurium* TA98، حيث كانت نسبة تثبيط ZnO NPs أقوى (76.24%) ثم (70%) Ag/Ag_2O NPS عند 250 ميكروجرام/بلات. جميع الجسيمات النانوية (ZnO NPs و Ag/Ag_2O NPs) منعت التخثر بشكل مشابه بالمقارنة مع الشاهد (EDTA). أما في ما يخص التجارب داخل الجسم الحي، أظهرت دراسة السمية للجسيمات النانوية عدم وجود وفيات لأكسيد الزنك (50 NPs مجم/كجم و100 مجم/كجم من وزن الجسم) و2.5) Ag/Ag_2O NPs مجم/كجم) للجرعة الواحدة خلال 28 يومًا. وعلى النقيض من ذلك، مات فأر واحد تلقى جرعة قدرها 5 ملغم/كغم من Ag/Ag_2O NPs بعد 24 ساعة، كما ظهرت علامات السمية واضحة جدا في هذه المجموعة. علاوة على ذلك، أدت النتائج التي تم إجراؤها على الفئران المعالجة بالميتريبوزين لمدة 21 يومًا إلى حدوث تغييرات كبيرة في مؤشرات الدم والكيمياء الحيوية وعدم التوازن في حالة الإجهاد التأكسدي وتدهور بنية الكبد والكلى والطحال مقارنة بالمجموعة الشاهدة. في حين أن المعاملة بأكسيد الزنك (2.5 ملجم/كجم و 5 ملجم/كجم) خففت معظم التأثيرات السامة وأعادت معظم التغيرات السابقة إلى الحالة الطبيعية. أما بالنسبة لـ Ag/Ag_2O NPs، فإن معظم تأثيرات التركيز المنخفض (0.062 ملجم/كجم) كانت مفيدة بشكل عام. بينما تأثير التركيز العالي (0.125 ملجم/كجم) كان ذو أثر سلبي بل وساماً، كما يتضح من التحاليل والصور النسيجية للأعضاء المدروسة. في الختام، هدف هذا العمل إلى إمكانية التوليف الأخضر للجسيمات النانوية من *O. europaea* حيث أظهرت هذه الجسيمات كفاءة بيولوجية عالية ومتنوعة فيما بينها، في حين أن Ag/Ag_2O NPs كان أكثر سمية إلى حد ما.

الكلمات المفتاحية: *O. europaea*، ZnO NPs، Ag/Ag_2O NPs، مضاد للبكتيريا، مضاد للطفرات، سمية، تأثير وقائي.